

Microcalorimetry beyond Adsorption: Basics and Applications in Heterogeneous Catalysis



S. Wrabetz

Fritz-Haber-Institute of the Max Planck Society

Department of Inorganic Chemistry, 14195 Berlin, Germany,

wrabetz@fhi-berlin.mpg.de

Nov 24, 2017

Lecture Series: Modern Methods in Heterogeneous Catalysis;

10:45 - 12:15

1. Introduction
2. Adsorptive microcalorimetric setup
3. Tian-Calvet calorimeter
Evolved adsorption heat
Differential heats of adsorption
4. Volumetric-Barometric System
calibration & measurement of adsorbed amount
5. Obtained physical quantities & evaluation criteria of
the calorimetric results
6. Applications of microcalorimetry in heterogeneous catalysis
 - H_2 and CO adsorption on 2%Pt / Al_2O_3 at $40^\circ C$
 - NH_3 adsorption on pure-phase MoVTeNb oxide at $80^\circ C$
 - CO_2 ads. on CeO_2 at $40^\circ C$
 - O_2 adsorption on supported CeO_2 at $200^\circ C$
 - Ethanol adsorption on $VO_x/\gamma-Al_2O_3$ at $40^\circ C$
 - Propane & ethane ads. on MoVTeNb oxide, V/SBA15, MoV oxide and P/oCNT at $40^\circ C$
 - Propylene adsorption on $MoO_x/SBA-15$ at $T_{reaction}=50^\circ C$
 - 1-Hexyne ads. on CeO_2/TiO_2 at $T_{reaction}=80^\circ C$
 - CO on IrOx at $T_{reaction}=r.t.$
 - CO on Ni/MgAl oxide at $30^\circ C$

Introduction

- adsorption steps, surface reaction processes, and desorption steps
- 1st step in the catalytic cycle: activation of the reacting molecules by **adsorption**
(*strength of chemisorption bond can effect the activation energy*)
- **adsorption phenomena** (*bond strength between adsorbate and surface*) play an important role in heterogeneous catalysis

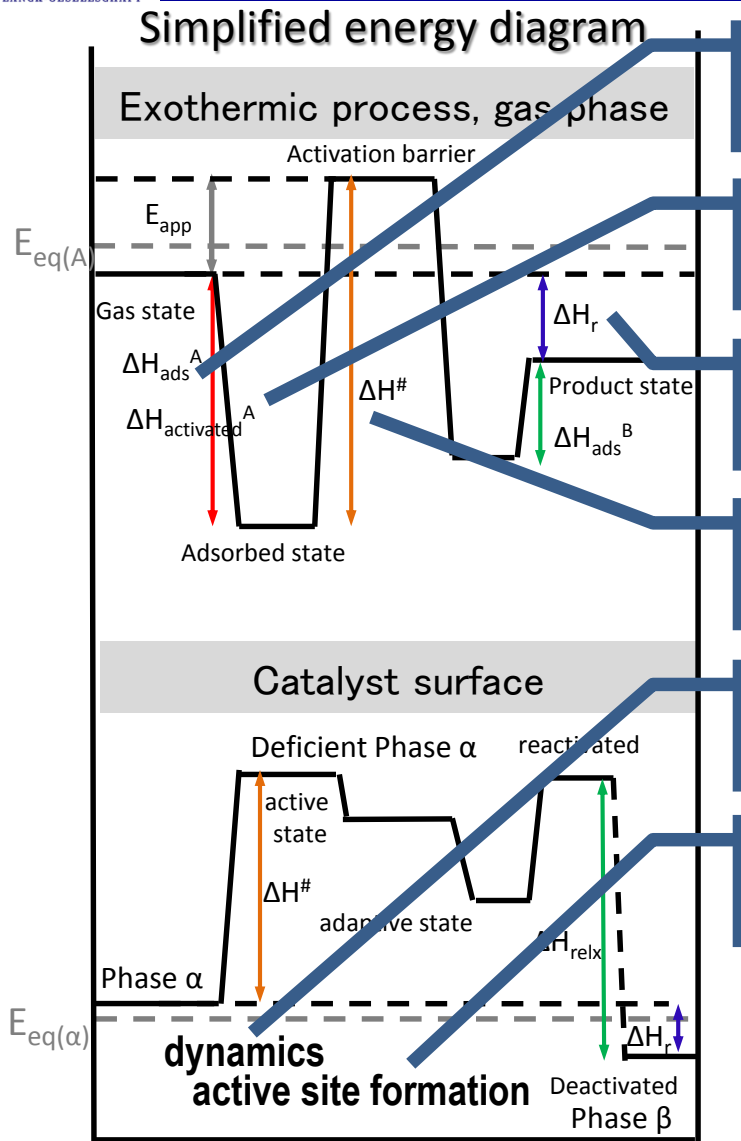
For a detailed understanding of complex reaction networks we need:

- **thermodynamic data of high accuracy**
 - **information about the nature of the catalyst surface**
- quantitatively study the adsorption, activation, and reaction phenomena close to the reaction parameters
- simulate reactants-induced responses of the surface

- **since perhaps only a minor fraction of all surface atoms form active centers**

Ads. Isothermal Microcalorimetry / Microcalorimetry beyond Ads.
direct method to determine number, strength and energy distribution of the adsorption sites

- key to the effective use of adsorptive microcalorimetry is the **careful choice of probe molecules and adsorption temperature** to study



CO₂ ads._{chemisorption} on CeO₂ for DEACON reaction ⁵

MoV oxide catalyst in oxidative dehydrogenation of alkanes

Ir-based catalysts for the oxygen evolution reaction at r.t. ¹

Vanadium Oxide-based and Metal-free Catalysts in the ODH of Ethane and Propane ²

Ni based catalysts for the dry reforming of methane ³

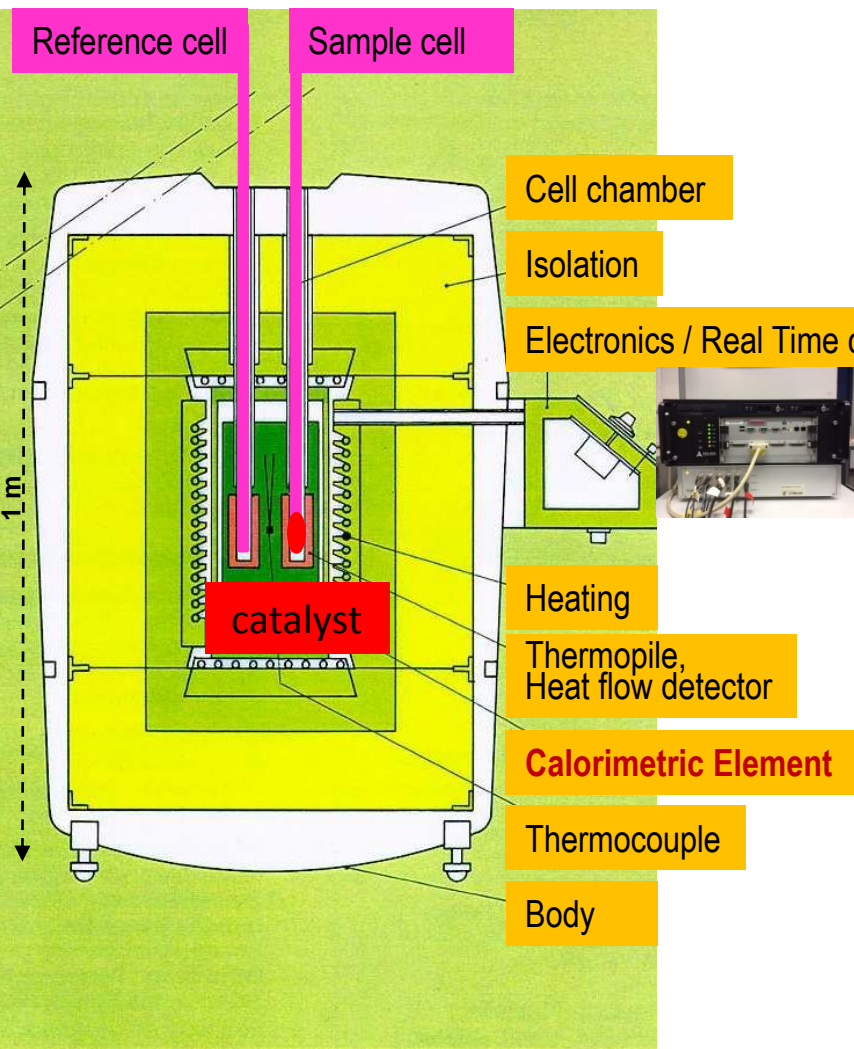
Propylene Metathesis over MoOx/SBA-15 ⁴

- 1 V. Pfeifer, T. Jones, S. Wrabetz, C. Massué, J. Velesco-Velez, R. Arrigo, M. Scherzer, S. Piccinin, M. Haevecker, A. Knop-Gericke and R. Schlögl, *Chem. Sci.*, 2016, 7, 6791-6795.
- 2 P. Kube, B. Frank, S. Wrabetz, J. Kröhnert, M. Hävecker, J. Valasco-Vélez, J. Noack, R. Schlögl, A. Trunschke, *ChemCatChem* 9 (2017) 1-14.
- 3 K. Mette, St. Kühl, A. Tarasov, M. G. Willinger, J. Kröhnert, S. Wrabetz, A. Trunschke, M. Scherzer, F. Girgsdies, H. Düdder, K. Kähler, K. Friedel Ortega, M. Muhler, R. Schlögl, M. Behrens, T. Lunkenbein, *ACS Catal.*, 2016, 6 (10), pp 7238-7248.
- 4 Amakawa, K., Wrabetz, S., Kröhnert, J., Tzolova-Müller, G., Schlögl, R., Trunschke, A.; *J. Am. Chem. Soc.*, 134 (28) (2012) 11462-11473.
- 5 Farra, R., Wrabetz, S., Schuster, M. E., Stötz, E., Hamilton, N., Amrute, A. P., Pérez-Ramírez, J., López, N., Teschner, D., *Phys. Chem. Chem. Phys.*, 15 (2013) 3454 - 3465.

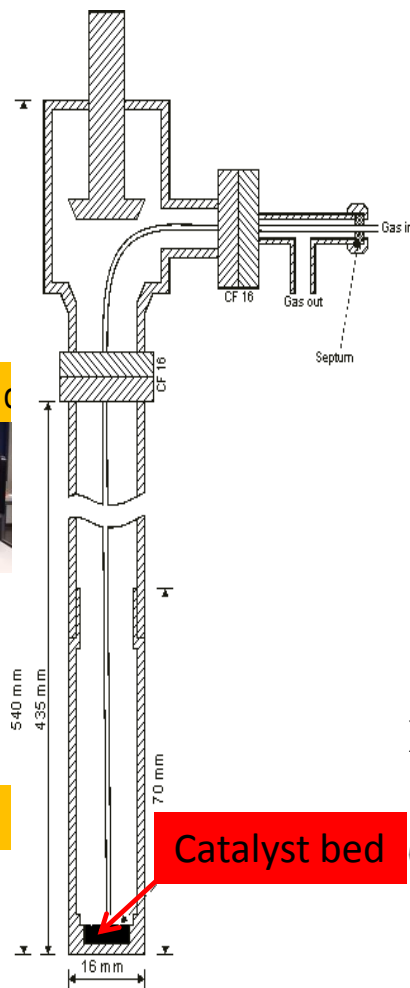
Adapted from van Santen, R. A., *Modern Heterogeneous Catalysis*, Wiley, 2017
 using Schlögl, R., *Introduction to Heterogeneous Catalysis*, Lecture, FHI Berlin, 2017

1. Introduction
2. Adsorptive microcalorimetric setup
3. Power balance of Tian-Calvet calorimeter & Evolved adsorption heat & Differential heats of adsorption
4. Volumetric-Barometric System calibration & measurement of adsorbed amount
5. Obtained physical quantities & evaluation criteria of the calorimetric results
6. Applications of microcalorimetry in heterogeneous catalysis
 - H_2 and CO adsorption on 2%Pt / Al_2O_3 at 40°C
 - NH_3 adsorption on pure-phase MoVTeNb oxide at 80°C
 - CO_2 ads. on CeO_2 at 40°C
 - O_2 adsorption on supported CeO_2 at 200°C
 - Ethanol adsorption on $VO_x/\gamma-Al_2O_3$ at 40°C
 - Propane ads. On MoVTeNb oxide at 40°C
 - Propylene adsorption on $MoO_x/SBA-15$ at $T_{reaction}=50^\circ C$
 - 1-Hexyne ads. on CeO_2/TiO_2 at $T_{reaction}=80^\circ C$

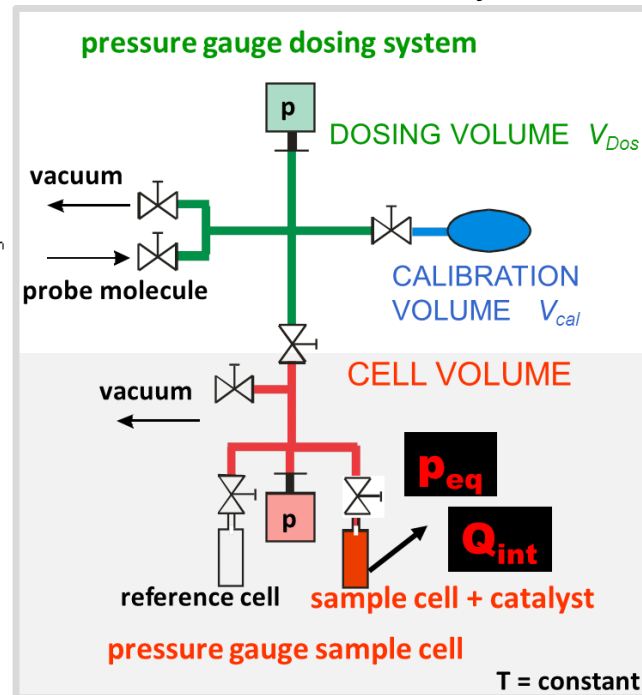
Tian-Calvet calorimeter of SETARAM



Sample cell (static, dynamic)



Volumetric-Barometric System



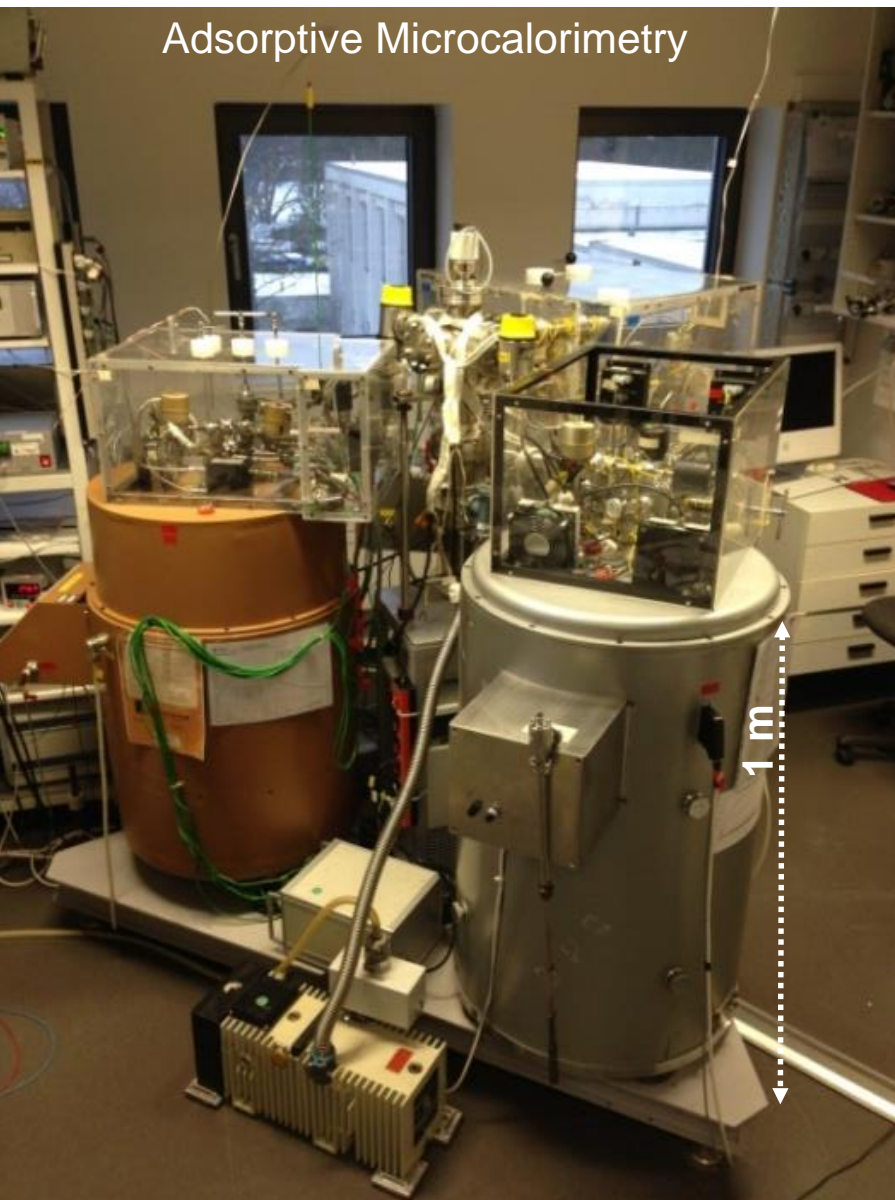
$$\Sigma n_{ads} \text{ vs } p_{eq} \quad , \quad \frac{\text{mmol} \cdot \text{g}^{-1}}{\text{mmol} \cdot \text{m}^{-2}}$$

$$q_{diff} = \frac{Q_{int}}{n_{ads}} = \Delta H_{ads} \quad , \quad \text{kJ/mol}$$

$$q_{diff} \text{ vs } n_{ads} \quad , \quad \text{kJ/mol}$$

$$K = K_o \exp \frac{\Delta H_{ads}}{RT} \quad , \quad \text{hPa}^{-1}$$

Adsorptive Microcalorimetry



HT1000 (rt-1000°C),

MS 70 (rt-100°C)

BT 2.15 (200°C–77K)

Tian-Calvet calorimeter of SETARAM

combined with a custom-designed high vacuum and gas dosing apparatus.

The **history** of modern calorimetry began at the University of Provence in Marseilles.



Prof. Albert Tian

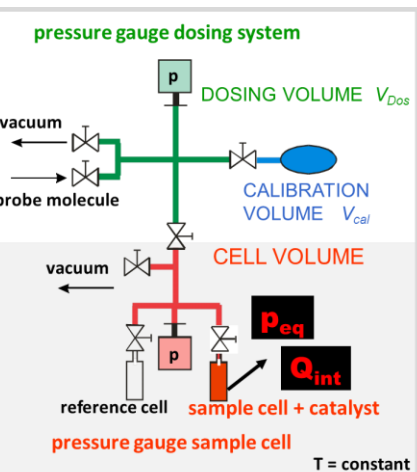
Tian described his compensation microcalorimeter for the first time in 1922, when he and his colleague COTTE used it to study the metabolism of insects. He brought further improvements to this thermocouple instrument in 1924 and 1926.



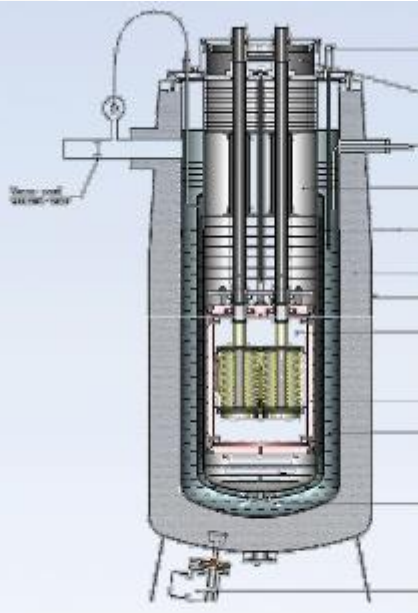
Prof. Edouard Calvet
(1895–1966)

CALVET introduced the differential setup (1948) and a rational construction of the **two twinned calorimetric elements**, transforming Tian's apparatus into a true laboratory instrument that today is commercialized by Setaram.

- Combination of LT-Calorimetry and LT-FTIR
 CO , CO_2 , CH_4 ads. on e.g. Cu catalysts,
Ni-catalysts, MgO

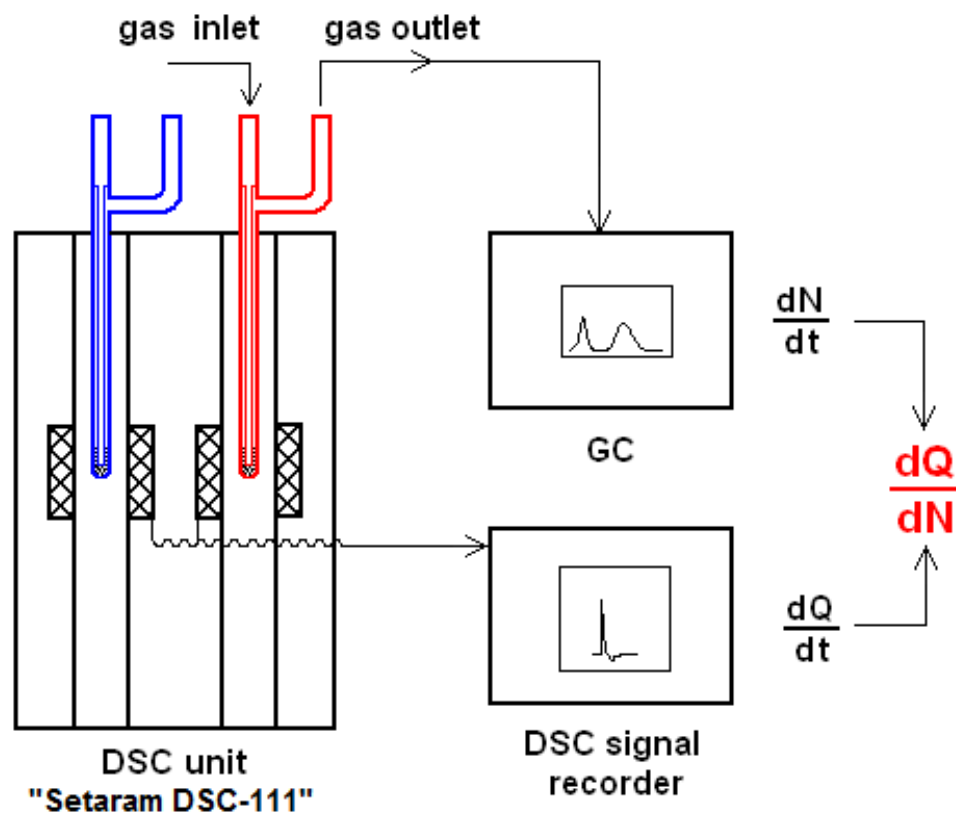
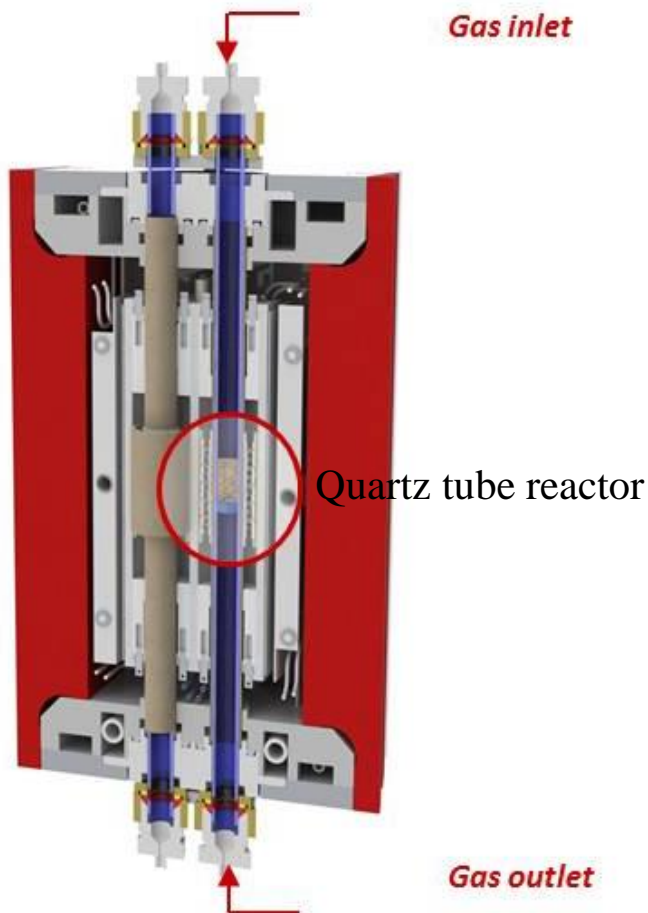


BT 2.15 Calorimeter



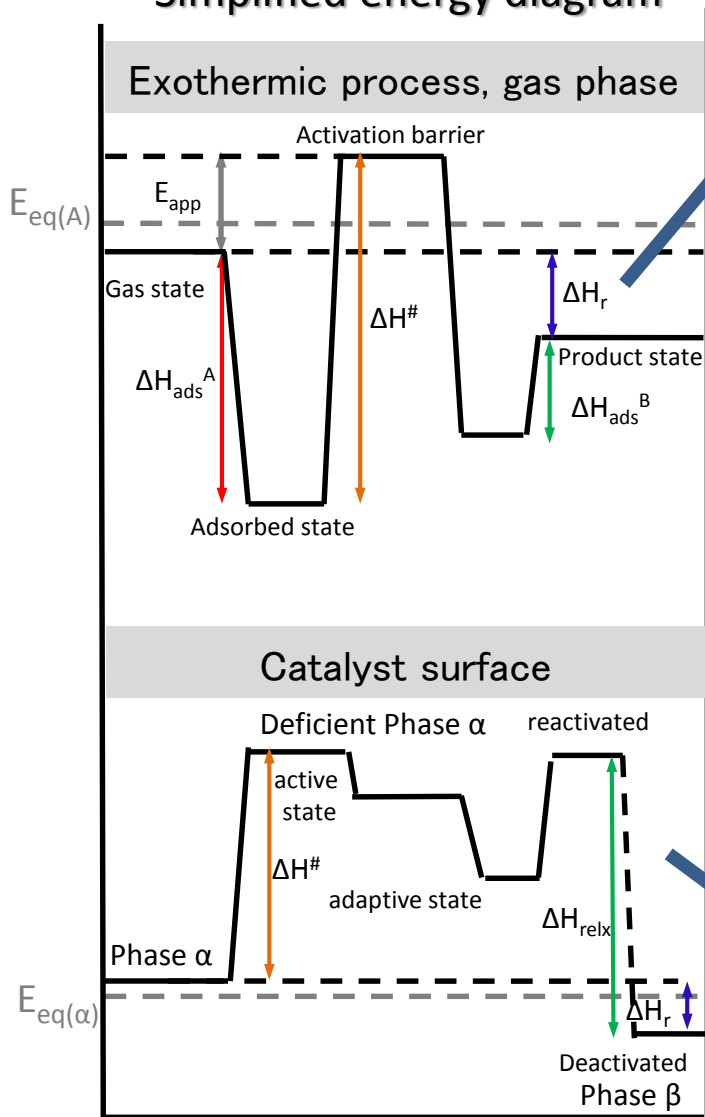
Cross-sectional view of the SETARAM BT 2.15

- Direct measurement of **reaction enthalpy**
- Precise **product analysis**



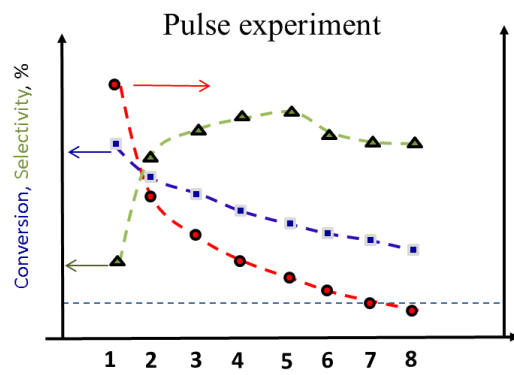
- Calvet calorimetric element
- 3D sensor totally surrounds the catalyst

Simplified energy diagram

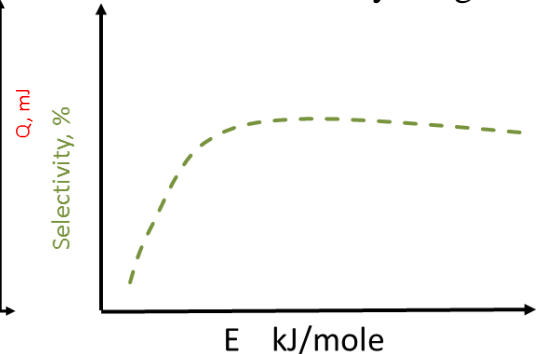


Transformation of gas phase molecules

- Information about reaction kinetics
- Simulation of different conditions *in situ*

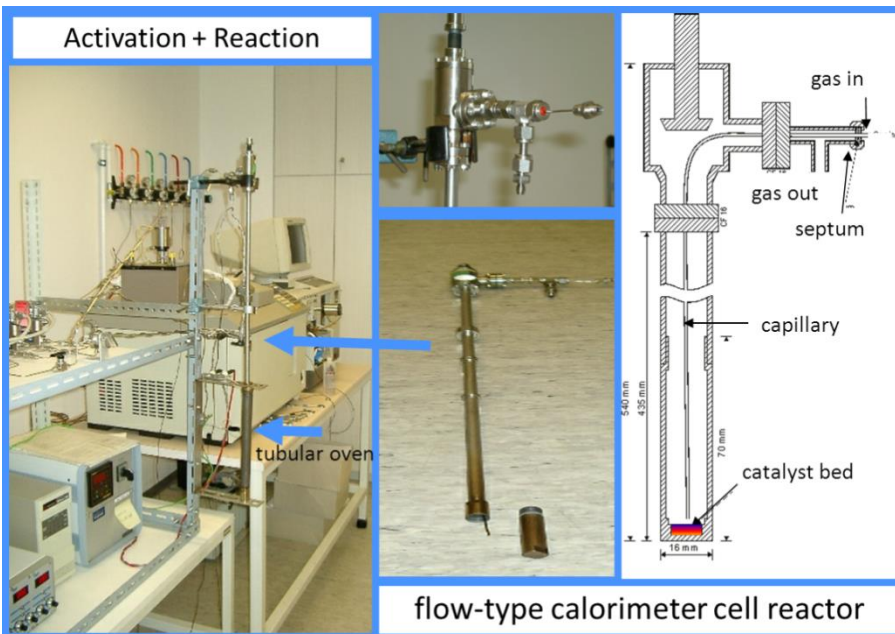


structure – selectivity diagram structure – reactivity diagram



Transformation in solid state

- Redox dynamics
- Thermochemistry of defects formation



Activation:

UHV (10^{-8} hPa), gases (H_2 , O_2 ),
rt - $600^\circ C$

Reaction:

Calorimeter cell can be used as a flow-type reactor.

Catalyst is used in the selected reaction until steady-state performance,
rt - $600^\circ C$

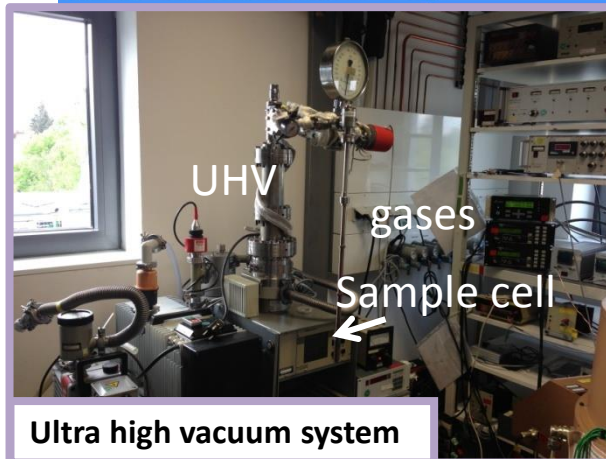
S. Wrabetz, F.C. Jentoft et al, J. Catal. 269 (2010) 351-358

Transfer

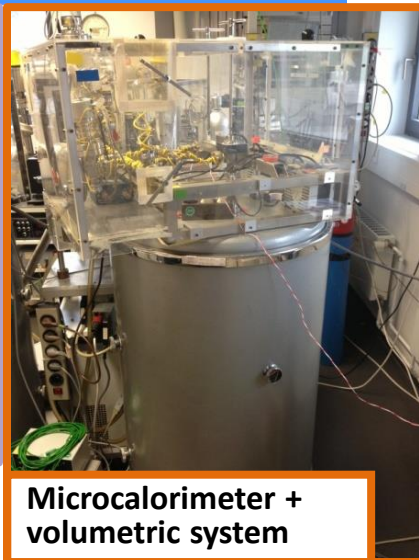
of the sample cell into the calorimeter and degassing/equilibration at T_{ads} .

Adsorptive microcalorimetric experiment:

Stepwise adsorption, desorption and re-adsorption of the selected probe molecule at the selected temperature.

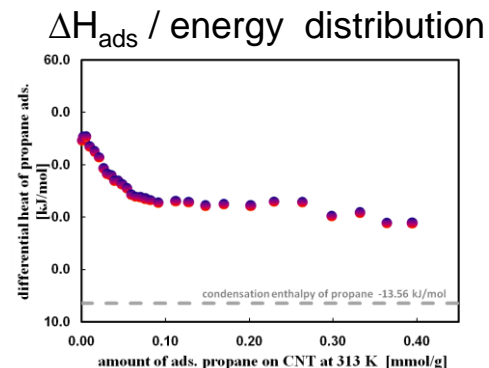
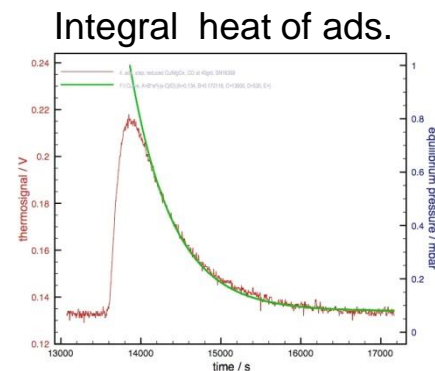
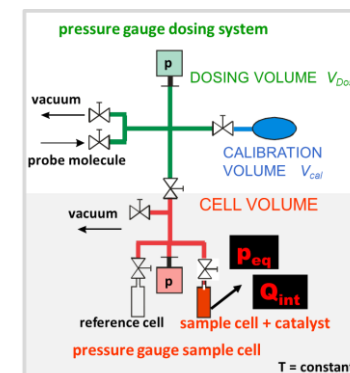
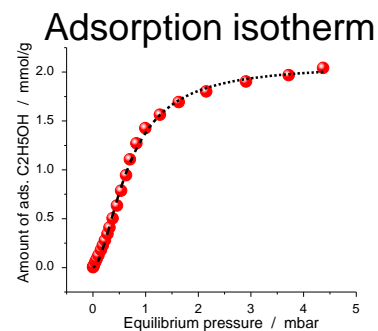


Ultra high vacuum system



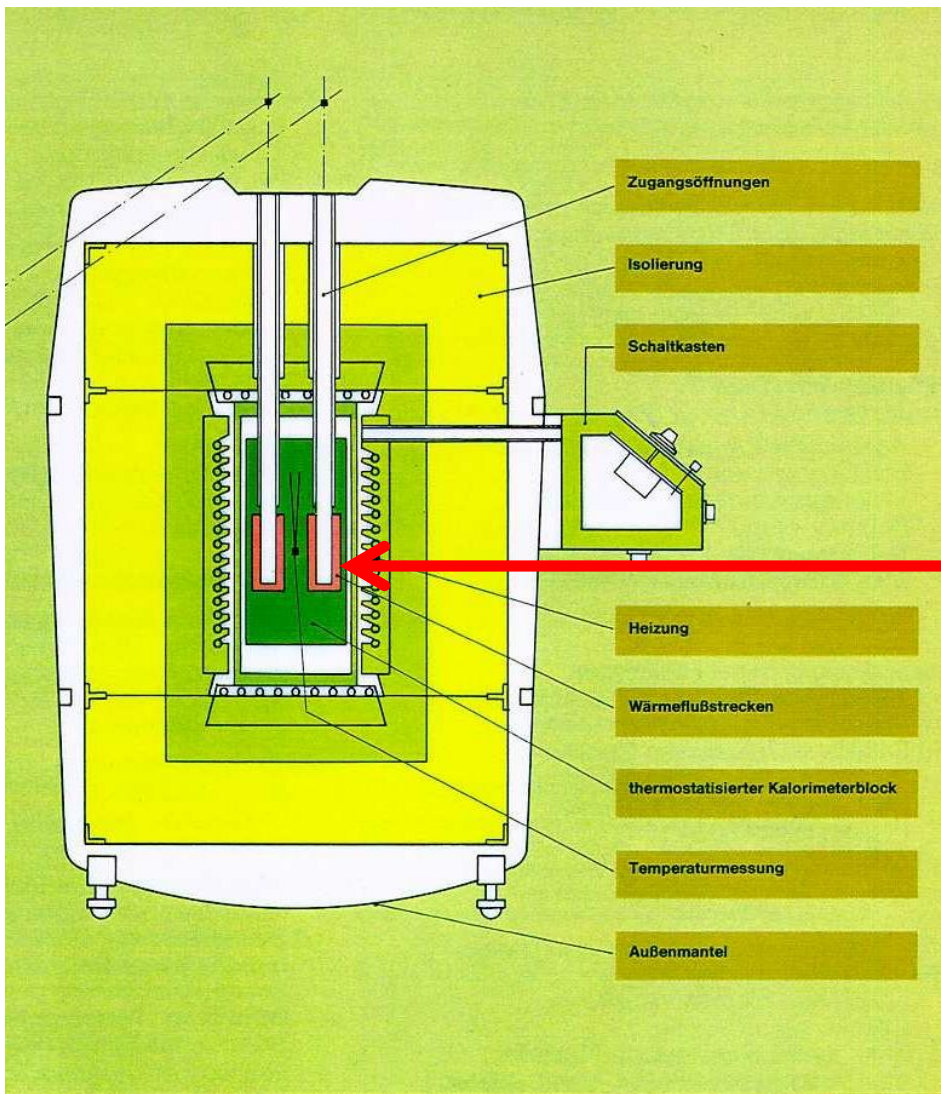
Microcalorimeter + volumetric system

- The probe molecule must be introduced **stepwise** at **constant temperature**, the pressure is increased slowly
- For each adsorption step, the **adsorbed amount** must be determined (isotherm)
- For each adsorption step, the **evolved heat** must be determined (integral heat of adsorption)
- The **differential heat** (ΔH_{ads}) can then be determined by dividing the evolved heat through the number of molecules adsorbed in a particular step



	Physisorption	Chemisorption
Type of interaction and heat of adsorption (negative enthalpy of adsorption)	van der Waals force $0 < \Delta_p H < 50$ kJ/mol Noble gases, CH ₄ , N ₂ Dipole-dipole interaction 20 – 25 kJ/mol H ₂ O, NH ₃	chemical bonding, electron transfer $60 < \Delta_c H < 400$ kJ/mol CO on metals (Pt, Pd) Dissociative adsorption (O ₂ , H ₂ on Pt, H ₂ O on oxides)
Reversibility	reversible	reversible , irreversible or partially irreversible
Speed	fast	can be slow (e.g. activated adsorption, dissociative adsorption)
Coverage	non-specific and weak multilayers possible	specific (chemisorbed molecule blocks surface sites) monolayer only

1. Introduction
2. Adsorptive microcalorimetric setup
3. Tian-Calvet calorimeter
Evolved adsorption heat
Differential heats of adsorption
4. Volumetric-Barometric System
calibration & measurement of adsorbed amount
5. Obtained physical quantities & evaluation criteria of
the calorimetric results
6. Applications of microcalorimetry in heterogeneous catalysis
 - H_2 and CO adsorption on 2%Pt / Al_2O_3 at 40°C
 - NH_3 adsorption on pure-phase MoVTeNb oxide at 80°C
 - CO_2 ads. on CeO_2 at 40°C
 - O_2 adsorption on supported CeO_2 at 200°C
 - Ethanol adsorption on $VO_x/\gamma-Al_2O_3$ at 40°C
 - Propane & ethane ads. on MoVTeNb oxide, V/SBA15, MoV oxide and P/oCNT at 40°C
 - Propylene adsorption on $MoO_x/SBA-15$ at $T_{reaction}=50^\circ C$
 - 1-Hexyne ads. on CeO_2/TiO_2 at $T_{reaction}=80^\circ C$
 - CO on IrOx at $T_{reaction}=r.t.$
 - CO on Ni/MgAl oxide at 30°C



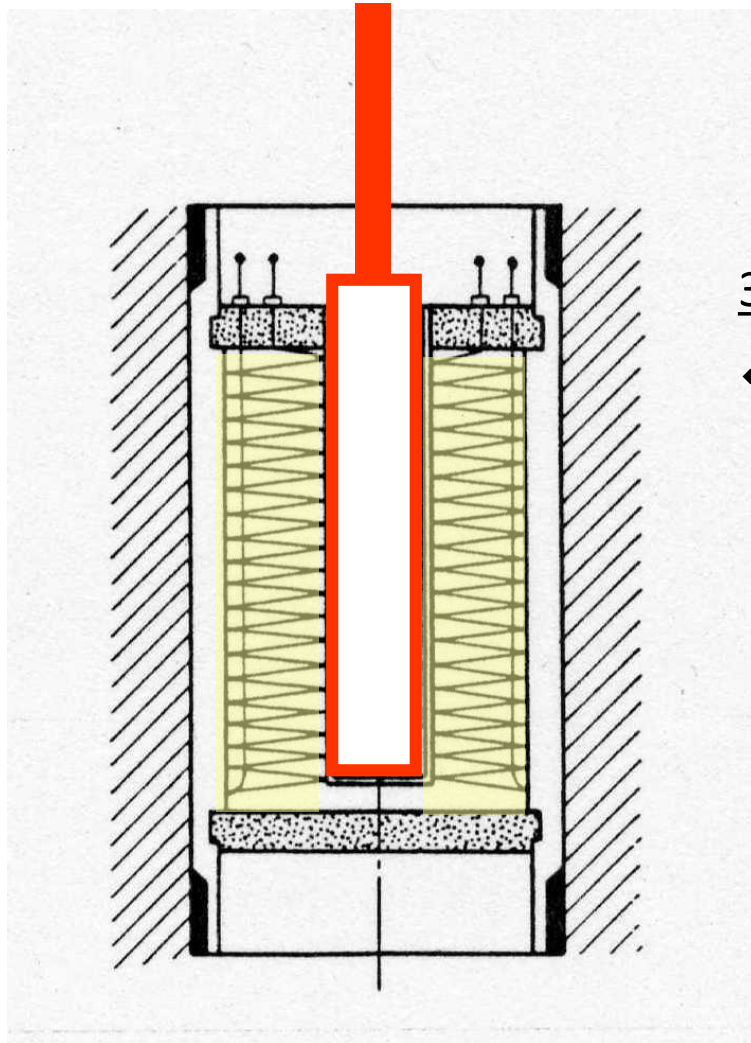
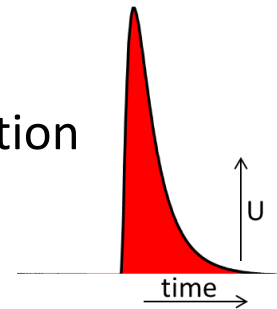
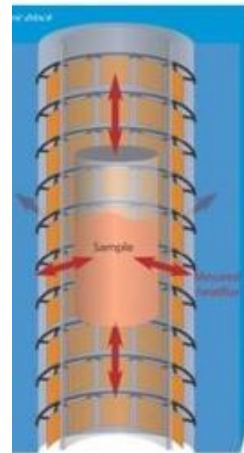
**Calorimetric
Element**

The Calorimetric Element

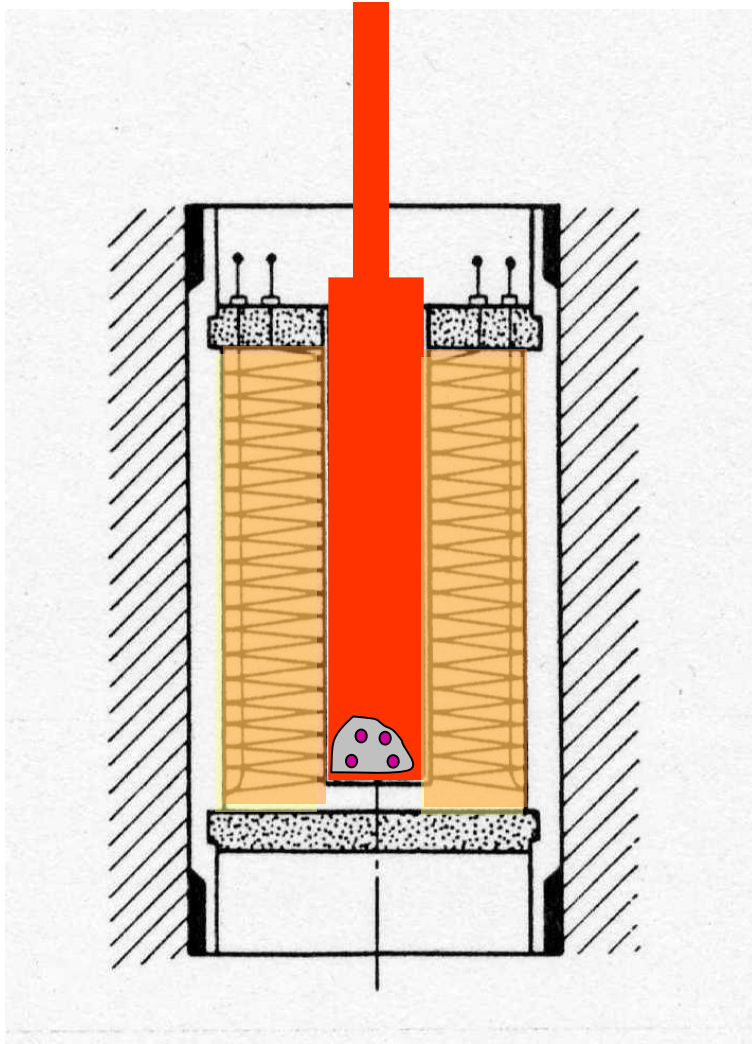
- ❖ The **sample cell** is placed into a calorimeter element

3D Calvet heat flow sensor

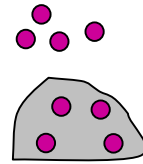
- ❖ The cell is totally surrounded by a **thermopile** made of more than 400 conductive thermocouples in series
- ❖ Thermopile has 2 functions:
 1. heat transfer
 2. signal generation



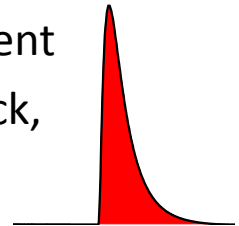
Heat and Heat Flow



➤ The **heat** produced by the adsorption/activation/reaction of a dosed **probe molecule** on/with the **catalyst** surface is consumed by 2 processes



1. Increase of the temperature of the sample cell
2. Once there is a temperature gradient between cell and surrounding block, heat flow through the thermopile

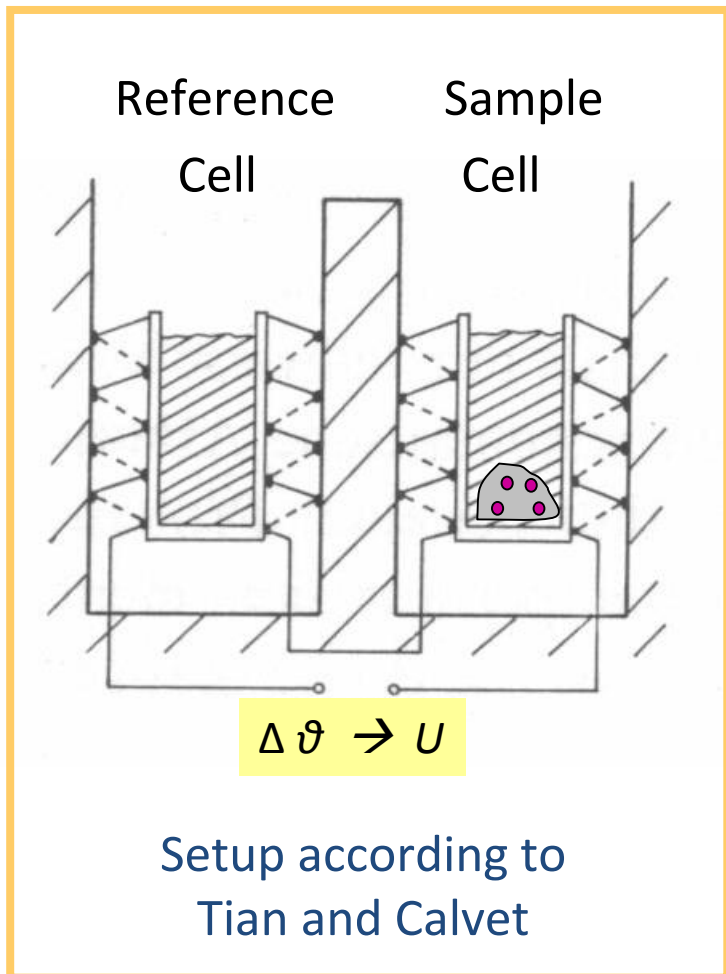


Reference cell

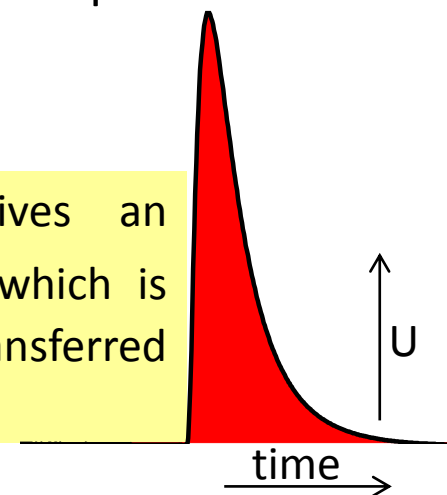
The calorimetric block consists of a sample cell and a reference cell.

The reference cell compensates external temperature fluctuations and it provides a good stability of the baseline.

Measurement of the temperature difference $\Delta \vartheta$



The heat-flow detector gives an **electrical signal "U"** which is proportional to the heat transferred per time unit.



The power P [W] necessary to heat the cell by $d\theta$ is proportional to the heat capacity C [J/K] of the cell

$$P = C \frac{d\theta}{dt}$$

The heat flow Φ [power] is proportional to the temperature gradient $\Delta\theta$ between cell and block and to the thermal conductivity G [W/K]

$$\Phi = G (\theta_{cell} - \theta_{block}) = G \Delta\theta$$

Total thermal power of calorimetric element

$$P_{total} = P + \Phi = C \frac{d\theta}{dt} + G \Delta\theta$$

The **electrical signal** is proportional to the temperature difference; (proportionality factor $g=f$ (number and type of the thermocouple))

$$U = g \Delta\theta$$

The relation between power and electrical signal is then

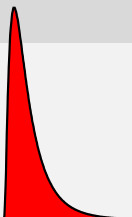
$$P_{total} = \frac{C}{g} \frac{dU}{dt} + \frac{G}{g} U$$

G [W/K] is constant and if C [J/K] can be considered constant, then C/G is a constant with units of time

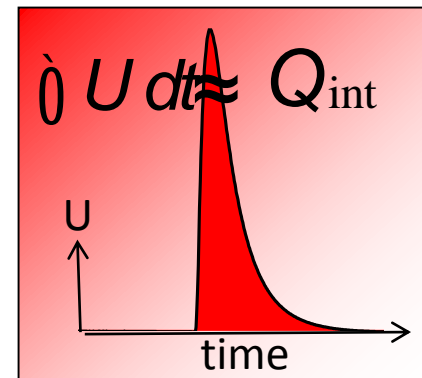
$$\tau = \frac{C}{G}$$

The **Tian equation** shows that the power is not proportional to the temperature difference, the power is delayed with respect to the signal **U** produced by the cell

$$P_{total} = \frac{G}{g} \left(U + \tau \frac{dU}{dt} \right)$$



- ◆ If heat is released in the cell for a limited period of time, e.g. through adsorption, then an **electrical signal U** with an exponential decrease is obtained .



- ◆ The integral under the curve is proportional to the evolved heat

$$Q_{\text{int}} = \frac{G}{g} \int U dt = f A$$

A: area under curve [Vs]

f: calibration factor [J/(Vs)]

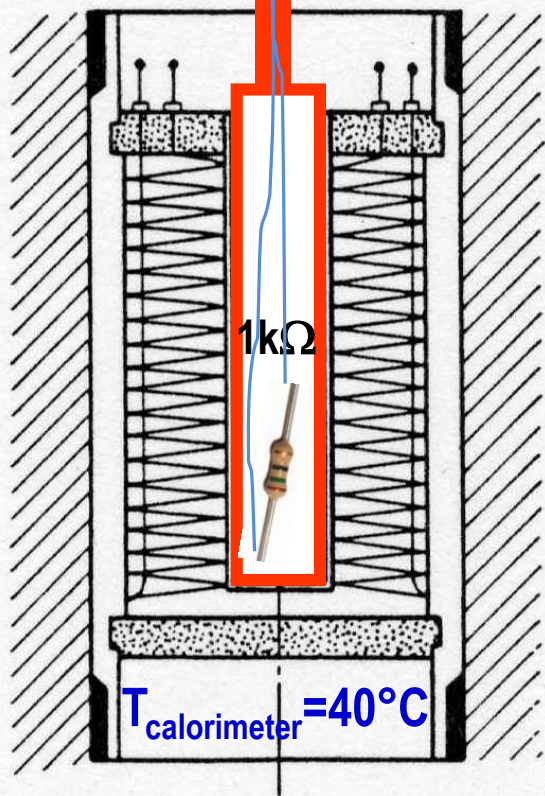
The heat signal of the calorimeter can be calibrated by:

- using an Ohm resistance which produces a certain amount of heat
- chemical reaction

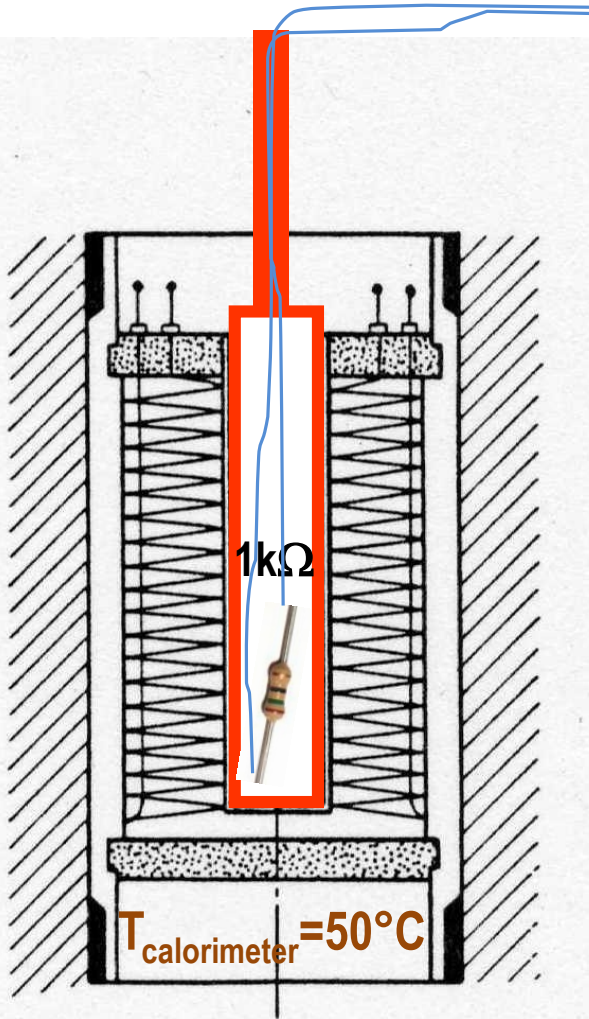
$$Q_{\text{Ohm resistance}} = U \cdot I \cdot t$$

$$f = Q_{\text{Ohm resistance}} / A_{\text{Ohm resistance}} \quad [\text{Ws/Vs}]$$

Calibration source:
Variation of voltage, current and time

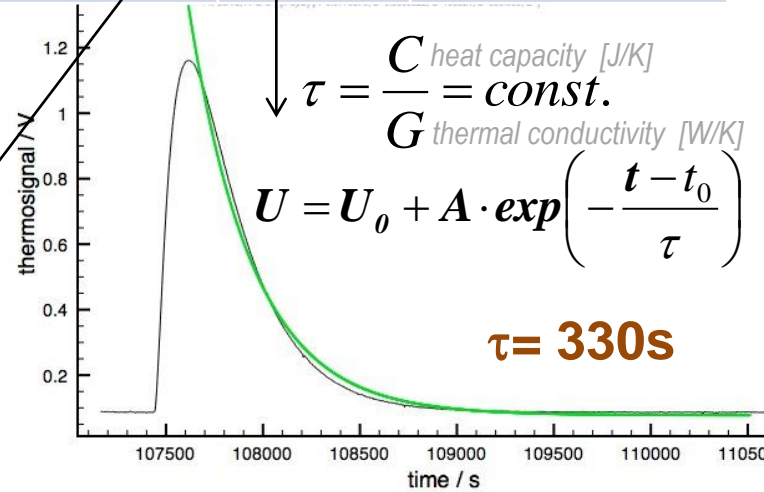
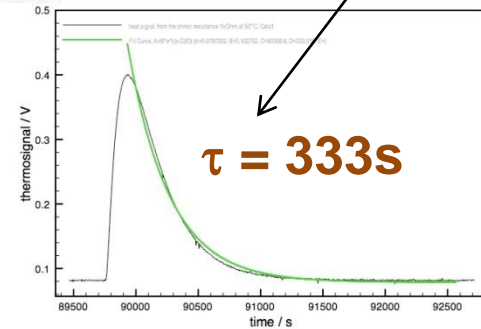
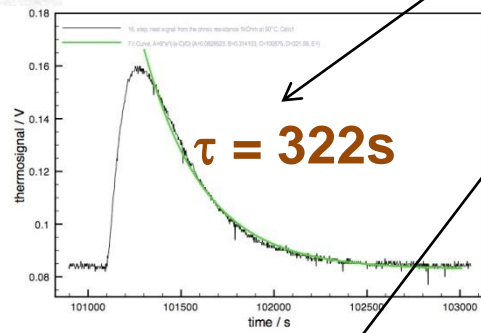


Voltage U [V]	Current I [mA]	time t [s]	Q introduced =U·I·t [mWs, mJ]	Q integral [Vs]	$f = \frac{Q_{\text{introduced}}}{Q_{\text{integral}}}$ [mJ/Vs]
3.0528	3	3	27.48	45.544	1657.64
3.0527	3	6	54.95	91.143	1658.69
10.1733	10	10	1017.33	1692.075	1663.25
3.0563	3	1	9.16	14.978	1635.30
					⋮
					f_{40°C} = 1659



Voltage U [V]	Current I [mA]	time t [s]	Q introduced =U·I·t [mWs, mJ]	Q integral [Vs]	$f = \frac{Q_{\text{introduced}}}{Q_{\text{integral}}}$ [mJ/Vs]
10.18	10	3	305.4	511.077	1673,47
2.03	2	5	20.30	34.631	1705.96
3.07	3	10	92.10	152.98	1661.02
10.17	10	3	305.10	514.63	1686.76

$f_{50^\circ\text{C}} = 1674$

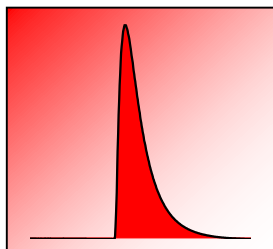


$$\tau = \frac{C \text{ heat capacity [J/K]}}{G \text{ thermal conductivity [W/K]}} = \text{const.}$$

$$U = U_0 + A \cdot \exp\left(-\frac{t-t_0}{\tau}\right)$$

$\tau_{\text{calorimeter}, 50^\circ\text{C}} = 300 - 350\text{s}$

Evolved Heat & Differential Heat of Adsorption



$$Q_{\text{int}} = \frac{G}{g} \int U dt = f A$$

A: area under curve [Vs]

f: calibration factor [J/(Vs)]

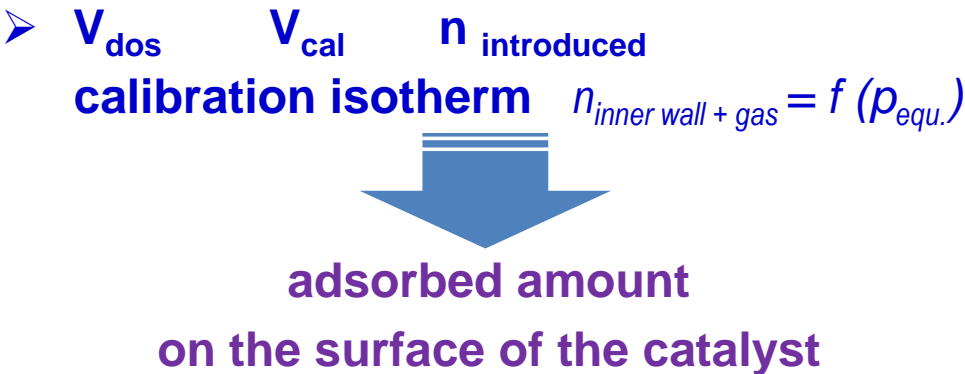
- ◆ Differential heats of adsorption as a function of coverage can be determined:

$$q_{\text{diff}} = \left(\frac{\delta Q_{\text{int}}}{\delta n} \right)_{T, V, p(\text{equ.})}$$

Calculation of the adsorbed amount

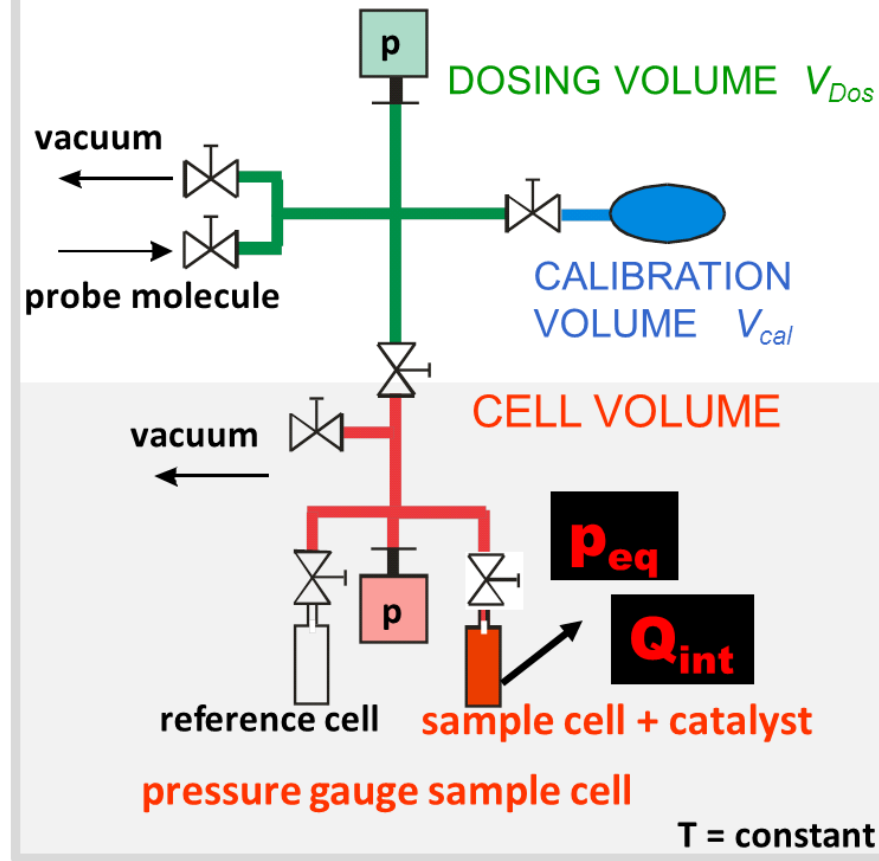
1. Introduction
2. Adsorptive microcalorimetric setup
3. Power balance of Tian-Calvet calorimeter & Evolved adsorption heat & Differential heats of adsorption
4. Volumetric-Barometric System calibration & measurement of adsorbed amount
5. Obtained physical quantities & evaluation criteria of the calorimetric results
6. Applications of microcalorimetry in heterogeneous catalysis
 - H_2 and CO adsorption on 2%Pt / Al_2O_3 at 40°C
 - NH_3 adsorption on pure-phase MoVTenb oxide at 80°C
 - CO_2 ads. on CeO_2 at 40°C
 - O_2 adsorption on supported CeO_2 at 200°C
 - Ethanol adsorption on $VO_x/\gamma-Al_2O_3$ at 40°C
 - Propane ads. On MoVTenb oxide at 40°C
 - Propylene adsorption on $MoO_x/SBA-15$ at $T_{reaction}=50^\circ C$
 - 1-Hexyne ads. on CeO_2/TiO_2 at $T_{reaction}=80^\circ C$

- adsorption via **stepwise dosing** of **probe molecule into the sample cell**
- Q_{int} , p , T are measured
- $q_{diff} = \Delta H_{cond} \rightarrow$ saturation of the surface
- The probe molecule is distributed into three partitions:
gas phase, wall adsorption, sample adsorption

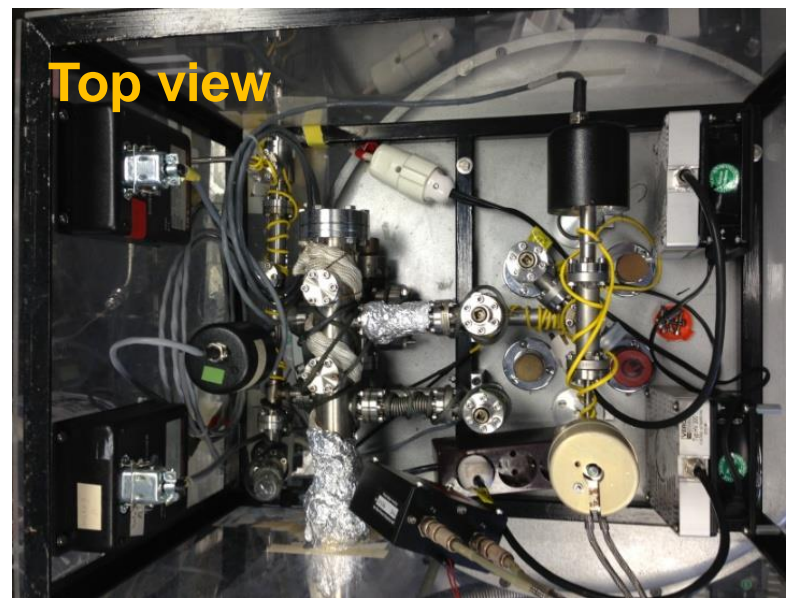
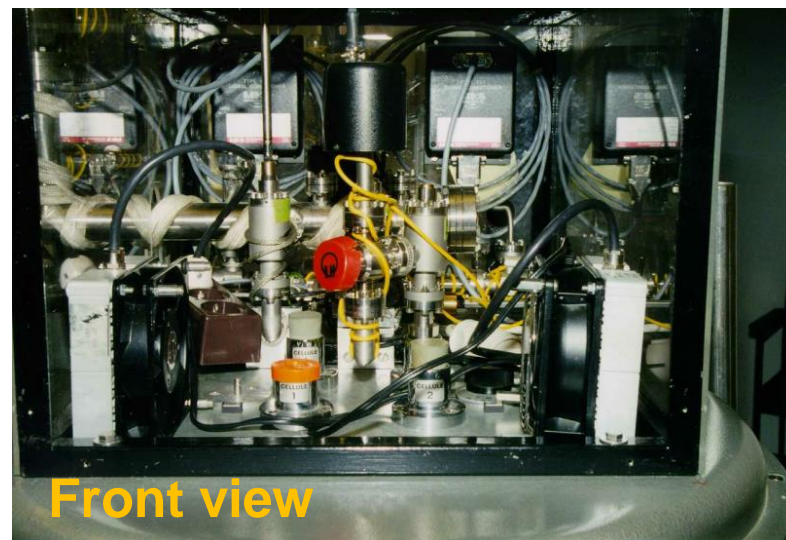
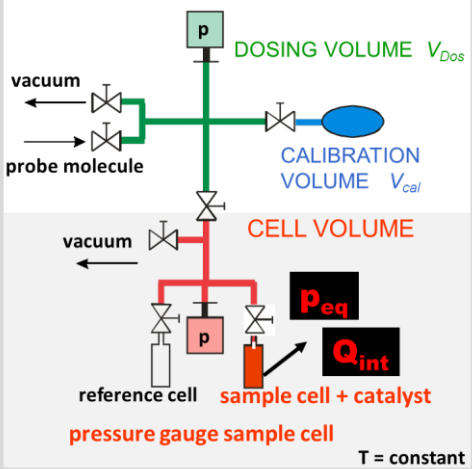


Volumetric-barometric system

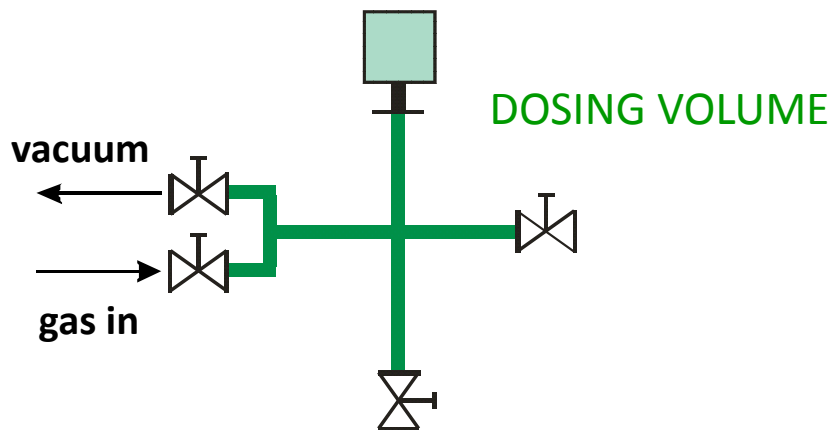
pressure gauge dosing system



pressure gauge dosing system



pressure gauge dosing system



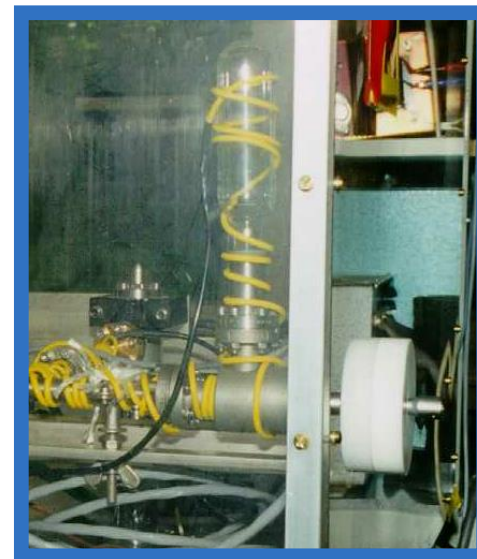
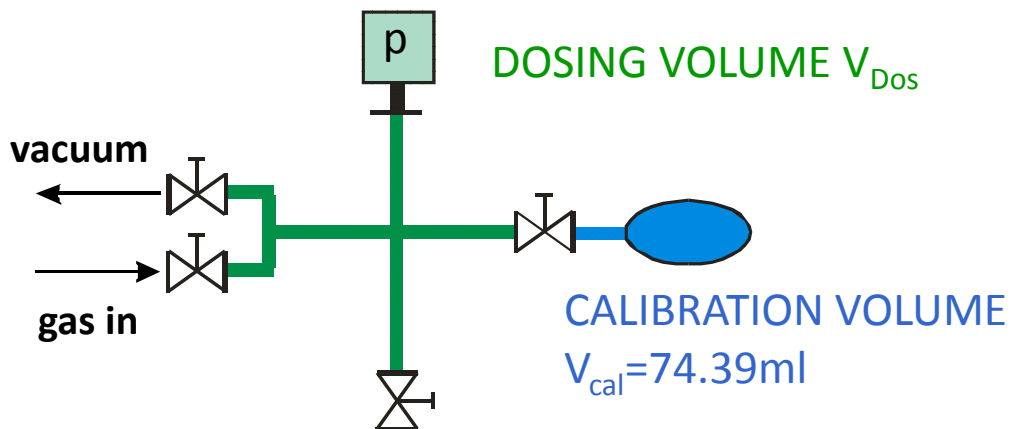
- ❖ p, T can be easily measured
- ❖ V needs to be determined

Volume Calibration

An unknown **volume** of any shape can then be determined through expansion from gas (*an ideal gas that does not stick much to the walls*) from one volume to the other and pressure measurement before and after the equilibration.

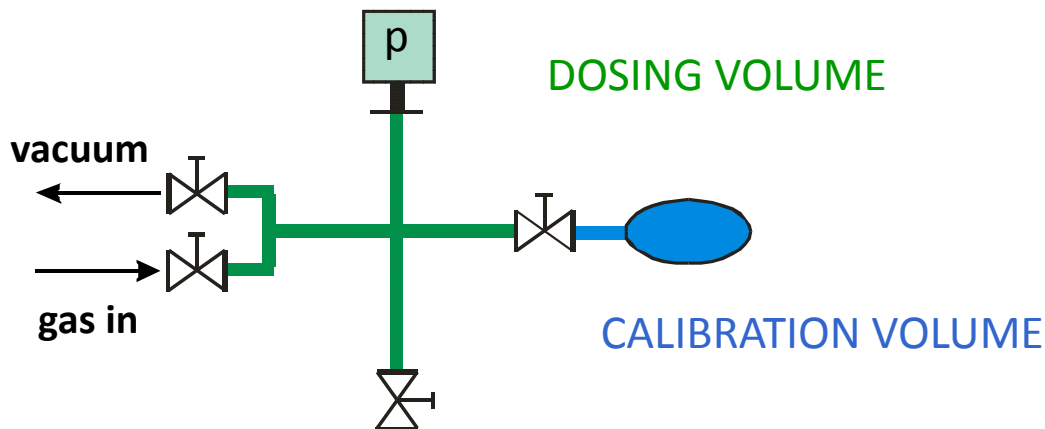
Calibrating the Dosing Volume

pressure gauge dosing system



- ❖ fill V_{Cal} and V_{Dos} , same pressure
- ❖ close valve between V_{Cal} and V_{Dos}
- ❖ set pressure in V_{dos} to p_{Dos}
- ❖ open valve, equilibrate

pressure gauge dosing system



❖ Initial situation:

$$nRT = p_{Cal} V_{Cal} + p_{Dos} V_{Dos}$$

❖ After opening valve:

$$nRT = p_{fin} (V_{Cal} + V_{Dos})$$

❖ n, T are constant

$$V_{Dos} = \frac{p_{Cal} - p_{fin}}{p_{fin} - p_{Dos}} V_{Cal}$$

Example Data

Propane at 40°C

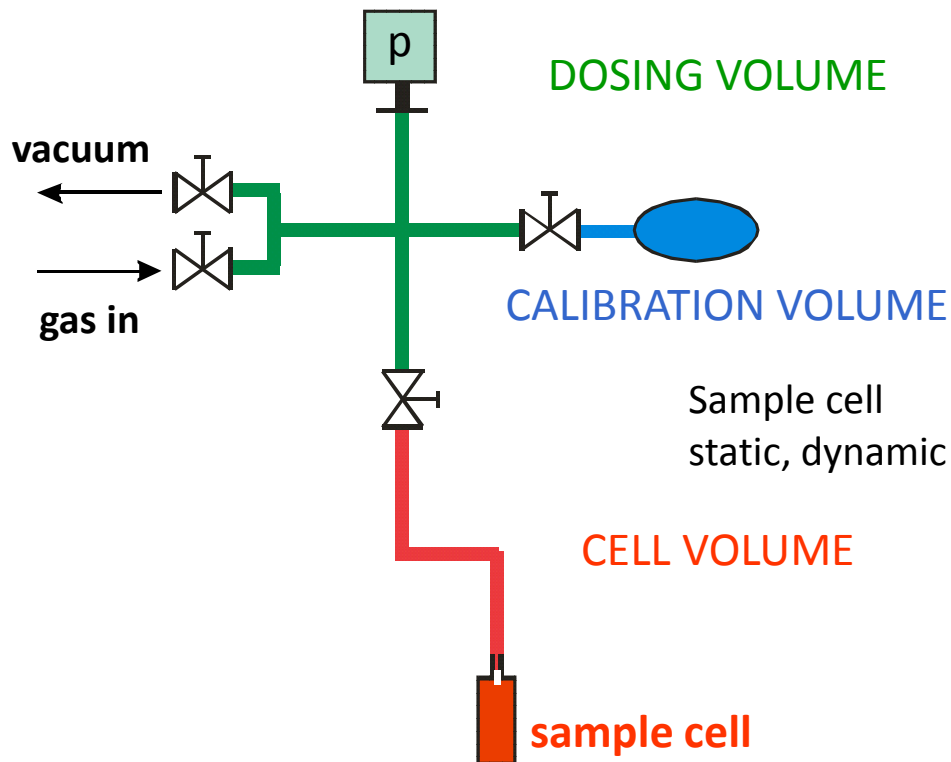
(Project: $V_xO_y/SBA15$ for ODH of propane)

Nr	p_{Cal} [mbar]	p_{Dos} [mbar]	p_{fin} [mbar]	V(Dos) [ml]
	before	before	after equilibration	
1	5,314	9,467	8,683	137
2	8,683	7,648	7,843	137
3	7,638	6,341	6,585	137
4	6,585	4,768	5,111	137
5	5,111	4,712	4,787	137
6	4,786	3,197	3,496	137
7	3,469	2,701	2,846	136

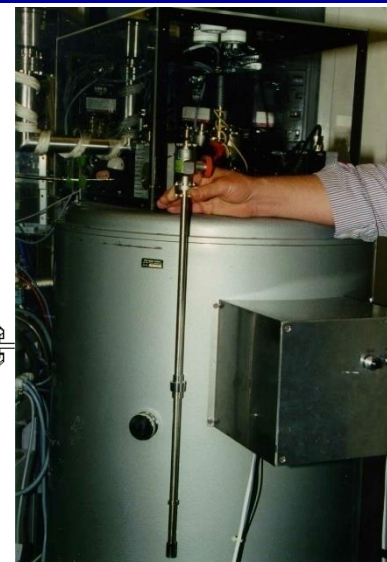
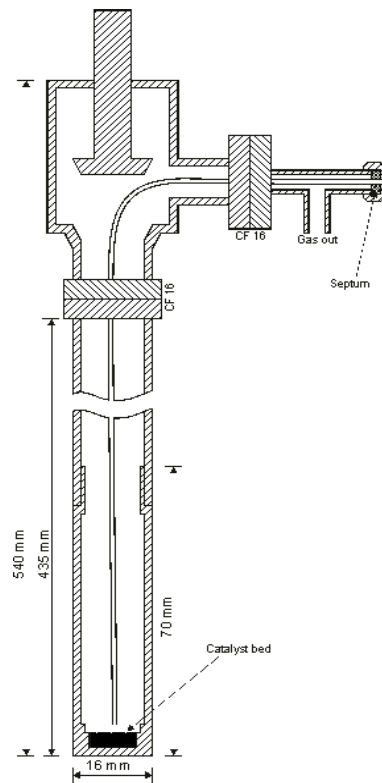
$$V_{Dos} = \frac{p_{Cal} - p_{fin}}{p_{fin} - p_{Dos}} V_{Cal}$$

- ❖ It is important that the entire system is at the same constant temperature!

pressure gauge dosing system



Sample cell
static, dynamic



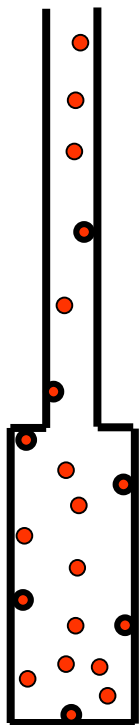
sample holder
L = 70 mm
Ø = 15 mm

$$n_{int,i} = \frac{(p_{Dos,bef} - p_{Dos,aft})V_{Dos}}{RT}$$

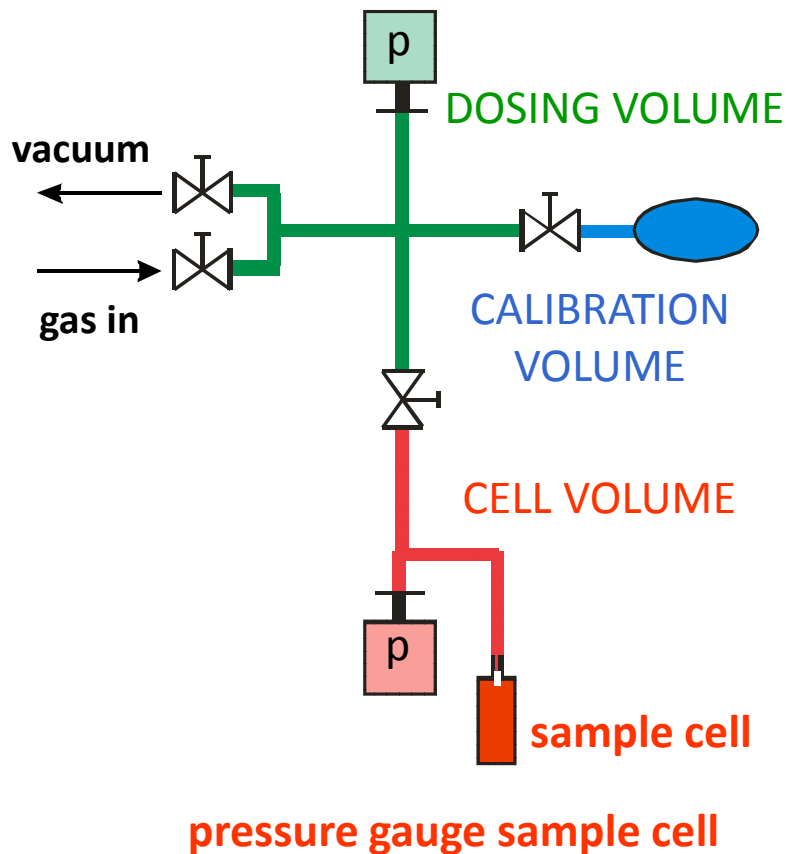
- ❖ Total number of molecules accumulated in cell

$$n_{SC,tot,i} = \sum_i n_{int,j} = n_{SC,tot,i-1} + n_{int,j}$$

- ❖ i.e. the sum of
 - the number of molecules already in the cell
 - the number of molecules introduced in the i^{th} step

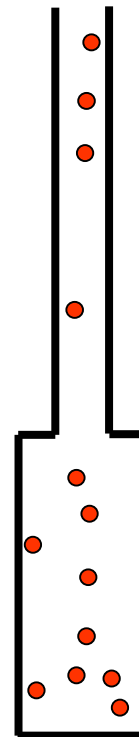


- Molecules are in the gas phase but also adsorbed on the inner wall surface
- Only the gas phase molecules contribute to the measured pressure
- The number of molecules adsorbed on the walls depends on the pressure
→ wall adsorption isotherm



- ❖ Measure the pressure in the cell as a function of the total number of molecules introduced into the cell
- ❖ **Without wall adsorption and without sample**, the relation between pressure and number of molecules in the sample cell would be given by the ideal gas law

$$p_{SC,i} = \frac{n_{SC,tot,i}RT}{V_{SC}}$$

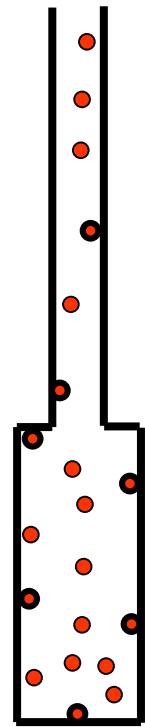


- ❖ With wall adsorption and with or without a sample, the relation between number of molecules in the gas phase + on the walls and the pressure can be written as a polynomial expression

$$n_{SC,w+g,i} = a(p_{SC,i}) - b(p_{SC,i})^2 + c(p_{SC,i})^3 - d(p_{SC,i})^4 \dots$$

- ❖ Without a sample, the coefficients can be determined

$$n_{SC,w+g,i} = n_{SC,tot,i}$$



Nr	$p_{D_{os,bef}}/mbar$	$p_{D_{os,aft}}/mbar$	$p_{SC,i}/mbar$	$n_{int,i}/\mu mol$	$n_{SCtot,i}/\mu mol$
1	9,682	9,674	0,007	0,04	0,04
2	9,653	9,641	0,026	0,06	0,10
3	9,607	9,591	0,054	0,08	0,18
4	9,562	9,544	0,081	0,09	0,27
5	9,499	9,481	0,117	0,09	0,36
6	9,442	9,428	0,147	0,07	0,43
7	9,392	9,371	0,181	0,11	0,54
9	9,230	9,195	0,283	0,18	0,72
10	9,128	9,091	0,344	0,19	0,91
11	9,024	8,988	0,403	0,19	1,10
13	8,814	8,758	0,537	0,29	1,39
14	8,644	8,582	0,640	0,32	1,71
15	8,466	8,386	0,755	0,42	2,13
16	8,209	8,122	0,909	0,45	2,58
17	7,783	7,612	1,208	0,90	3,48
19	6,672	6,487	1,870	0,97	3,45
20	5,893	5,526	2,436	1,93	5,38
21	4,477	4,041	3,314	2,30	7,68
22	9,146	8,409	4,056	3,88	11,56

Isobutane at 40°C

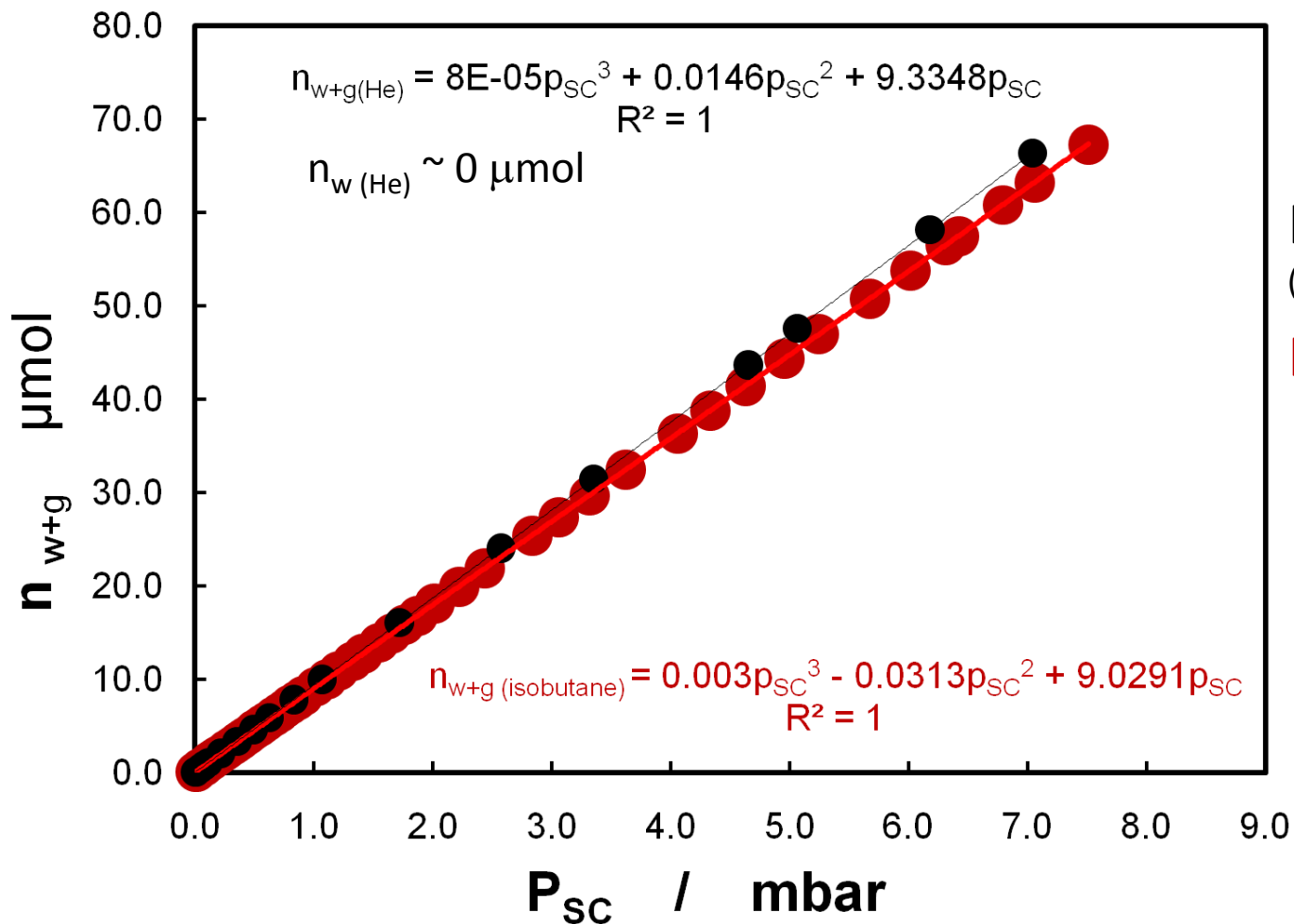
without catalyst

(Project:
isomerisation of
n-butane to isobutane
over sulf. ZrO₂)

$$n_{int,j} = \frac{(p_{D_{os,bef}} - p_{D_{os,aft}})V_{D_{os}}}{RT}$$

$$n_{SC,tot,i} = \sum_i n_{int,i} = n_{SC,tot,i-1} + n_{int,i}$$

Correction for Wall Adsorption

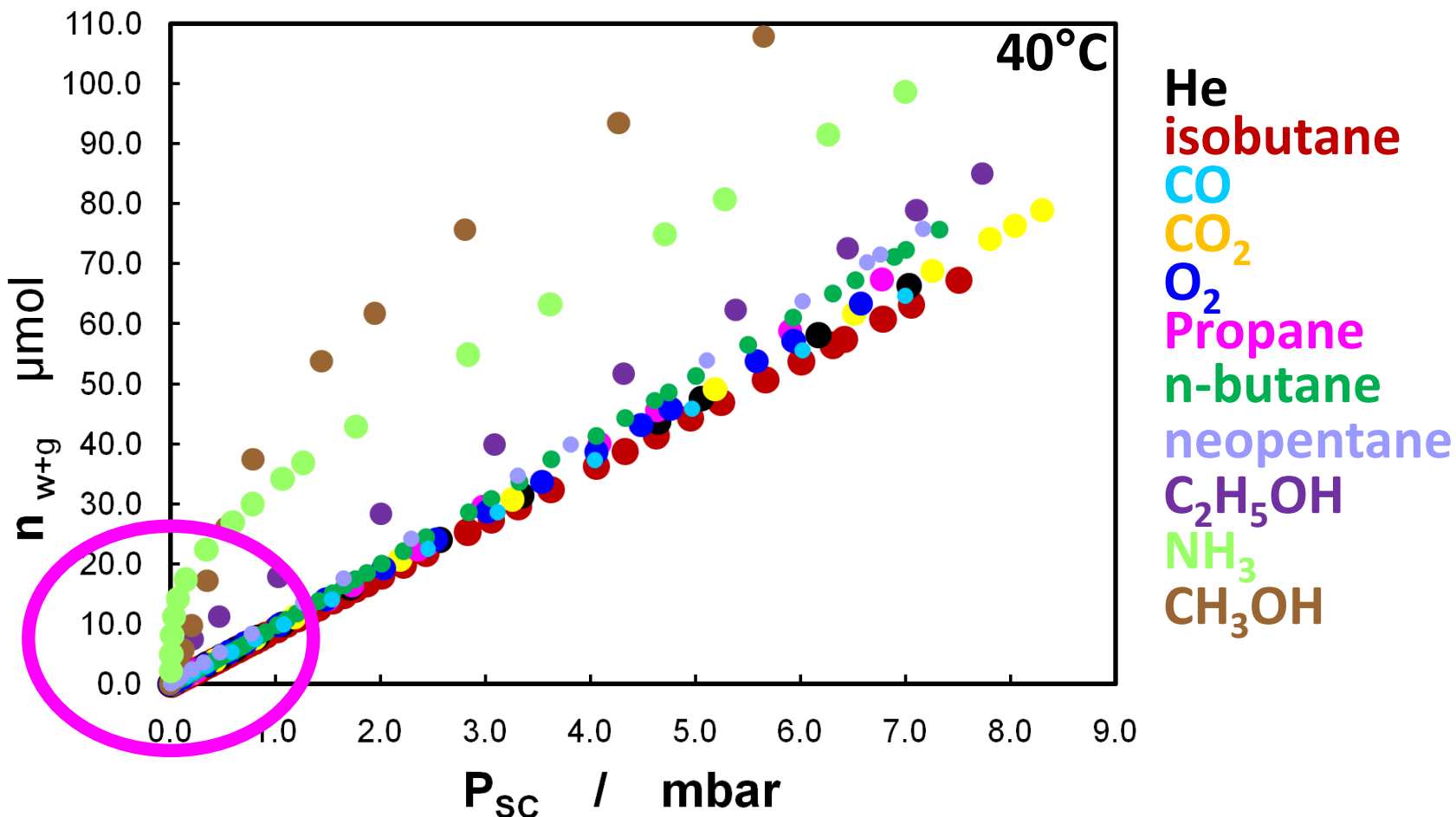


He @ 40°C

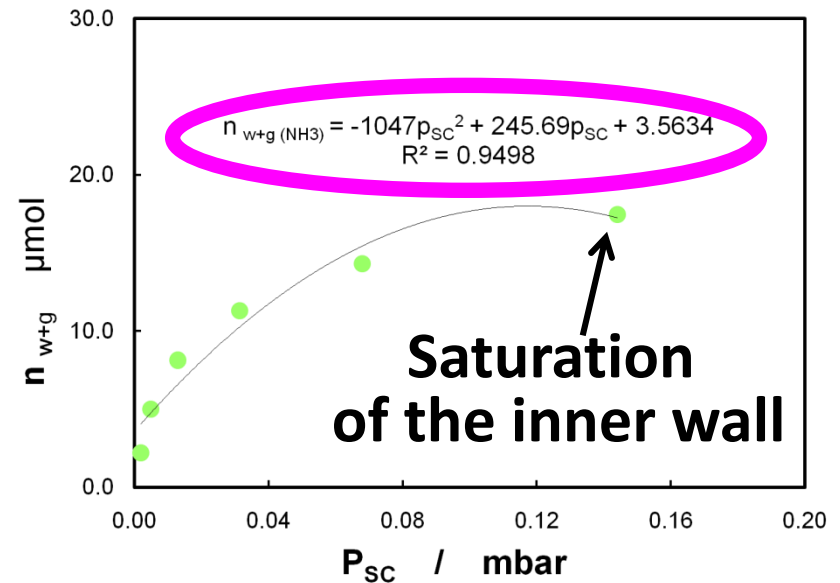
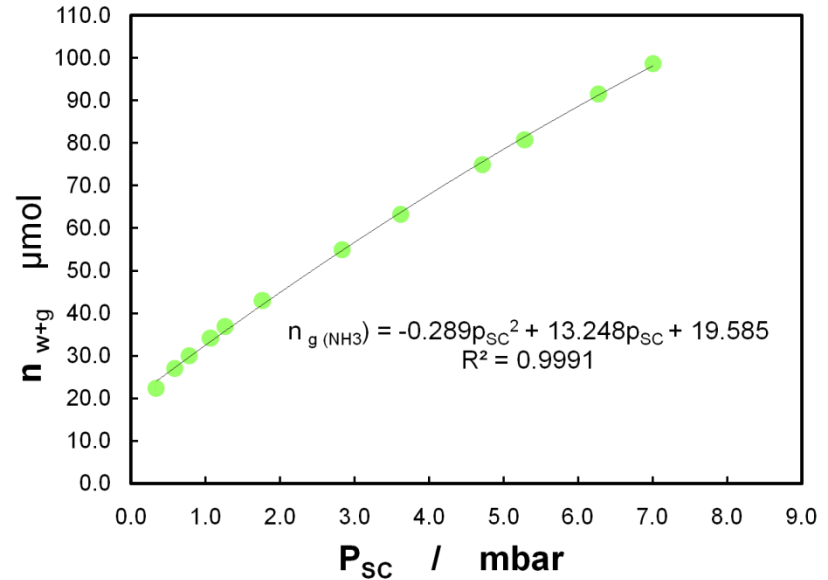
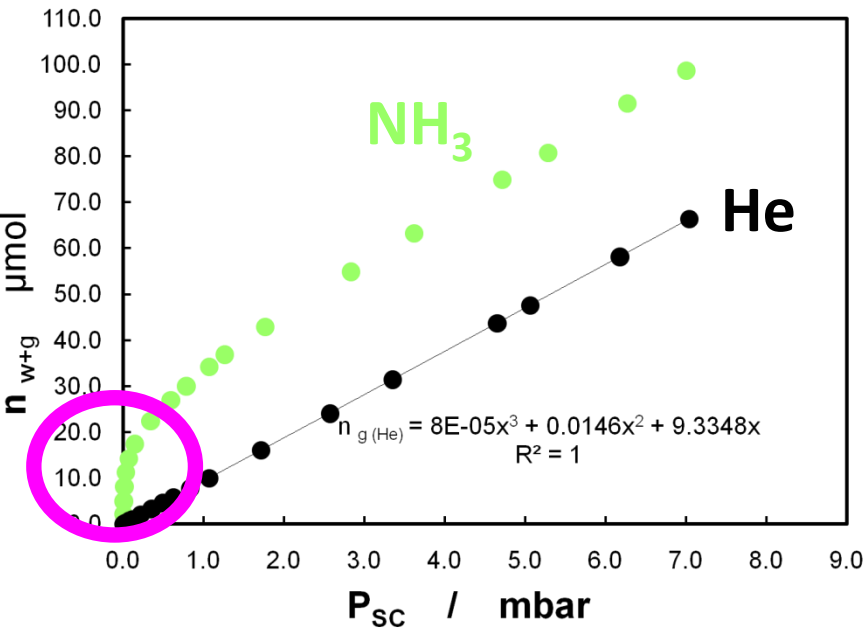
(does not stick to the walls)

Isobutane @ 40°C

- The adsorption of isobutane on the walls is insignificant



- The adsorption of e.g. C₂H₅OH NH₃ CH₃OH on the walls is significant

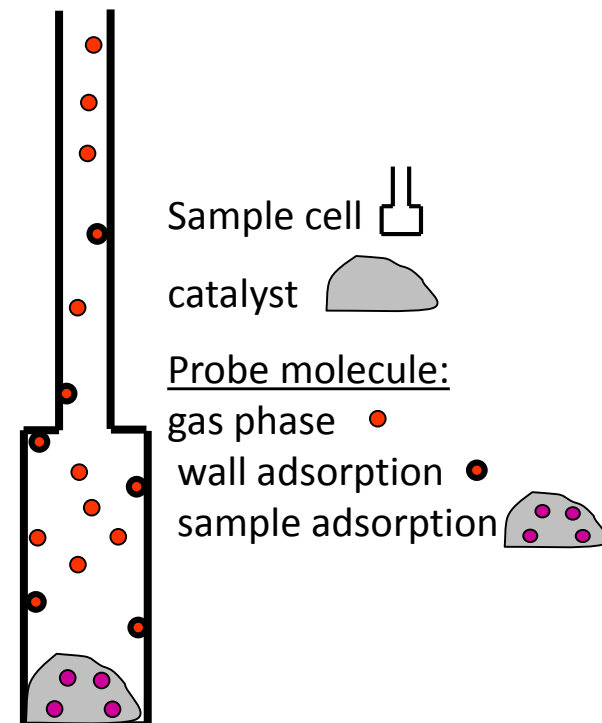


- ❖ Total number of molecules in sample cell after the i^{th} step

$$n_{SC,tot,i} = n_{ads,tot,i} + n_{SC,w+g,i}$$

- ❖ Total number of molecules in sample cell after the $(i+1)^{\text{th}}$ step

$$n_{SC,tot,i+1} = n_{ads,tot,i} + n_{SC,w+g,i} + n_{ads,i+1} + n_{SC,w+g,i+1}$$



- ❖ The difference in number of molecules between i^{th} and $(i+1)^{\text{th}}$ step is the number of molecules introduced in the $(i+1)^{\text{th}}$ step

- ❖ The number of molecules adsorbed in the $(i+1)^{\text{th}}$ step is then

$$n_{ads,i+1} = n_{int,i+1} + n_{SC,w+g,i} - n_{SC,w+g,i+1}$$

- ❖ The total number of molecules adsorbed after $(i+1)$ steps is

$$n_{ads,tot,i+1} = n_{ads,tot,i} + n_{ads,i+1}$$

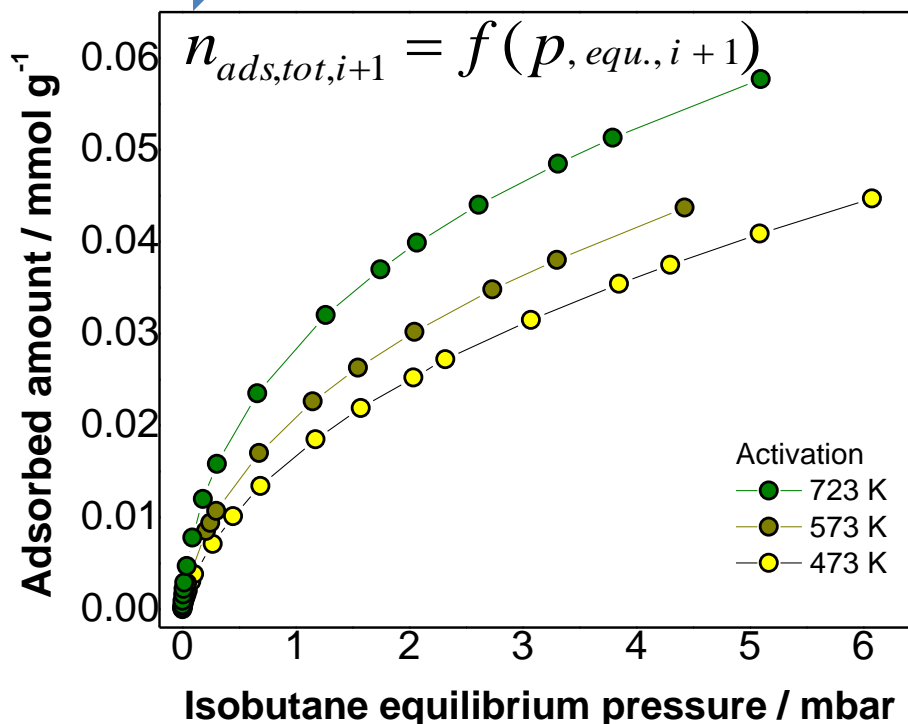


Adsorption isotherm

Isobutane adsorption on different activated sulf. ZrO_2 at $40^\circ C$.

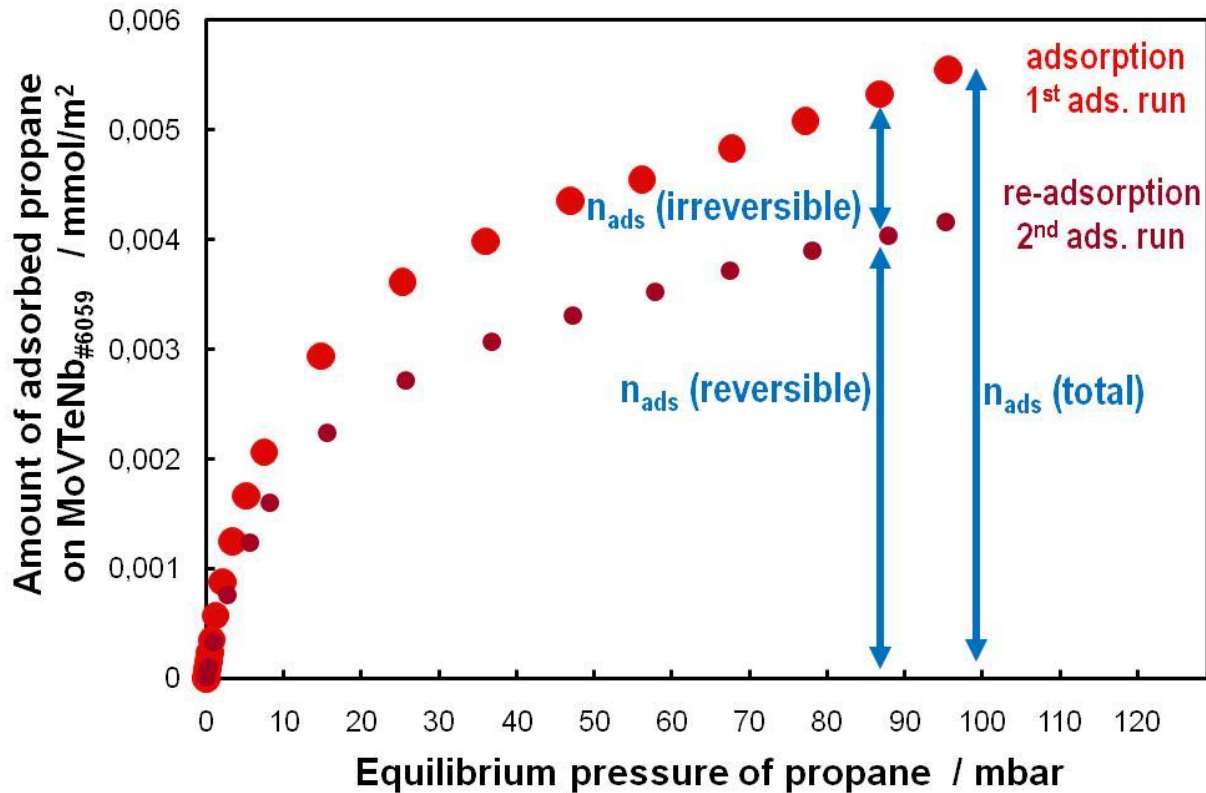
(Project: isomerisation of n-butane to isobutane over sulf. ZrO_2)

[S. Wrabetz, F.C. Jentoft et al, J. Catal. 269 (2010) 351-358.]



1. Introduction
2. Adsorptive microcalorimetric setup
3. Power balance of Tian-Calvet calorimeter & Evolved adsorption heat & Differential heats of adsorption
4. Volumetric-Barometric System calibration & measurement of adsorbed amount
5. Obtained physical quantities & evaluation criteria of the calorimetric results
6. Applications of microcalorimetry in heterogeneous catalysis
 - H_2 and CO adsorption on 2%Pt / Al_2O_3 at 40°C
 - NH_3 adsorption on pure-phase MoVTeNb oxide at 80°C
 - CO_2 ads. on CeO_2 at 40°C
 - O_2 adsorption on supported CeO_2 at 200°C
 - Ethanol adsorption on $VO_x/\gamma-Al_2O_3$ at 40°C
 - Propane ads. On MoVTeNb oxide at 40°C
 - Propylene adsorption on $MoO_x/SBA-15$ at $T_{reaction}=50^\circ C$
 - 1-Hexyne ads. on CeO_2/TiO_2 at $T_{reaction}=80^\circ C$

Adsorption Isotherm - $n_{\text{ads}} = f(p_{\text{equ.}})$

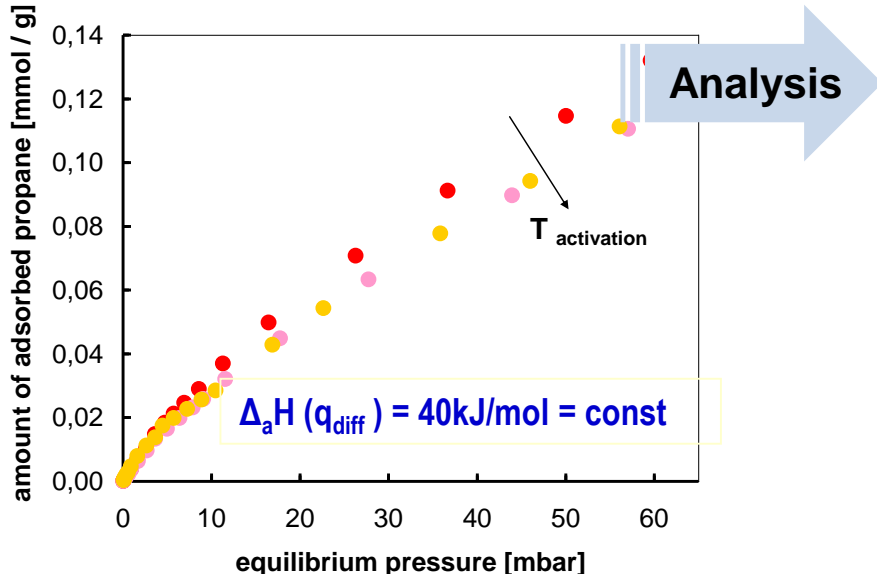


$n_{\text{ads}}(\text{total})$: overall adsorbed amount under an equilibrium pressure of 95 mbar

$n_{\text{ads}}(\text{irrev.})$: chemisorbed amount

Adsorption Isotherm

of propane on 10%V/SBA15 catalyst active in oxidation of propane



Langmuir model: The enthalpy of adsorption $\Delta_a H$ per site is constant with coverage Θ

➤ Langmuir model for dissociative adsorption

$$\theta_H = \frac{n_{ads}}{n_m} = \frac{\sqrt{p_{H_2} K_{ads}}}{1 + \sqrt{p_{H_2} K_{ads}}}$$
e.g., dissociative ads. of H_2 on Pt supported on Al_2O_3 at $40^\circ C$

➤ Higher order Langmuir model

$$N_{ads} = \frac{N_{mono} (Kp)^{\frac{1}{n}}}{1 + (Kp)^{\frac{1}{n}}}$$
e.g., activated ads. of n-butane (educt) on sulf. ZrO_2 at $40^\circ C < T_{reaction} = 60^\circ C$
[S. Wrabetz et al., Catal. 2010, 269, 351–358.]

➤ Langmuir model $\theta = \frac{Kp}{1 + Kp}$

Freundlich isotherm:

The enthalpy of adsorption $\Delta_a H$ per site decreases exponential with coverage Θ

$$N_{ads} = \frac{A p^{\frac{1}{n}}}{1 + A p^{\frac{1}{n}}}$$

Tempkin isotherm: The enthalpy of adsorption $\Delta_a H$ per site decreases linear with coverage Θ

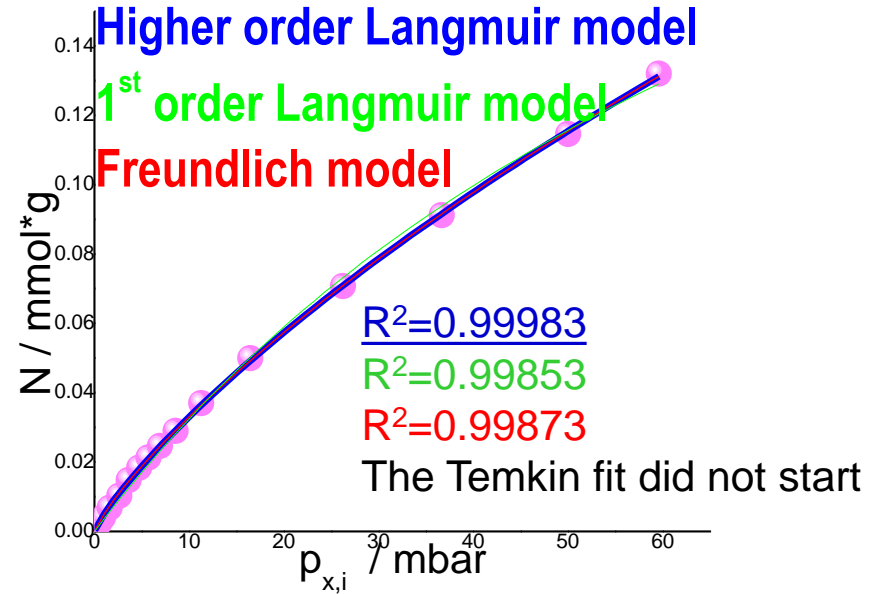
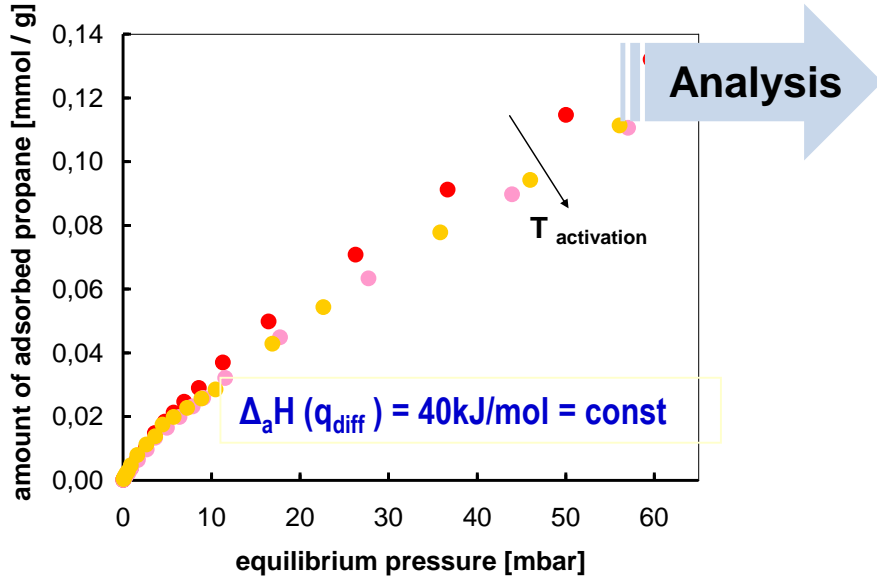
$$\theta = \frac{RT}{q_{ads}^{(\theta=0)} - q_{ads}^{(\theta=1)}} \ln \left(\frac{1 + \frac{p}{p^*} \exp \frac{q_{ads}^{(\theta=0)}}{RT}}{1 + \frac{p}{p^*} \exp \frac{q_{ads}^{(\theta=1)}}{RT}} \right)$$

e.g., propane adsorption (313 K) on the oxygen surface groups of CNT and B_2O_3 -CNT catalysts used in ODH of propane [B. Frank, S. Wrabetz et al., ChemPhysChem 2011, 12, 2709 – 2713]

CO Adsorption on supported Gold nanoparticle catalysts [Ch. J. Pursell et al., J. Phys. Chem.C, 2012, 116(20),11117]

Adsorption Isotherm

of propane on 10%V/SBA15 catalyst active in oxidation of propane



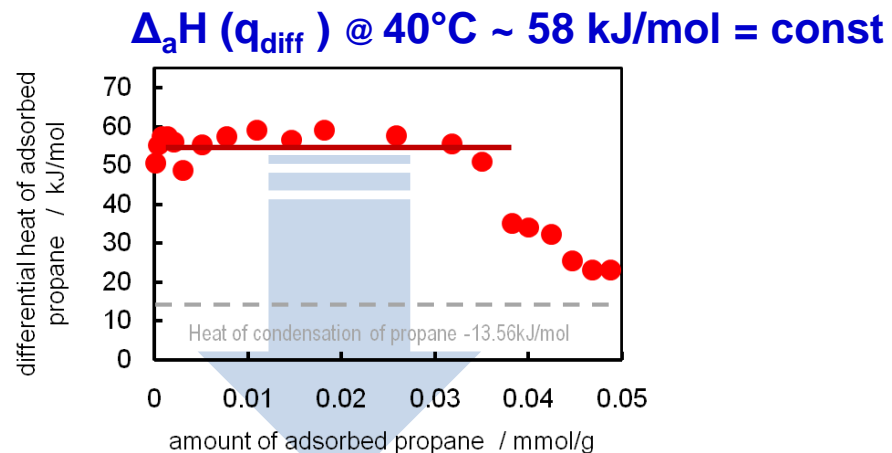
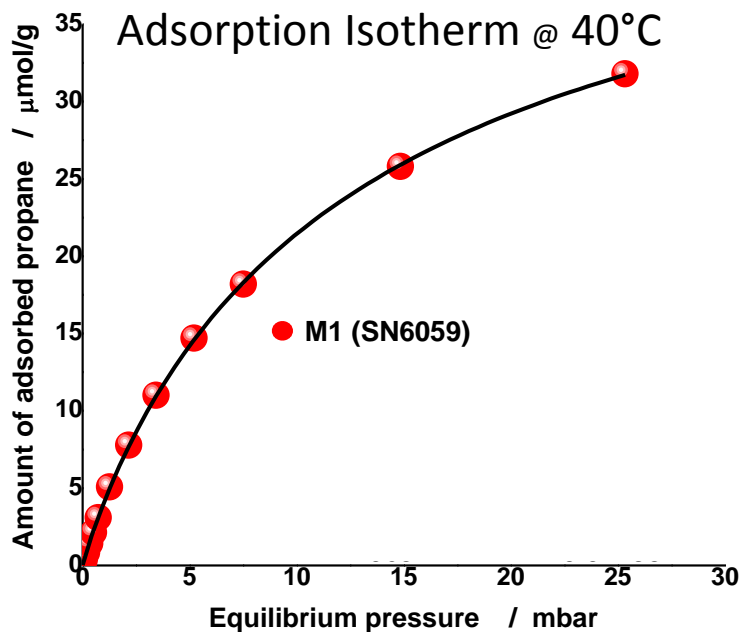
Specific surface area = N_{mono} * Avogadro constant * $S_{1:1, \text{ assumed}}$ * cross-section area 39\AA^2 for propane
 [A. L. McClellan et al., J. of Colloid and Interface Science, 23 (1967) 577]

$$N_{\text{ads}} = \frac{N_{\text{mono}} (Kp)^{\frac{1}{n}}}{1 + (Kp)^{\frac{1}{n}}}$$

n = 1 non-activated ads.
n > 1 activated ads.

10%V/SBA15 dehydration temperature	N_{mono} $\mu\text{mol} * \text{g}^{-1}$	n	R^2	S_{propane} $\text{m}^2 * \text{g}^{-1}$	BET S_{N_2} $\text{m}^2 * \text{g}^{-1}$
373 K	0.9 (2)	1.20 (2)	0.99983	226 (10)	329 (4)
573 K	1.3 (4)	1.22 (2)	0.99982	304 (10)	
673 K	1.2 (3)	1.22 (2)	0.99905	290 (10)	

Propane adsorption on **pure-phase M1** catalyst (MoVTenb oxide #6059) active in selective oxidation of propane



$$N_{ads} = \frac{N_{mono} (Kp)^{\frac{1}{n}}}{1 + (Kp)^{\frac{1}{n}}}$$

Langmuir model for activated ads.:
The enthalpy of adsorption $\Delta_a H$ per site is constant with coverage Θ

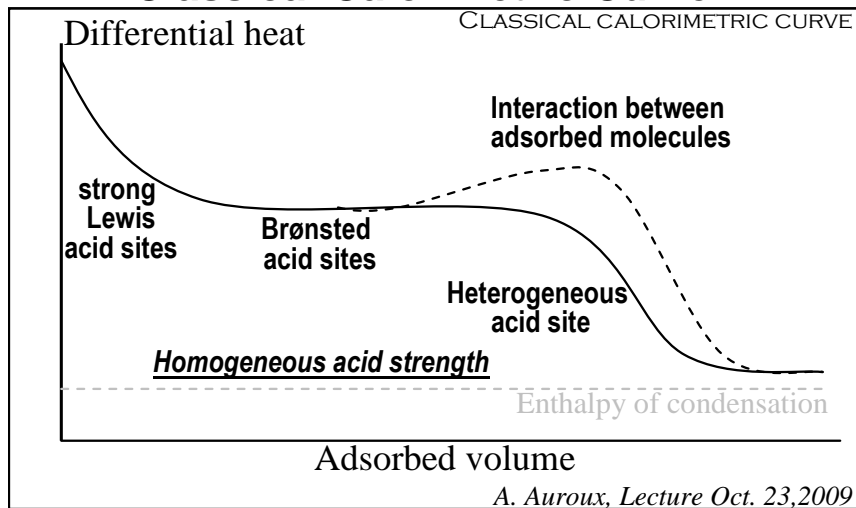
Specific surface area = $N_{mono} * \text{Avogadro constant} * S_{1:1, \text{assumed}} * \text{cross-section area}$ 39 \AA^2 for propane
[A. L. McClellan et al., J. of Colloid and Interface Science, 23 (1967) 577]

Catalyst (ID)	$N_{monolayer}$ $\mu\text{mol} * \text{g}^{-1}$	R^2	$S_{propane}$ $\text{m}^2 * \text{g}^{-1}$ $A_{propane} \sim 39 \text{ \AA}^2$	BET $\text{m}^2 * \text{g}^{-1}$ $A_{N_2} = 16.2 \text{ \AA}^2$
M1 (5630)	34.9 (2)	0.99951	8.2 (1)	6.6
M1 (6059)	48.5 (8)	0.99991	11.3 (1)	8.8
M1 (5737)	42.3 (8)	0.99986	9.9 (1)	13.4

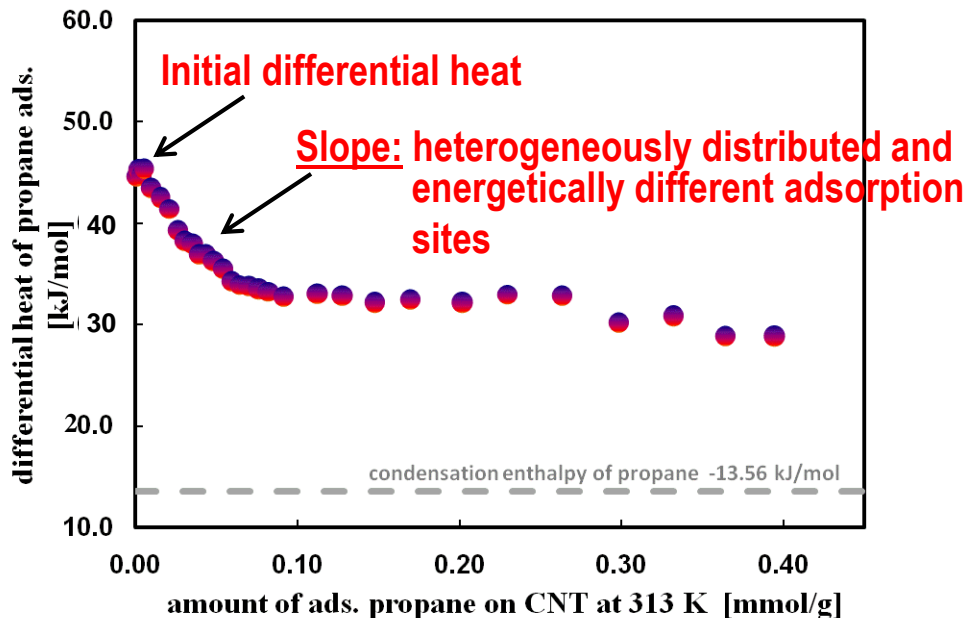
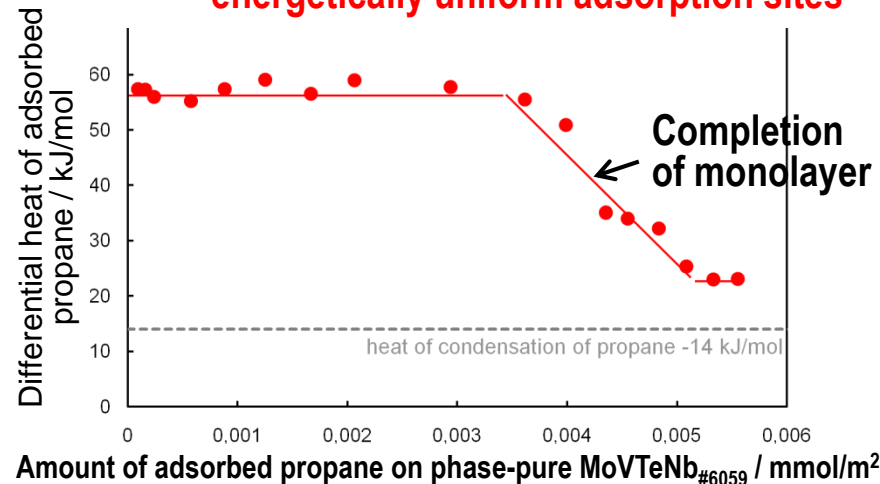
N_{ads} - coverage with certain equilibrium pressure
 N_{mono} - monolayer coverage

p - equilibrium pressure
 n - adsorption order
 K/A - adsorption equilibrium constant
 R^2 - correlation coefficient; goodness of fit
 S - stoichiometry

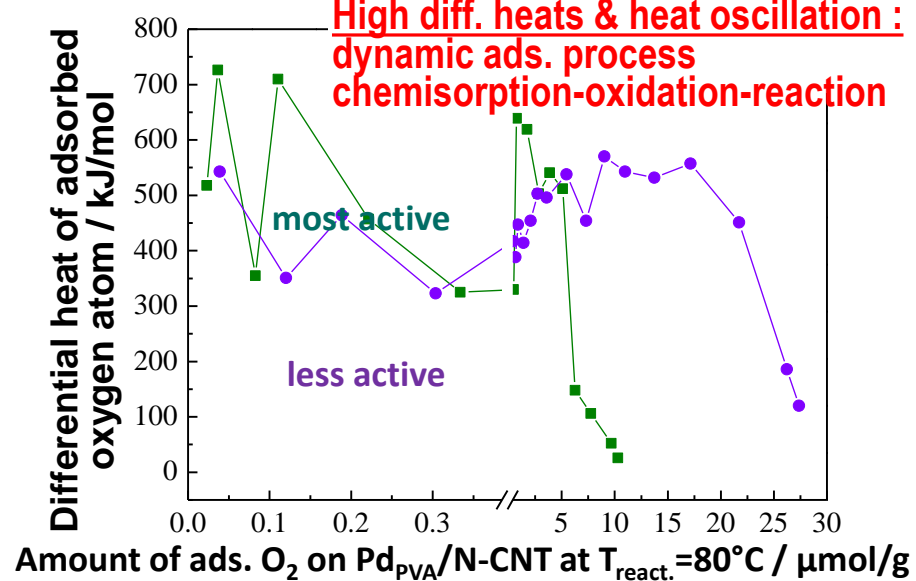
Classical Calorimetric Curve



Plateau: homogeneously distributed and energetically uniform adsorption sites

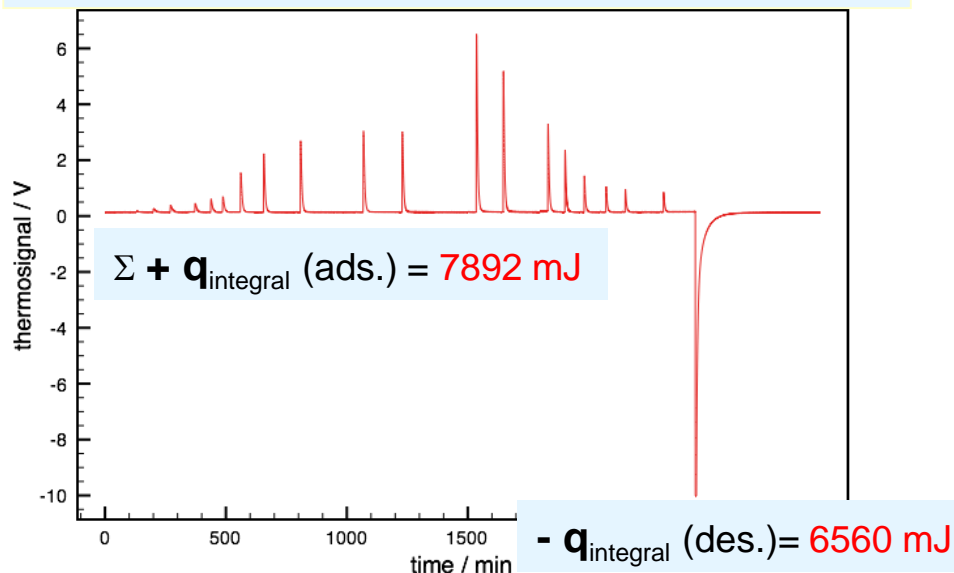


High diff. heats & heat oscillation : dynamic ads. process chemisorption-oxidation-reaction



Integral heat signal of adsorption and desorption

stepwise adsorption of propane on MoVTaNb oxide at 40°C



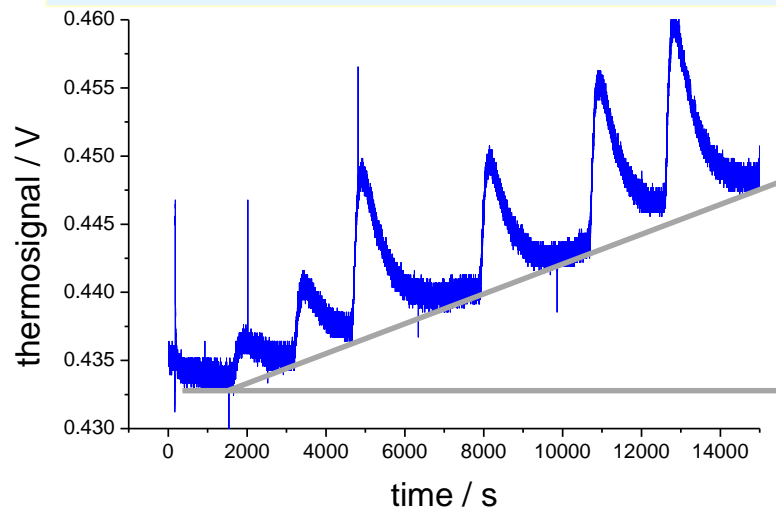
$\Sigma q_{\text{int}} (\text{ads.}) > q_{\text{int}} (\text{des.}) \rightarrow$ partially irreversible ads.;
activated ads. process

$\Sigma q_{\text{int}} (\text{ads.}) < q_{\text{int}} (\text{des.}) \rightarrow$ instability of the catalyst
in the presence of probe molecule

$\Sigma q_{\text{int}} (\text{ads.}) = q_{\text{int}} (\text{des.}) \rightarrow$ reversible ads. process

Background of the thermo signal during the stepwise adsorption

stepwise n-butane ads. on sulf. ZrO₂
at 40°C < 60°C = T_{reaction}



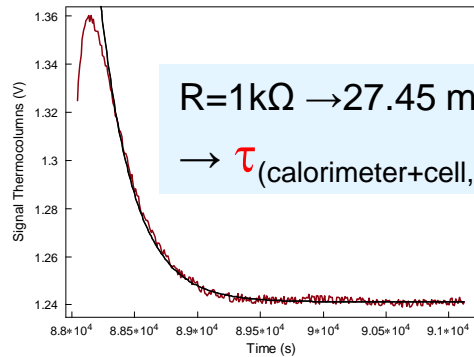
Heat signal deviates from the base-line

\rightarrow Adsorption process is accompanied by secondary processes
e.g. during n-butane ads. a partial isomerization of n-butane to isobutane in the calorimeter cell was observed

Determination of the time constant τ of the integral heat signal

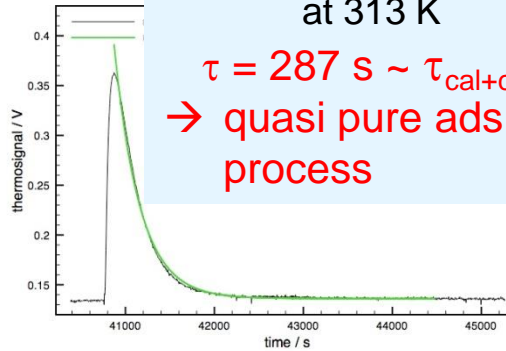
$$\frac{\text{heat capacity } C}{\text{thermal conductivity } G}$$

$$y = y_0 + A \cdot \exp\left(-\frac{x - x_0}{\tau}\right)$$



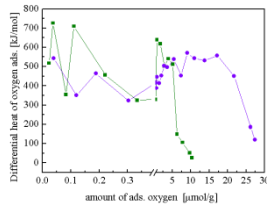
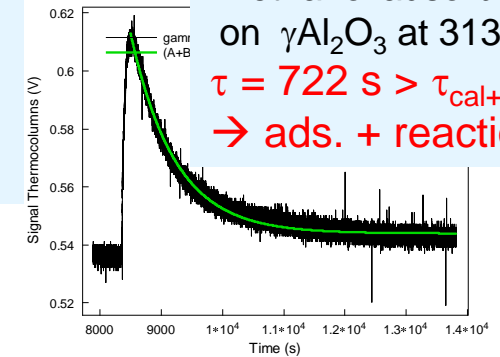
5.9 $\mu\text{mol/g}$ propylene adsorbed on MoVTeNb at 313 K

$\tau = 287\text{ s} \sim \tau_{\text{cal+cell}}$
 \rightarrow quasi pure ads. process



4.8 $\mu\text{mol/g}$ methanol adsorbed on $\gamma\text{Al}_2\text{O}_3$ at 313 K

$\tau = 722\text{ s} > \tau_{\text{cal+cell}}$
 \rightarrow ads. + reaction



Shape of the integral heat signal O_2 adsorption on 2%Pd/N-CNT473K at $353\text{K}=T_{\text{reaction}}$

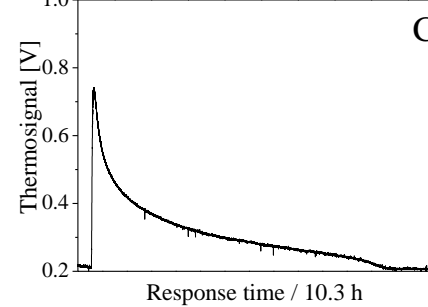
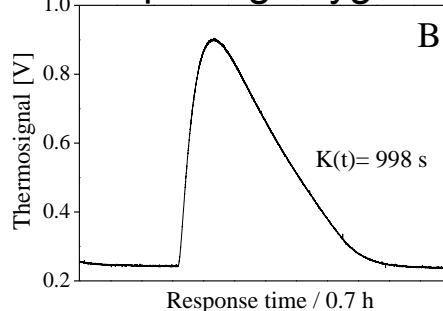
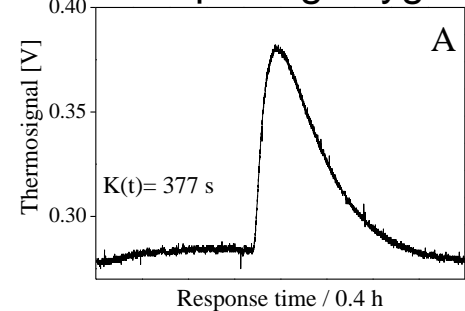
At low coverage quasi pure oxygen chemisorption on Pd

At higher coverage oxygen chemisorption is accompanied by dissociative secondary processes

0.039 $\mu\text{mol/g}$ oxygen

2 $\mu\text{mol/g}$ oxygen

14 $\mu\text{mol/g}$ oxygen



6. Applications of microcalorimetry in heterogeneous catalysis

Specific surface area of Pt:

H₂ and CO ads. on 2%Pt/Al₂O₃ at 40°C

Titration of acid or basic surface sites:

- *NH₃ ads. on pure-phase MoVTeNb oxide at 80°C*
- *NH₃ ads. on H-ZSM5 at 80°C; Validation of the TP-surface chemical probe reaction of n-propylamin*
- *CO₂ ads. on CeO₂ at 40°C*

Investigation of the oxidation process: - *O₂ ads. on supported CeO₂ at 200°C*

Study of catalytic relevant sites via calorimetry close to the reaction conditions:

- *Ethanol ads. on VO_x/γ-Al₂O₃ at 40°C*
- *Propane ads. on MoVTeNb oxide at 40°C*
- *Propane and EB adsorption on the oCNT*

Study of catalytic relevant sites via calorimetry under reaction conditions:

- *Propylene chemisorption on MoO_x/SBA-15 at T_{reaction}=50°C*
- *O₂ ads. on Ag for ethylene epoxidation at T_{reaction}=230 °C*
- *1-Hexyne chemisorption on CeO₂/TiO₂ at T_{reaction}=80°C*
- *CO chemisorption on Ir based catalysts for OER at r.t.*

Reactants induced dynamic responses of catalyst surface:

- *CO chemisorption cycles (30°C) on Ni/MgAl oxide catalyst for dry reforming of methane (DRM)*
- *propane and ethane ads./des. cycles on MoV oxide at 40°C*

Estimation of the enthalpy of formation of the transition state (activation barrier):

- *ethane & ethylene and propane & propylene ads. on the Vanadium oxide-based and Metal-free catalysts for ODH*

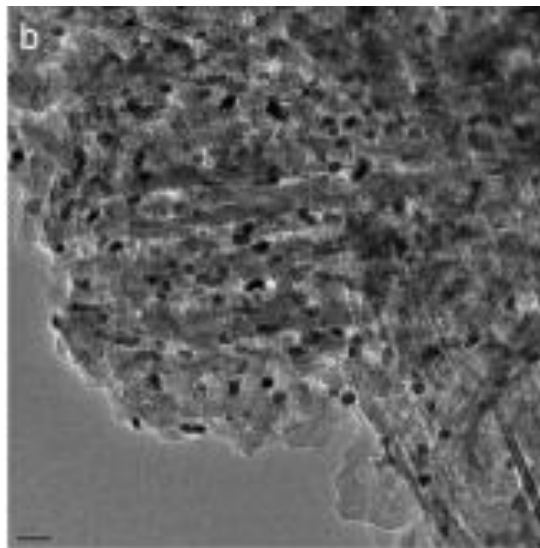
VALIDATION

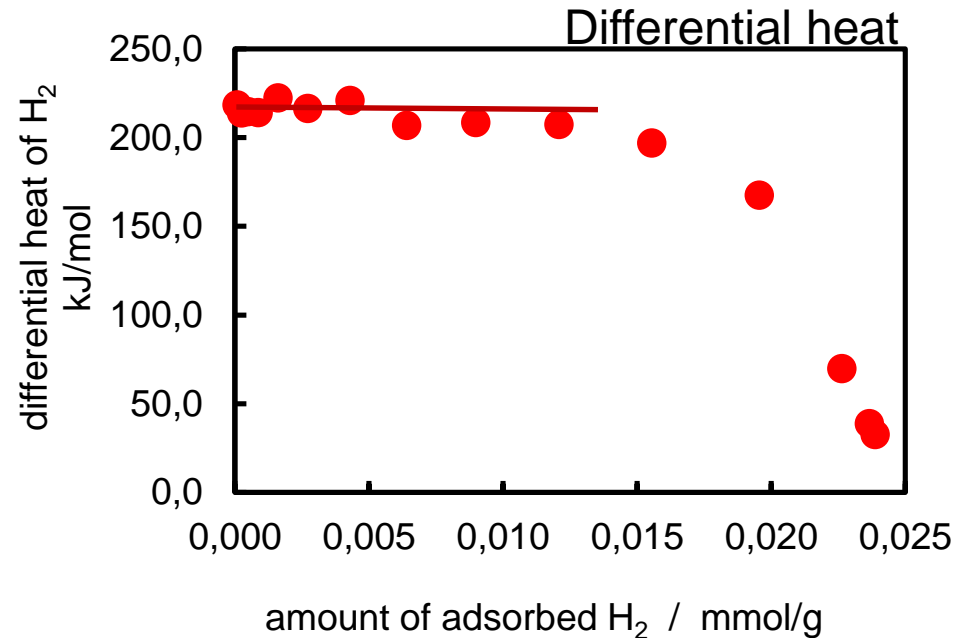
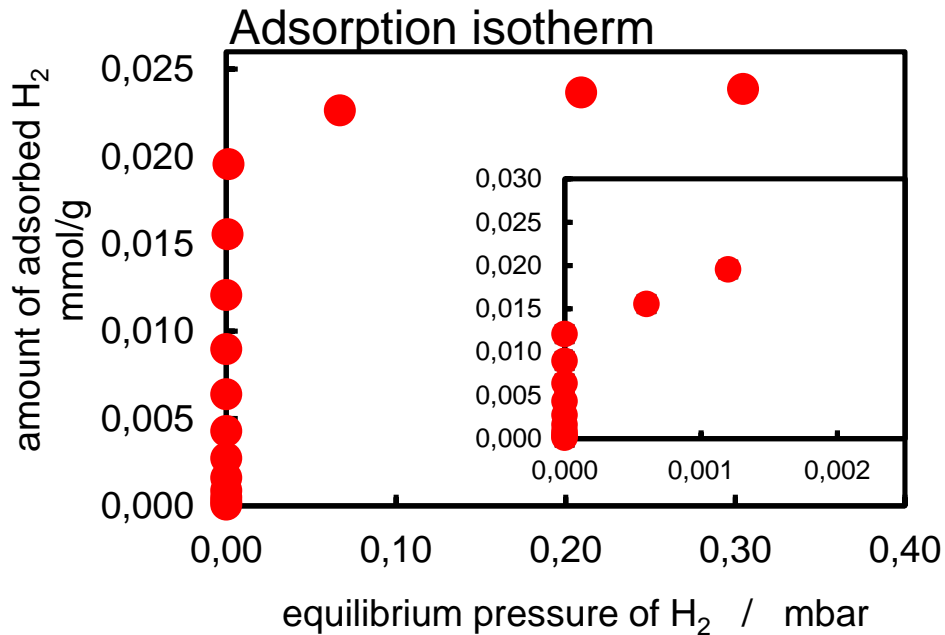
H_2 chemisorption on 2 wt.% Pt_{H2-673K-2h}/Al₂O₃ at 40°C

Reference Material from



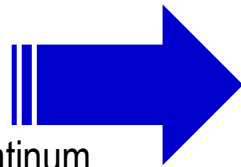
Active Metal Surface Area = 1.146 m² g⁻¹





Heat plateau: homogeneously distributed and **energetically uniform** adsorption sites

q_{diff} = 215 kJ/mol : chemisorption ! $\Delta_c H = 215$ kJ/mol
 Hydrogen is dissociative adsorbed on platinum
 $H_2 + Pt + Pt \rightarrow Pt-H + Pt-H$ $\Delta_c H = 266$ kJ/mol
 2.5% Pt/silica
 J.A. Dumesic et.al., Catal. Letters 45 (1997) 155-163.



Langmuir isotherm for dissociative adsorption

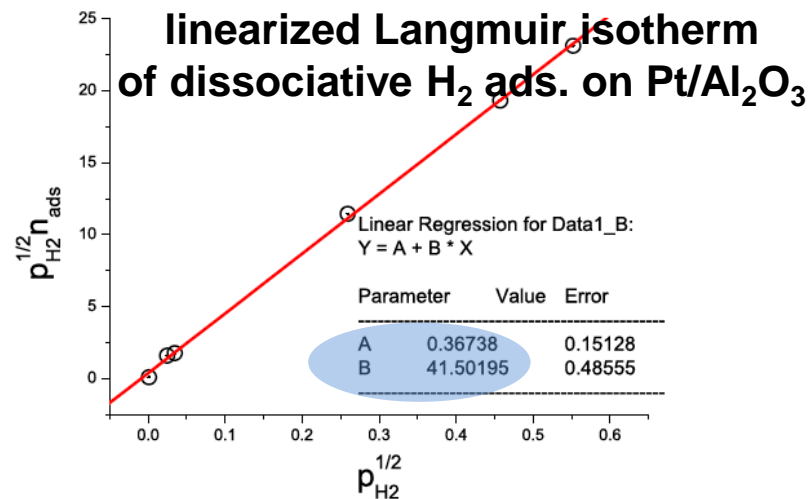
$$\theta_H = \frac{n_{ads}}{n_m} = \frac{\sqrt{pH_2 K_{ads}}}{1 + \sqrt{pH_2 K_{ads}}}$$

Linearization

$$\theta_H = \frac{n_{ads}}{n_m} = \frac{\sqrt{p_{H_2} K_{ads}}}{1 + \sqrt{p_{H_2} K_{ads}}}$$

$$n_{ads} \left(1 + \sqrt{p_{H_2} K_{ads}}\right) = n_m \sqrt{p_{H_2} K_{ads}}$$

$$\frac{1}{n_m \sqrt{K_{ads}}} + \frac{1}{n_m} \sqrt{p_{H_2}} = \frac{\sqrt{p_{H_2}}}{n_{ads}}$$



registered	$\frac{p_{H_2}}{\text{mbar}}$	10 ⁻⁶	6 · 10 ⁻⁴	1.2 · 10 ⁻³	6.69 · 10 ⁻²	2.09 · 10 ⁻¹	3.05 · 10 ⁻¹
calculated from the calibrated volumetric system	$\frac{n_{ads}}{(\text{mmol} \cdot \text{g}^{-1})}$	1.208 · 10 ⁻²	1.555 · 10 ⁻²	1.956 · 10 ⁻²	2.264 · 10 ⁻²	2.366 · 10 ⁻²	2.387 · 10 ⁻²
calculated	$\frac{\sqrt{p_{H_2}}}{\sqrt{\text{mbar}}}$	10 ⁻³	24.5 · 10 ⁻³	34.6 · 10 ⁻³	259 · 10 ⁻³	457 · 10 ⁻³	552 · 10 ⁻³
calculated	$\frac{n_{ads}}{\frac{\sqrt{\text{mbar}} \cdot \text{g}}{\text{mmol}}}$	0.083	1.58	1.77	11.44	19.32	23.13

B

$$\frac{1}{n_m} = 42 \frac{\text{g}}{\text{mmol}} \Rightarrow n_m = 24 \cdot 10^{-3} \frac{\text{mmol}}{\text{g}}$$

Specific surface area of Pt m^2_{Pt}/g_{cat}

A

$$\frac{1}{n_m \sqrt{K_{ads}}} = 0.4 \frac{\sqrt{\text{mbar}} \cdot \text{g}}{\text{mmol}} \Rightarrow K_{ads} = \left(\frac{1 \cdot \text{g} \cdot \text{mmol}}{24 \cdot 10^{-3} \text{mmol} \cdot 0.4 \sqrt{\text{mbar}} \cdot \text{g}} \right)^2$$

$$\Rightarrow K_{ads} = 10851 \text{ mbar}^{-1}$$

H₂ adsorption on Pt/Al₂O₃ Quantachrome at 40°C

Specific surface area of Pt m^2_{Pt}/g_{cat}

$$S_{Pt} = \frac{n_m \cdot \text{Avogadro constant}}{\text{Surface sites density } \Gamma_{\text{fcc lattice, Pt}}}$$

$$S_{Pt} = \frac{24 \cdot 10^{-6} \text{ mol} \cdot 6.022 \cdot 10^{23} \text{ particles} \cdot \text{cm}^2}{\text{g} \cdot 1.5 \cdot 10^{15} \text{ atoms} \cdot \text{mol}}$$

$$S_{Pt} = 9667 \text{ cm}^2/\text{g} \approx 1 \text{ m}^2/\text{g}$$

$$S_{Pt}; \text{ certified by Quantachrome} = 1.146 \text{ m}^2/\text{g}$$

Final Results

Kinetic parameters determined for the H₂ ads. on Pt/Al₂O₃

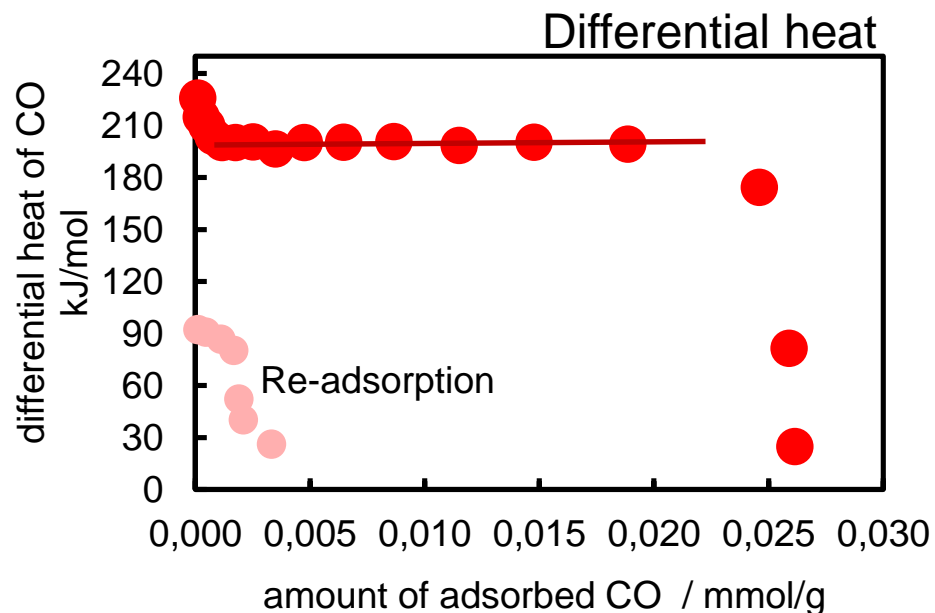
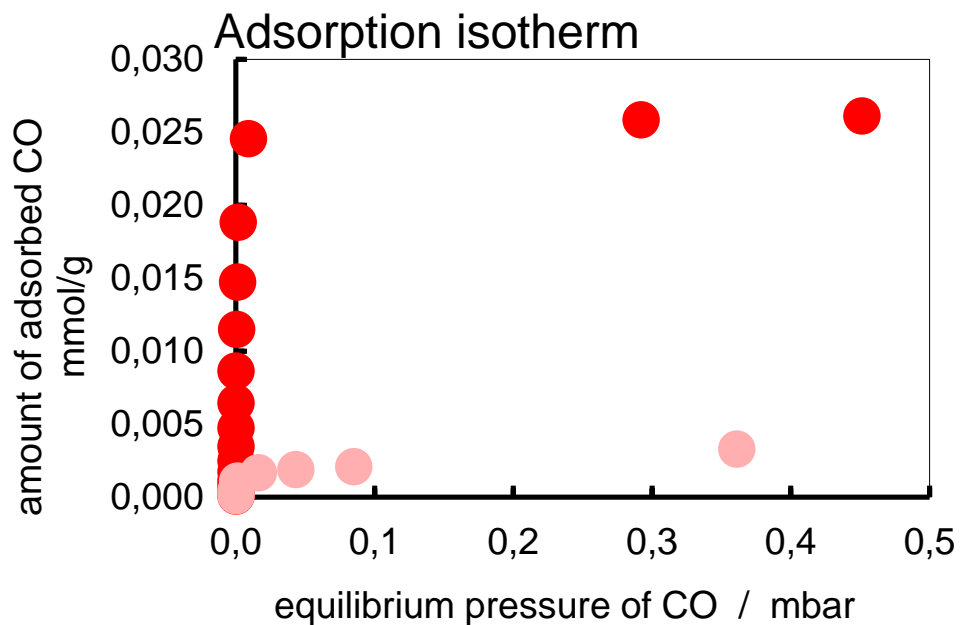
$$\begin{aligned} n_{\text{mono}} &= 24 \cdot 10^{-6} \text{ mol} \cdot \text{g}^{-1} \\ K_{\text{ads}} &= 10851 \text{ mbar}^{-1} \\ \Delta H_{\text{ads.}} &= 215 \pm 4 \text{ kJ} \cdot \text{mol}^{-1} \\ S_{\text{Pt}} &\approx 1.0 \text{ m}^2 \cdot \text{g}^{-1} \end{aligned}$$



MAX-PLANCK-GESELLSCHAFT



CO adsorption on Pt_{H2-673K-2h}/Al₂O₃ *Quantachrome* at 40°C



Heat plateau: homogeneously distributed and **energetically uniform** adsorption sites

Reversibility: CO is mainly irreversible adsorbed on Pt at 40°C

q_{diff} = 200 kJ/mol : chemisorption ! $\Delta_c H = 200$ kJ/mol

Pt-CO terminal CO $\Delta_c H = 209$ kJ/mol

(Pt)_n; n>1 -CO bridged CO $\Delta_c H = 94$ kJ/mol

J. Therm. Anal. Cal., 82, 2005 105

$\nu_{CO} \sim 2055$ cm⁻¹

$\nu_{CO} \sim 1822$ cm⁻¹

higher order Langmuir model for activated adsorption

$$N_{ads} = \frac{N_{mono} (Kp)^{\frac{1}{n}}}{1 + (Kp)^{\frac{1}{n}}}$$



$$N_{ads} = \frac{N_{mono} (Kp)^{\frac{1}{n}}}{1 + (Kp)^{\frac{1}{n}}}$$

$$1/(n_{mono} K_{ads}^{1/n}) + (1/n_{mono}) p_{CO} = p_{CO} / n_{ads}$$

$$1/n_{mono} = 38.29 \text{ g/mmol} \rightarrow n_{mono} = 26.11 \times 10^{-3} \text{ mmol/g}$$

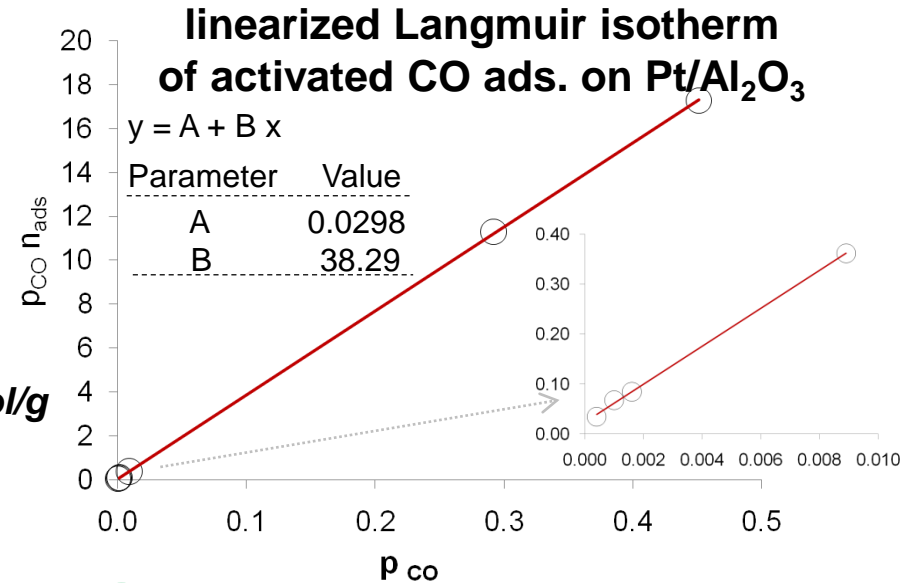
$$1/(n_{mono} K_{ads}^{1/n}) = 0.0298 \text{ mbar} \cdot \text{g/mmol} \rightarrow K_{ads} = (1/n_{mono} A)^n$$

$$K_{ads} = (1 \text{ g mmol} / 26.11 \times 10^{-3} \text{ mmol} \cdot 0.0298 \text{ mbar g})^{1.1567}$$

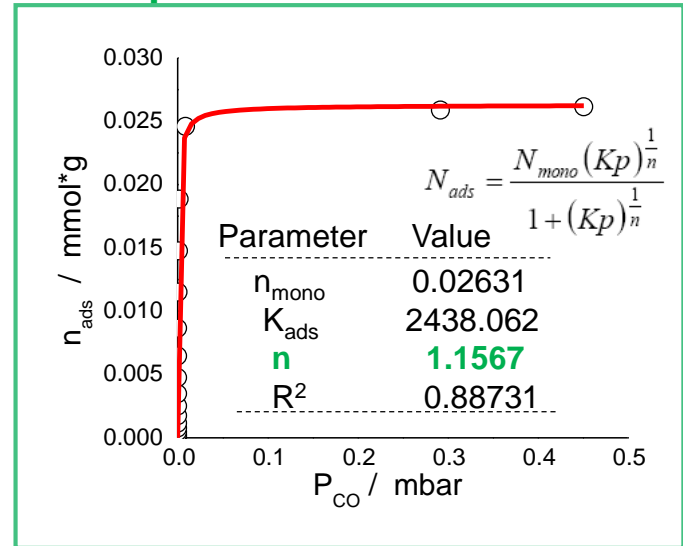
$$K_{ads} = 3945,96 \text{ mbar}^1$$

$$S_{Pt} = 10563 \text{ cm}^2/\text{g} \approx 1.1 \text{ m}^2/\text{g} ;$$

$$S_{Pt} ; \text{ certified by Quantachrome} = 1.146 \text{ m}^2/\text{g}$$



Adsorption order ?



Comparison

Kinetic parameters determined for the **CO** ads. on Pt/Al₂O₃

$$\begin{aligned}n_{\text{mono}} &= 26 * 10^{-6} \text{ mol} \cdot \text{g}^{-1} \\K_{\text{ads}} &= 3946 \text{ mbar}^{-1} \\ \Delta H_{\text{ads.}} &= 200 \pm 4 \text{ kJ} \cdot \text{mol}^{-1} \\ S_{\text{Pt}} &\approx 1.1 \text{ m}^2 \cdot \text{g}^{-1}\end{aligned}$$

Kinetic parameters determined for the **H₂** ads. on Pt/Al₂O₃

$$\begin{aligned}n_{\text{mono}} &= 24 * 10^{-3} \text{ mmol} \cdot \text{g}^{-1} \\K_{\text{ads}} &= 10851 \text{ mbar}^{-1} \\ \Delta H_{\text{ads.}} &= 215 \pm 4 \text{ kJ} \cdot \text{mol}^{-1} \\ S_{\text{Pt}} &\approx 1.0 \text{ m}^2 \cdot \text{g}^{-1}\end{aligned}$$

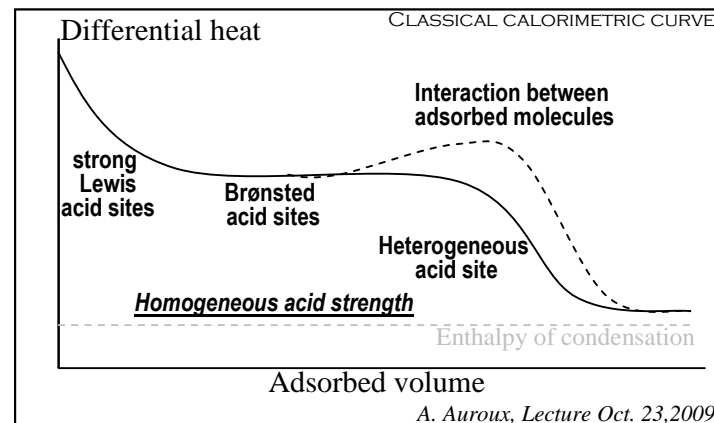
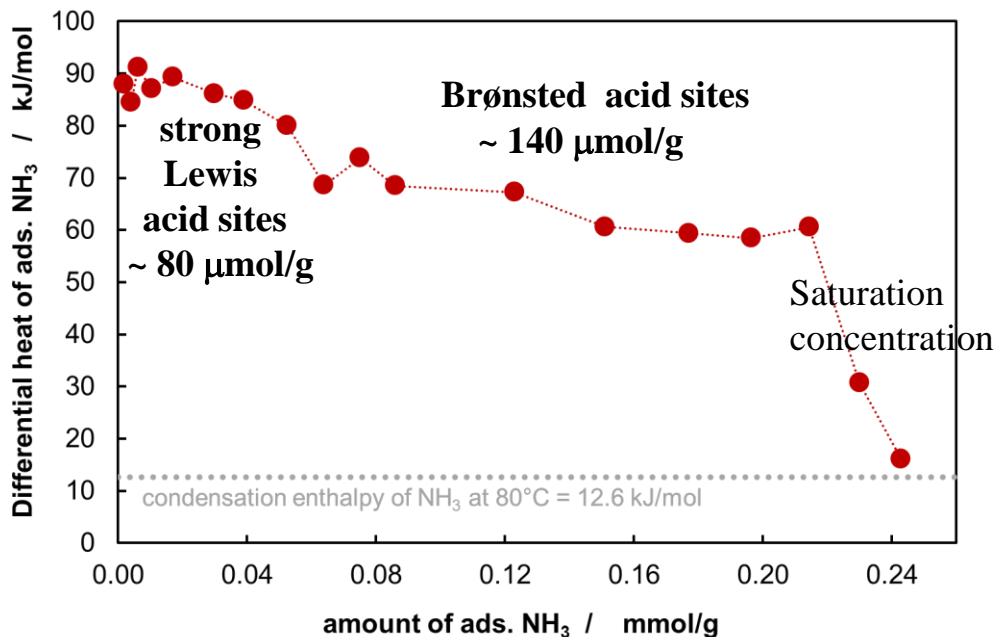
Validation

of the SETARAM calorimeter combined with a custom-designed high vacuum and gas dosing apparatus.

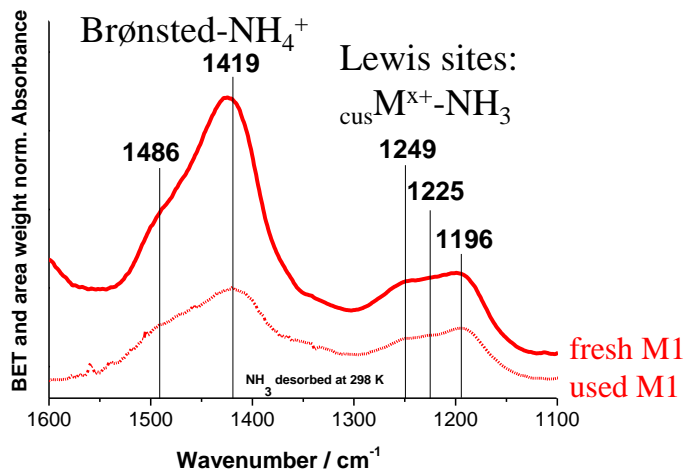
$$\begin{array}{l} J. \text{Therm. Anal. Cal.}, 82 (2005)105 : \text{Pt-CO } \Delta_{\text{C}}H = 209 \text{ kJ/mol} \\ S_{\text{Pt}} ; \text{ certified by Quantachrome} = 1.146 \text{ m}^2/\text{g} \end{array} \quad \Rightarrow \quad \begin{array}{l} \Delta_{\text{C}}H = 200 \pm 4 \text{ kJ/mol} \text{ (Dept. AC FHI)} \\ S_{\text{Pt}} = 1 \pm 0.1 \text{ m}^2/\text{g} \end{array}$$



**Titration of acid sites
on the surface of MoVTeNb oxide catalyst #6059
using NH₃ at 80°C**



FTIR spectra



Determination of the amount of Brønsted and Lewis acid sites using the extinction coefficients from the literature:

Brønsted acid sites: ~ 40 $\mu\text{mol/g}$

Lewis acids sites: ~ 90 $\mu\text{mol/g}$



Development of a NEW METHODE:



Quantification of Brønsted Acid Sites on Catalyst Surfaces via Temperature Programmed Surface Reaction of n-Propylamine

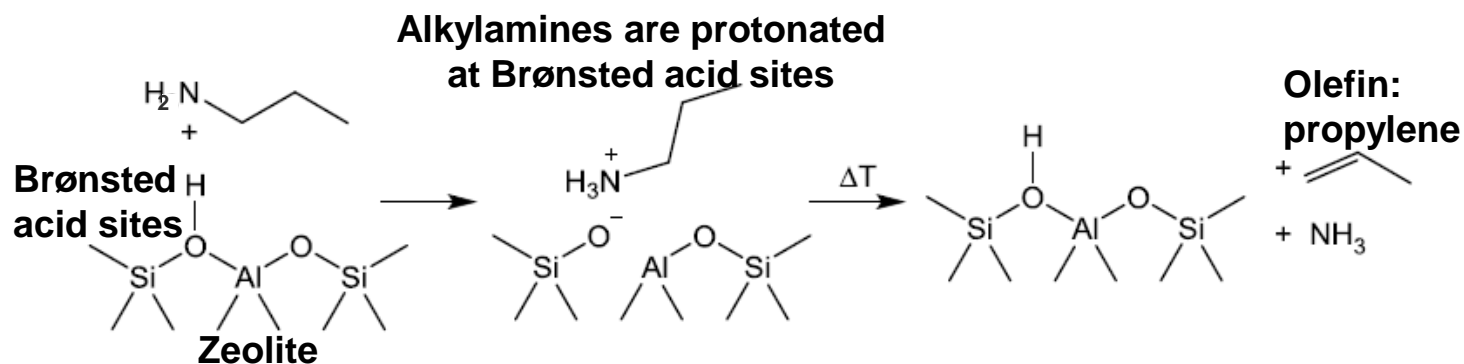
VALIDATION via Calorimetry
NH₃ ads. on H-ZSM5 zeolite at 80°C

Motivation:

Development of a standard characterization method for the **quantification of acid sites on surfaces**.

Gorte et al. developed a method that uses alkylamines as reactive probe molecules for TPSR experiments on zeolites.

It was investigated if the needed information can be readily obtained by a **commercial TPD machine**.



Combination of TPSR and TPD/MS:
quantify Brønsted acid sites is the amount of desorbed olefin

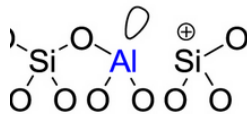
- Samples:**
- H-ZSM5-30 (H-ZSM5 zeolite with a $\text{SiO}_2/\text{Al}_2\text{O}_3$ ratio of 30)
 - H-ZSM5-80 (H-ZSM5 zeolite with a $\text{SiO}_2/\text{Al}_2\text{O}_3$ ratio of 80)

H-ZSM5-30

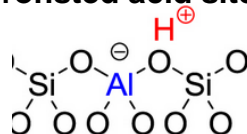
SiO₂/Al₂O₃ ratio of 30

n Brønsted acid sites = **560 μmol/g**

Lewis acid sites



Brønsted acid sites



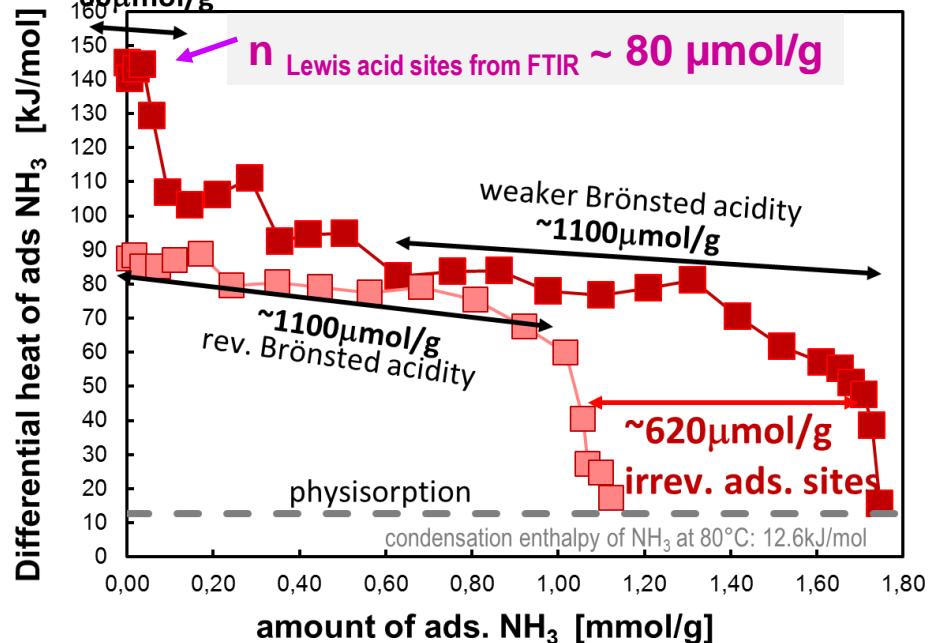
H-ZSM5-80

SiO₂/Al₂O₃ ratio of 80

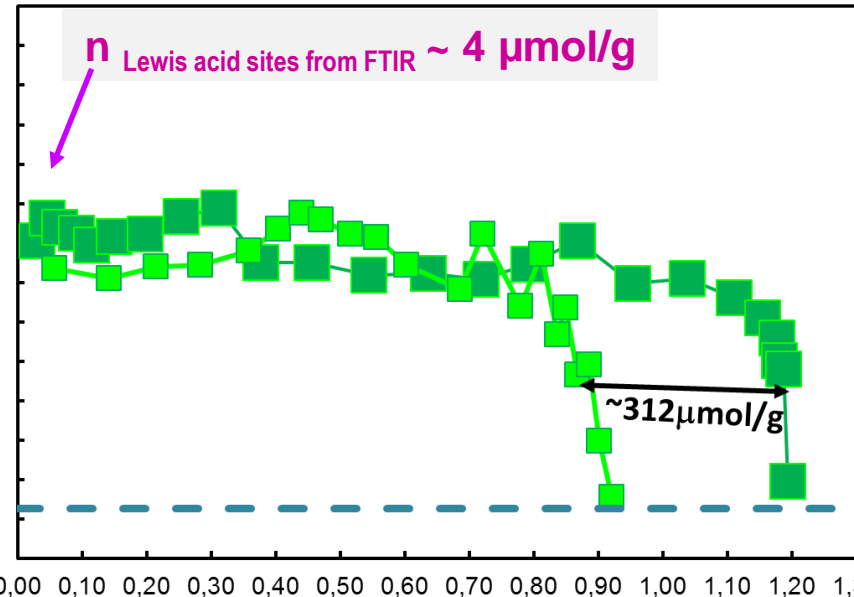
n Brønsted acid sites = **312 μmol/g**

strong acidity Lewis

~60 μmol/g



Differential heat of ads NH₃ [kJ/mol]



amount of ads. NH₃ [mmol/g]

$$n_{\text{relevant Brønsted acid sites}} = n_{\text{irrev. ads sites}} - n_{\text{Lewis acid sites}}$$

Stoichiometric and measured acidities for H-ZSM5 zeolites TPSR/TPD & microcalorimetry & FTIR

Quantification of Brønsted Acid Sites

Sample	Stoichiometric acidity ^[5] μmol/g	FTIR ^[6] μmol/g	Microcalorimetry ^[7] μmol/g	Alkylamine TPD μmol/g
H-ZSM5-30	525	437	560	557
H-ZSM5-80	204	269	312	297

- The comparison shows that the obtained results from the TPSR are consistent with the microcalorimetry and IR measurements.

[5] A. S. Al-Dughaiter, H. de Lasa, *Ind. Eng. Chem. Res.* 2014, 53, 15303–15316.

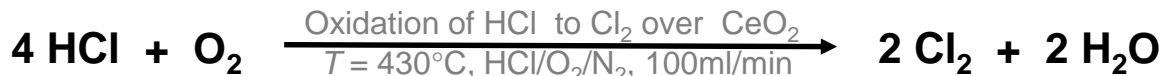
[6] O. Bortnovsky, Z. Melichar, Z. Sobalík, B. Wichterlová, *Micropor. Mesopor. Mat.* 2001, 42, 97–102.

[7] S. Wrabetz, X. Yang, G. Tzolova-Müller, R. Schlögl, F. C. Jentoft, *J. Catal.* 2010, 269, 351–358.; Klaus Dieter Friedel Ortega, Dissertation, „6.3.4. Investigation of gas-phase acidity by NH₃ microcalorimetry and NH₃-TPD,, S. Wrabetz, page102.



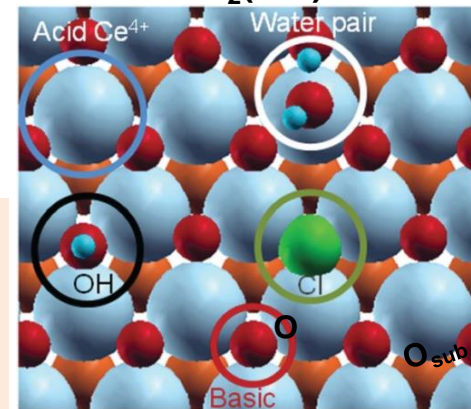
Titration of basic sites on the surface of ceria using CO₂ at 40°C

DEACON reaction



Intention: Understanding CeO₂ as a Deacon catalyst, characterize ceria in its fresh **CeO₂-F** and post-reaction states **CeO₂-D**

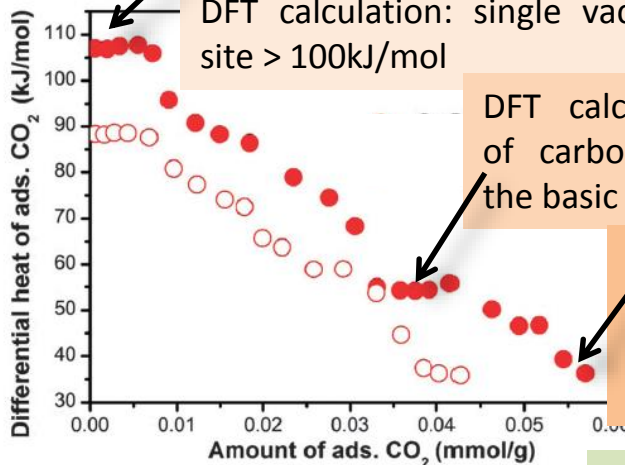
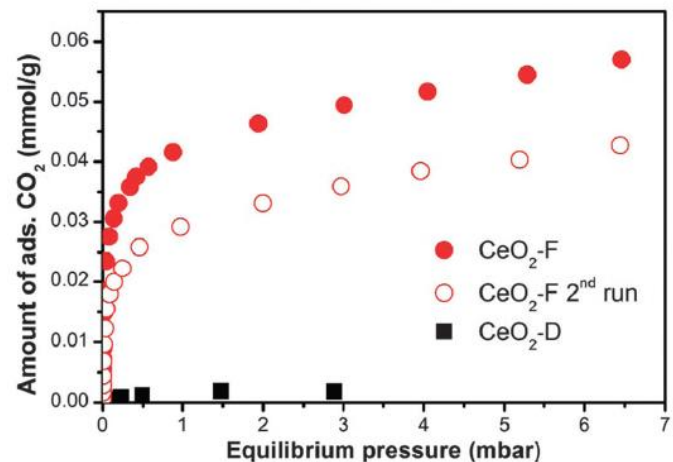
Adsorption sites on the CeO₂(111) surface



Structural defects such as edges in nanoparticles¹ or vacancies in more open facets such as (110)²
DFT calculation: single vacancy site > 100kJ/mol

DFT calculation: formation of carbonate species with the basic O atoms 43kJ/mol

DFT calculation: partially hydroxylated surfaces or oxygen vacancies are filled by one of the O atoms of the CO₂ molecules 18kJ/mol



➤ The basic character of the ceria surface has been eliminated upon reaction, indicating that most of the basic lattice O sites are exchanged by chlorine and that the OH groups formed are rather acidic.

NH₃ ads. 40°C
fresh: 30 kJ/mol 75 μmol/g acid sites
used: 50 kJ/mol 75 μmol/g acid sites
➤ increased acidity of the chlorinated surface

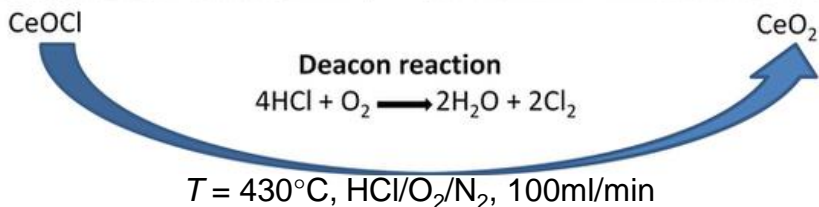
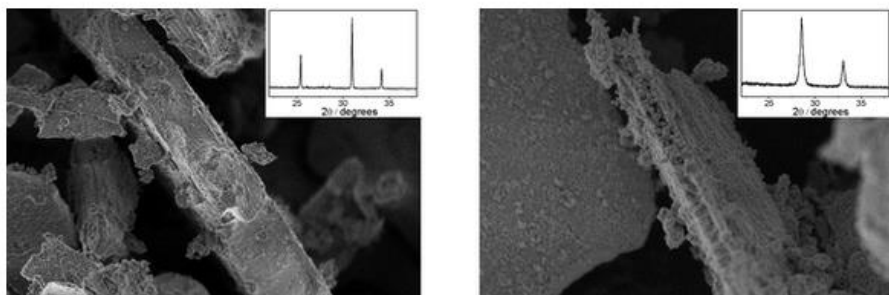
(1) G. N. Vayssilov, M. Mihaylov, P. S. Petkov, K. I. Hadjiivanov and K. M. Neyman, J. Phys. Chem. C, 2011, 115, 23435–23454.

(2) M. Nolan, S. C. Parker and G. W. Watson, Phys. Chem. Chem. Phys., 2006, 8, 216–218.

(3) Farra, R., Wrabetz, S., Schuster, M. E., Stotz, E., Hamilton, N., Amrute, A. P., Pérez-Ramírez, J., López, N., Teschner, D., Phys. Chem. Chem. Phys., 15 (2013) 3454 - 3465 .



Investigation of the oxidation process:
Oxidation of HCl to Cl₂ over bare and supported CeO₂

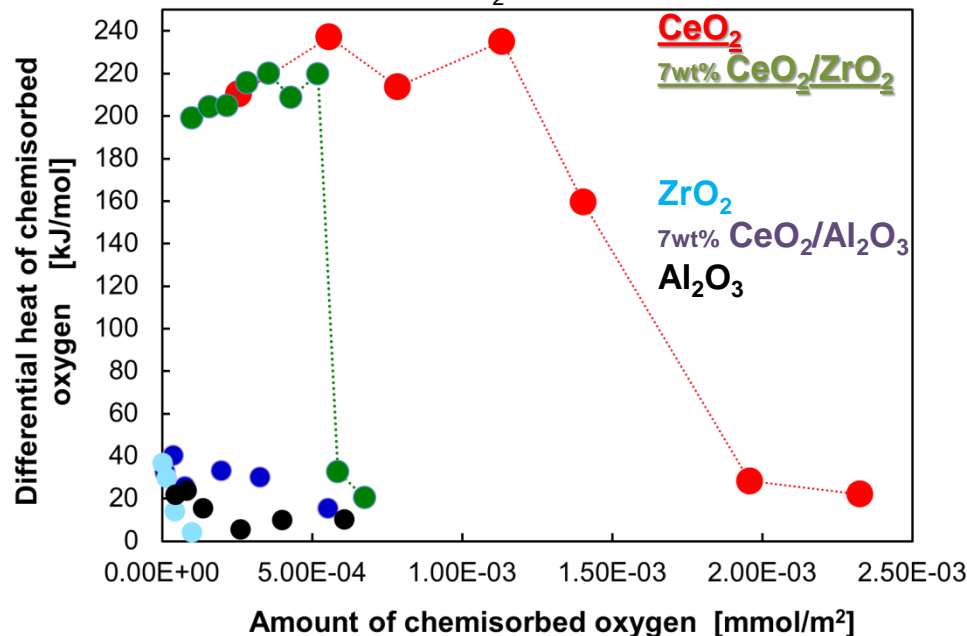


➤ **Best reactivity** was obtained from bare **CeO₂** and **CeO₂/ZrO₂**.

➤ One essential parameter seems to be the **reducibility** of the catalyst in order to create catalytically important oxygen vacancies.

Heat of adsorption of O₂ at 200° C / HT1000

Pretreatment: H₂ reduction at 200° C

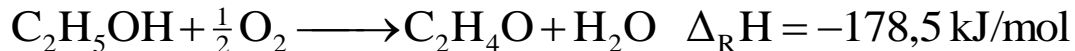


➤ **Reactivity** seems to be linked with the **reducibility** of the surface.



Study of catalytic relevant sites
via calorimetry close to the reaction conditions:

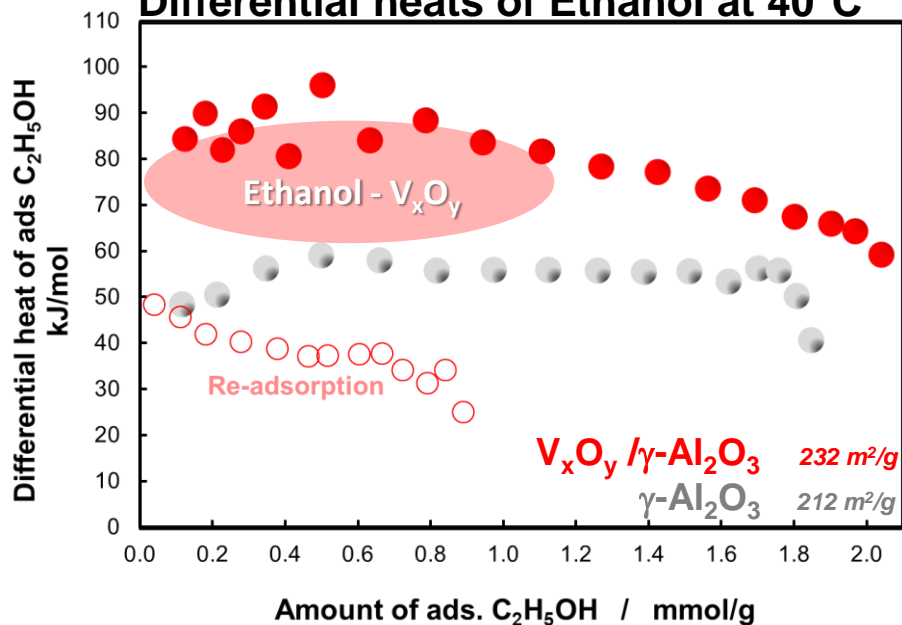
Oxidation of alcohol over vanadium supported Al_2O_3



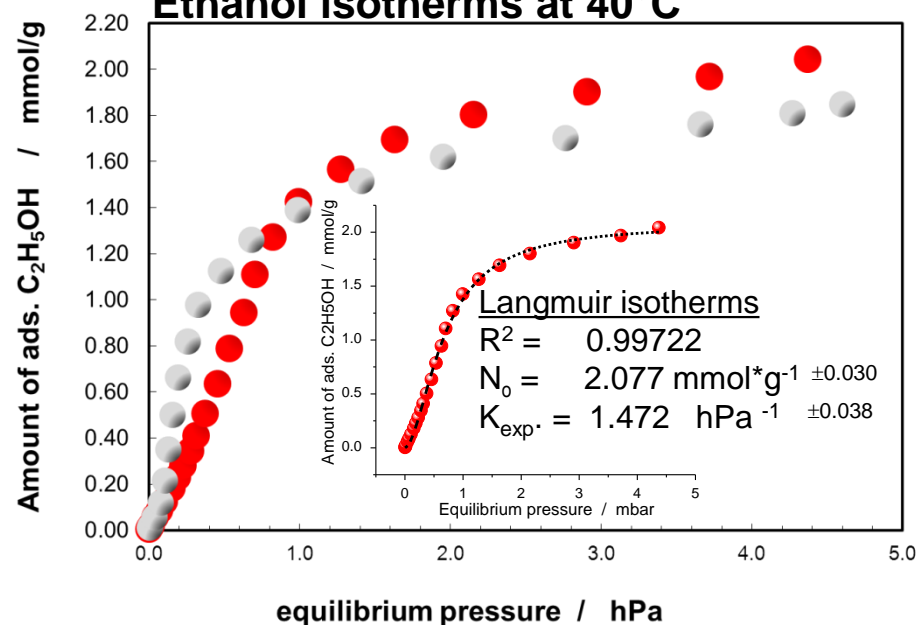
Catalyst: $\text{V}_x\text{O}_y / \gamma\text{-Al}_2\text{O}_3$
 $T_{\text{reaction}} = 140 - 200 \text{ }^\circ\text{C}$

Intention: Determination of kinetic data: N_{ads} , K_{ads} and ΔH_{ads} of Ethanol on $\text{V}_x\text{O}_y/\text{Al}_2\text{O}_3$

Differential heats of Ethanol at 40°C



Ethanol isotherms at 40°C



Kinetic parameters determined for the ethanol ads. on $\text{V}_x\text{O}_y/\text{Al}_2\text{O}_3$

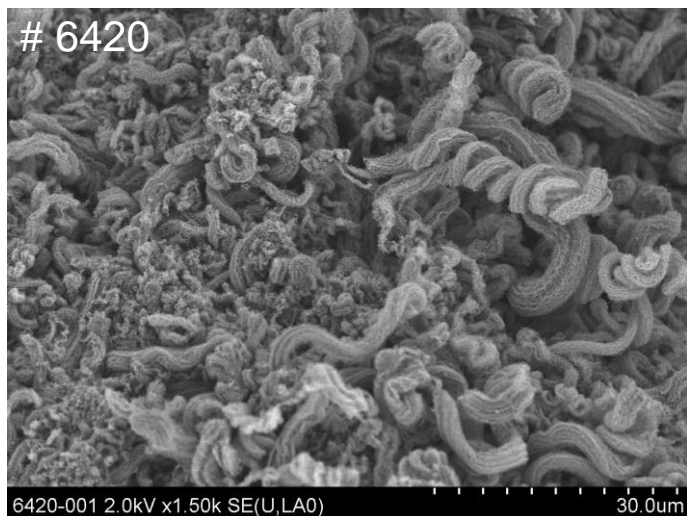
N_{mono}	=	2.077	$\text{mmol} \cdot \text{g}^{-1}$
$K_{\text{ads.}}$	=	1.47	hPa^{-1}
$\Delta H_{\text{ads.}}$	=	90 ± 10	$\text{kJ} \cdot \text{mol}^{-1}$



Study of catalytic relevant sites
via calorimetry close to the reaction conditions:

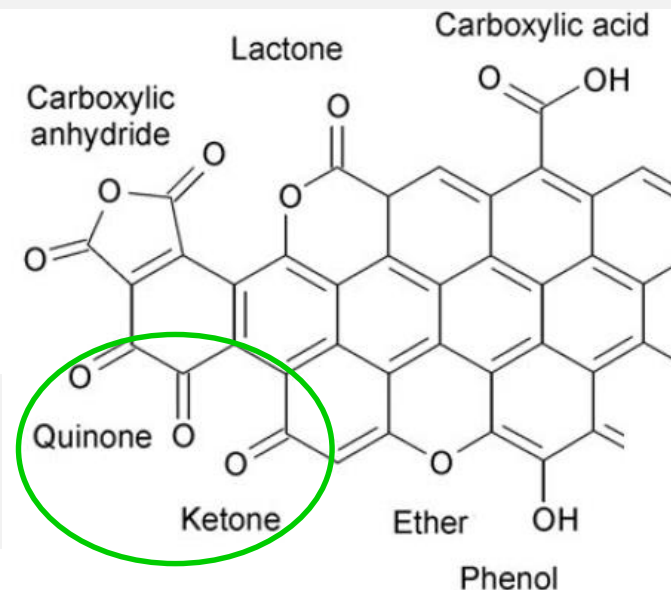
**New insights on
active sites of oxygen functionalized carbon nanotube (*oCNT*)
for oxidative dehydrogenation (*ODH*)**

Carbon based materials are active catalysts for the oxidative dehydrogenation (ODH) reaction [1]



Quinone groups are believed to be the active sites. These **nucleophilic oxygen** species can selectively abstract hydrogen atoms [2-5]

The well defined active surface oxygen sites will be created by oxygen functionalization of the CNTs with HNO_3 .



Intention:

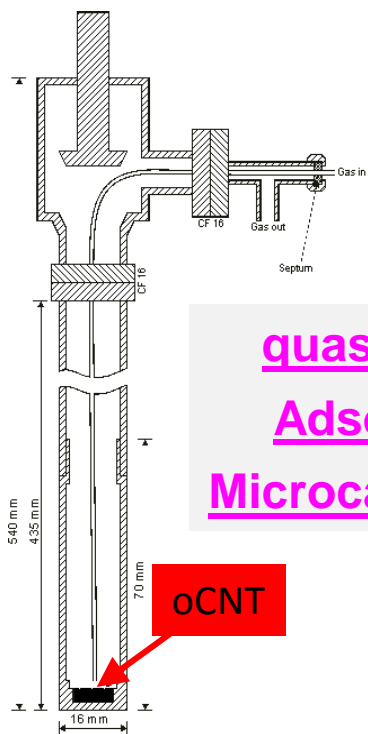
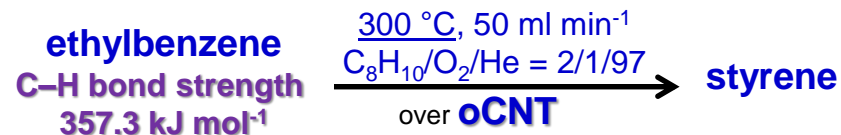
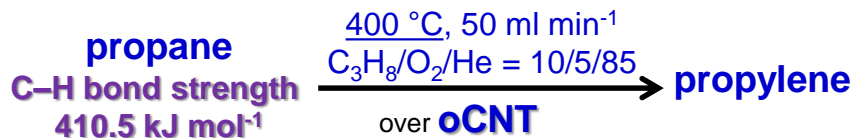
To establish a mechanistic model for carbon catalyzed ODH.

Ads. properties are important input for kinetic modeling.

The research project was performed in a multidisciplinary approach (quasi *in situ* adsorption microcalorimetry, *in situ* XPS, kinetics, DFT).

We choose the ODH of propane and ethylbenzene (EB) as the model reactions.

Model reaction



quasi in situ

Adsorption

Microcalorimetry

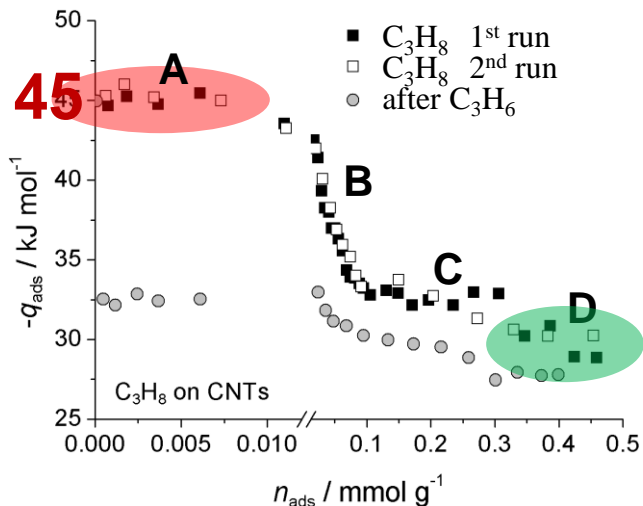
★ probe molecule: propane, propylene and ethylbenzene

★ T_{adsorption} = 313K < 673K = T_{reaction}

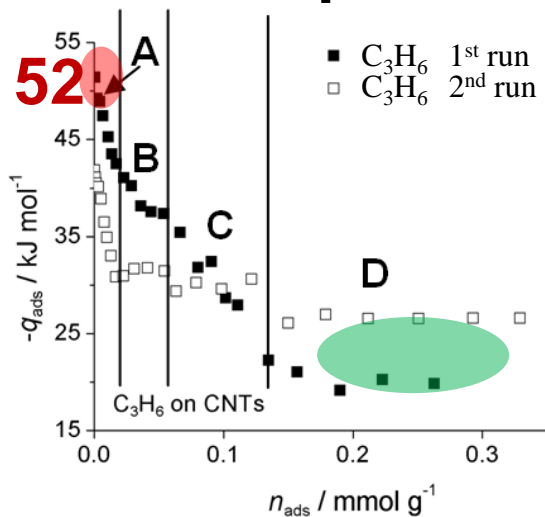
★ selected catalyst: 370mg used MW oCNT #6420

oCNT

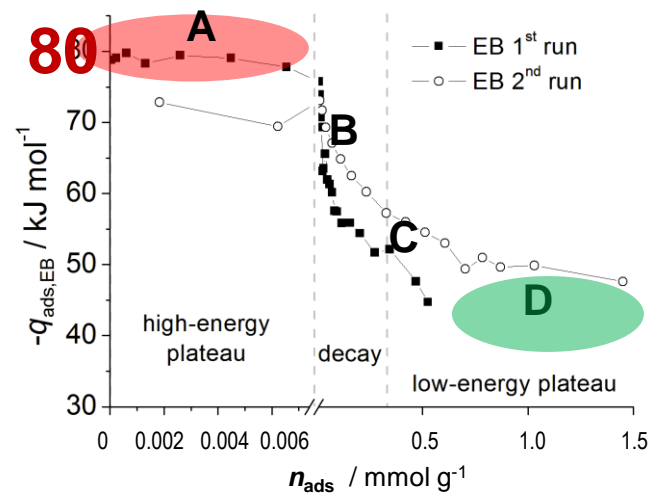
Propane



Propene



Ethylbenzene

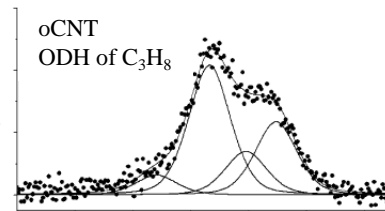
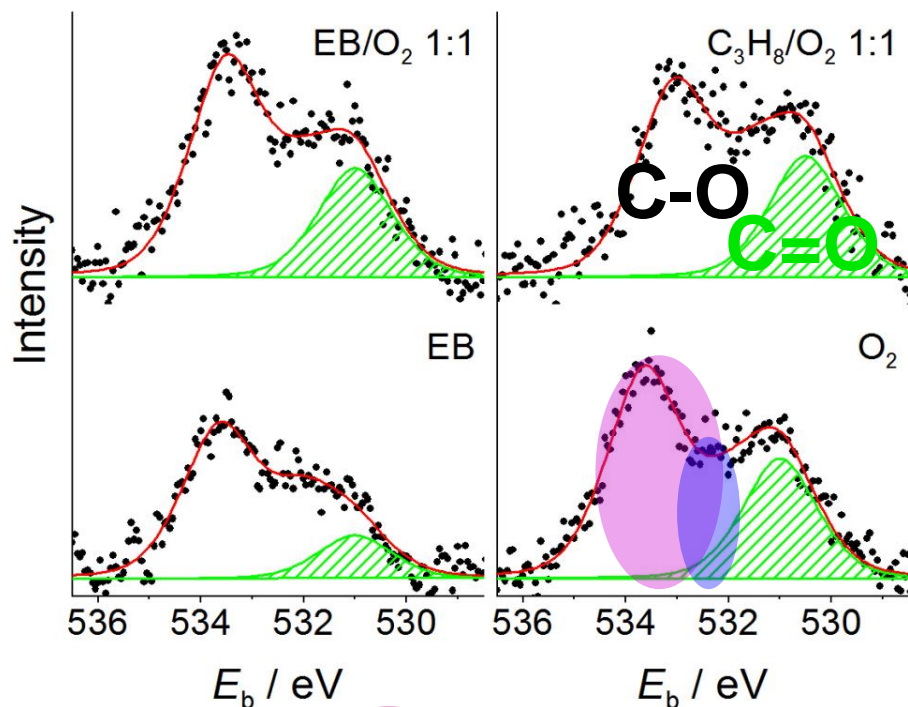


- ~8 $\mu\text{mol/g}$ active sites equilibrated in EB and propane ODH reaction
- 3-5% of the surface is covered by high-energy adsorption sites which can be correlated to 4-5% of surface oxygen determined by XPS [2]
- EB reacts stronger (80 kJ/mol) than propane (45 kJ/mol).
- Graphite (free of oxygen) shows a constant low level of diff. heats for propane (32kJ/mol) and propylene (40kJ/mol); reversible

[1] B. Frank, S. Wrabetz, O.V. Khavryuchenko, R. Blume, A. Trunschke, R. Schlögl, *ChemPhysChem* 12 (2011) 2709.

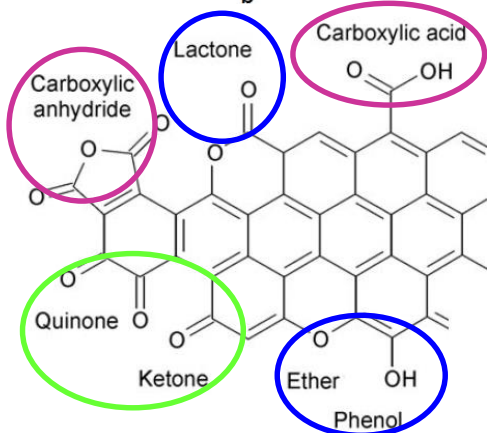
[2] B. Frank, J. Zhang, R. Blume, R. Schlögl, D. S. Su, *Angew. Chem.* 2009, 121, 7046–7051; *Angew. Chem. Int. Ed.* 2009, 48, 6913–6917.

MW oCNT catalyst under different atmospheres @ 350°C.



Atmosphere	$I_{C=O} / I_{C-O}$
EB	0.168
EB/O ₂	0.283
C ₃ H ₈ /O ₂	0.313
O ₂	0.315

↑ REACTIVITY

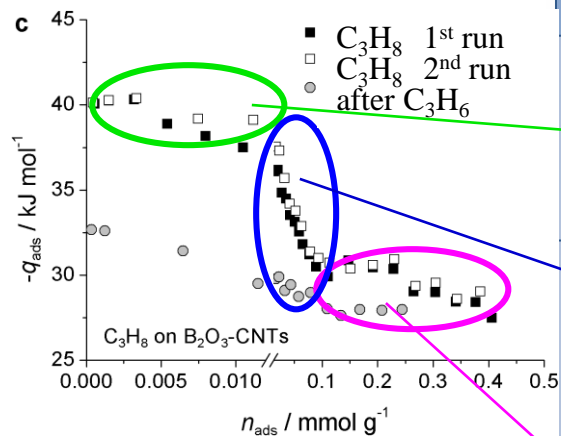


nucleophilic oxygen
ketones & quinones

quasi neutral oxygen
lactone/ester, ethers,
phenols

electrophilic oxygen
carboxylic anhydrides,
carboxylic acid

Site classification & quantification from microcalorimetric analyses, XPS, and TPD_{not shown} of active surfaces of oCNT catalysts in ODH of propane and EB [1,2]



ODH substrate	C ₃ H ₈ [1]	EB [2]	
	$-q_{\text{ini}}$ (kJ mol ⁻¹)	45	80
nucleophilic oxygen ketones & quinones	n_{ads} (μmol g ⁻¹)	0 - 8	0 - 8
high energy plateau	$-q_{\text{ads}}$ (kJ mol ⁻¹)	45±0.5	80±0.5
quasi neutral oxygen lactone/ester, ethers, phenols	n_{ads} (μmol g ⁻¹)	10 - 120	10 - 110
steady decay range	$-q_{\text{ads}}$ (kJ mol ⁻¹)	45 - 33	80 - 55
electrophilic oxygen carboxylic anhydrides, carboxylic acid	n_{ads} (μmol g ⁻¹)[a]	-	-
low energy plateau	$-q_{\text{ads}}$ (kJ mol ⁻¹)[b]	33	55
capacity at 40 mbar	$n_{\text{ads,total}}$ (μmol g ⁻¹)	220	220

$S_{\text{propane}} = 51 \text{ m}^2 \text{ g}^{-1}$

$S_{\text{EB}} = 122 \text{ m}^2 \text{ g}^{-1}$

BET_{used oCNT} = 544 m² g⁻¹

[a] could not be determined

[b] Maximum differential adsorption heat.

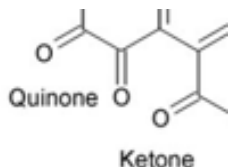
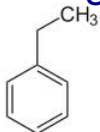
[1] B. Frank, S. Wrabetz, O.V. Khavryuchenko, R. Blume, A. Trunschke, R. Schlögl, ChemPhysChem 12

[2] Benjamin Frank, Raoul Blume, Oleksiy V. Khavryuchenko, Pierre Kube, Sabine Wrabetz, Jian Zhang,

"A Unifying Concept of Hydrocarbon Oxidative Dehydrogenation over Carbon-Based Catalysts", in prog

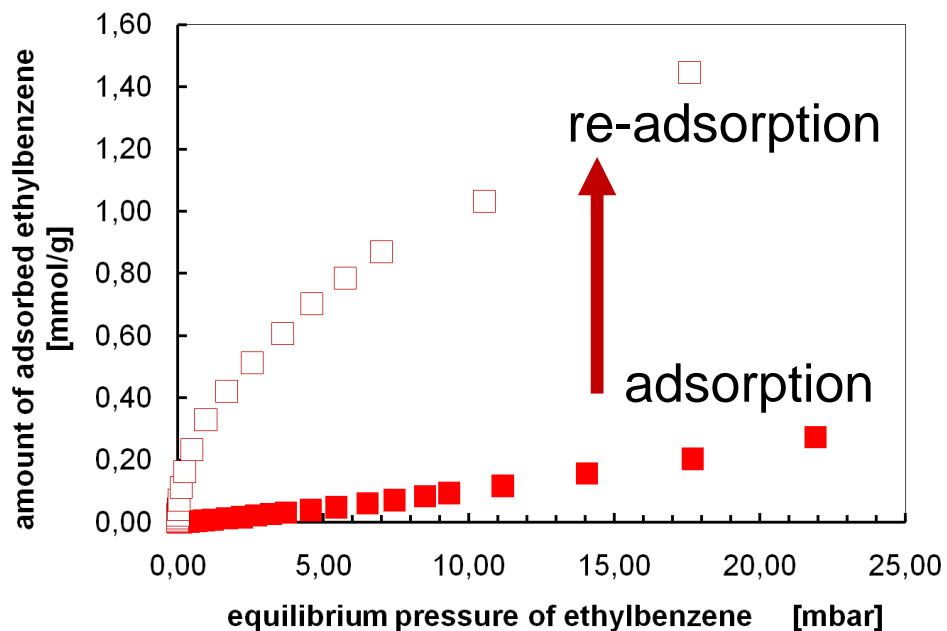
Explanation:

- high energy ads. sites reacts with CC1=CC=CC=C1 irreversibly to C-OH groups



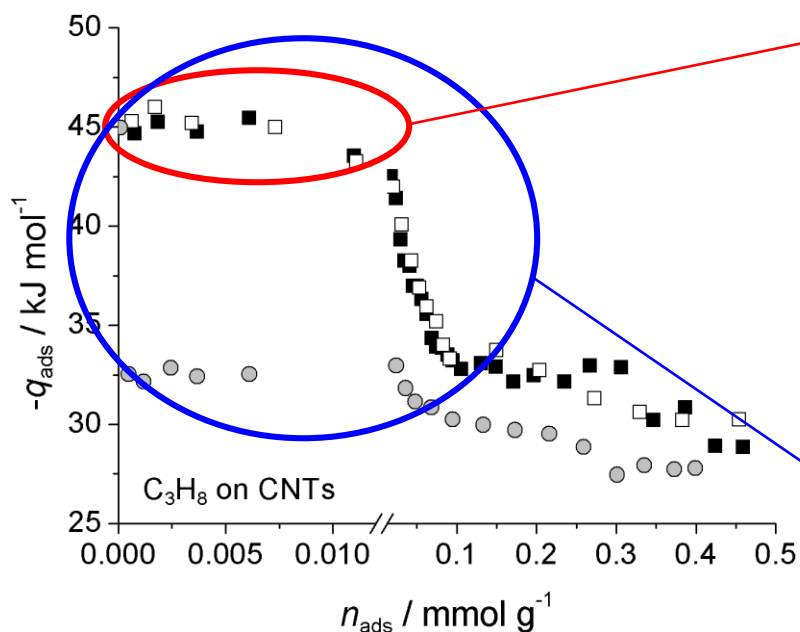
- formation of H₂O during initial reaction → blocked active sites → turns the surface more hydrophilic → hindering the ads. of non-polar EB molecule
- reversible 2nd ads. run of EB without reaction (consumed C=O groups) and hence no formation of H₂O
- more weak ads. sites available for EB

Ethylbenzene on used oCNT



- 2nd run of EB ads. reveals a drastic increase of the total adsorption capacity

Note: - Adsorption Isotherms only for oxygenated sites which are relevant for catalysis
 - Adsorption isotherms of propylene and EB have not been evaluated because of irreversible processes and surface reactions.



Energetically uniform sites

→ **Langmuir model**

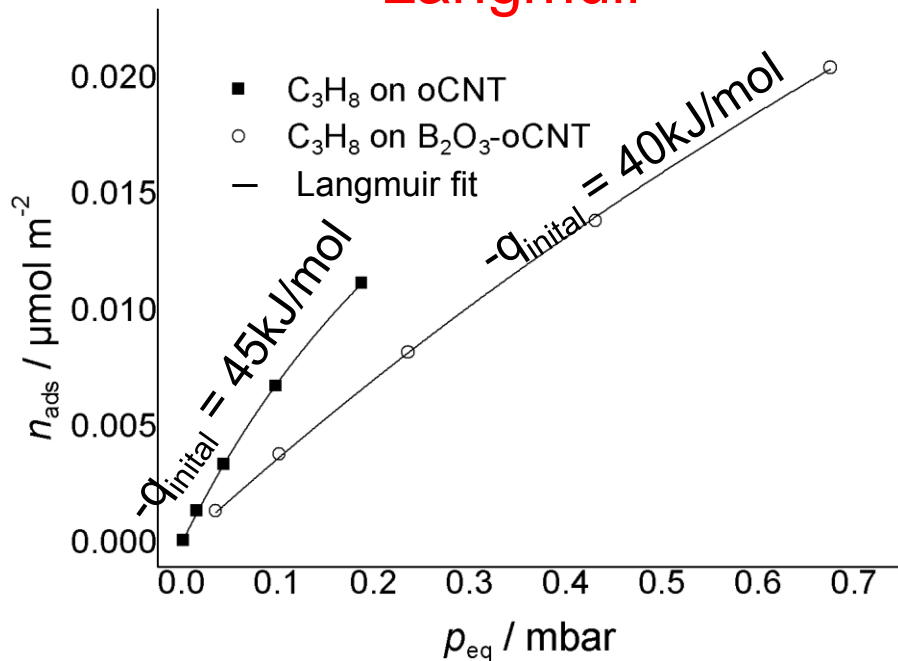
$$\theta = \frac{K p}{1 + K p} \quad K: \text{Langmuir adsorption constant}$$

$$\theta = \frac{RT}{q_{ads}^{(\theta=0)} - q_{ads}^{(\theta=1)}} \ln \left(\frac{1 + \frac{p}{p^*} \exp \frac{q_{ads}^{(\theta=0)}}{RT}}{1 + \frac{p}{p^*} \exp \frac{q_{ads}^{(\theta=1)}}{RT}} \right)$$

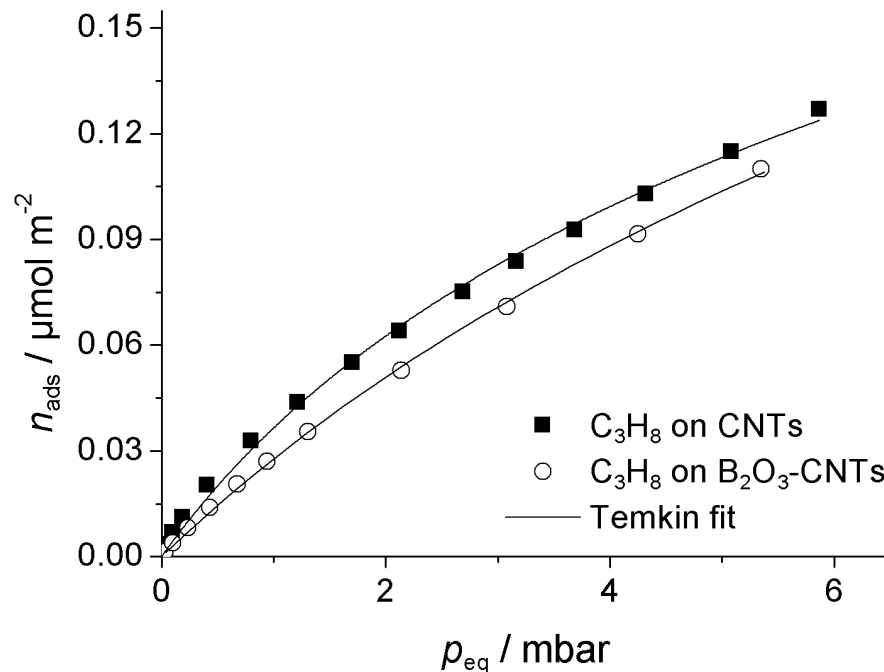
p^* : is a constant combining surface and molecular properties

Energetically non-uniform sites
 (decay of q_{ads} with increasing coverage) → **Temkin model**

Langmuir

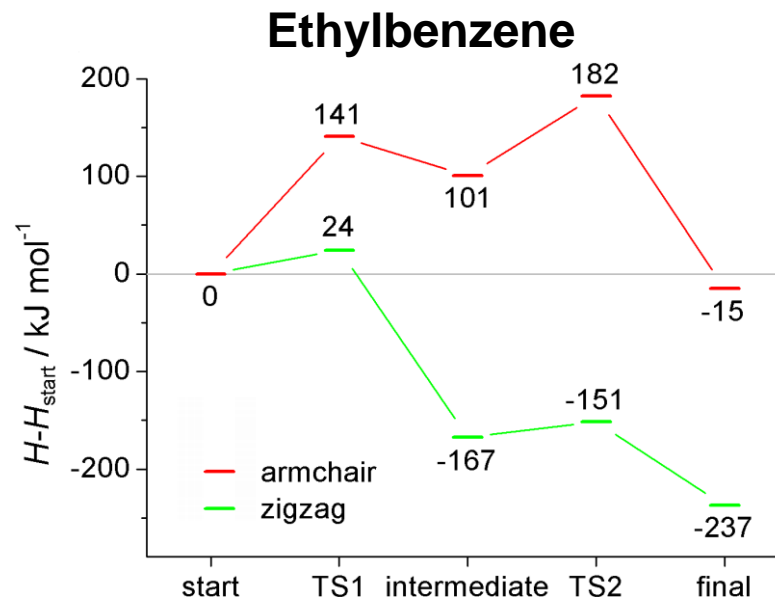
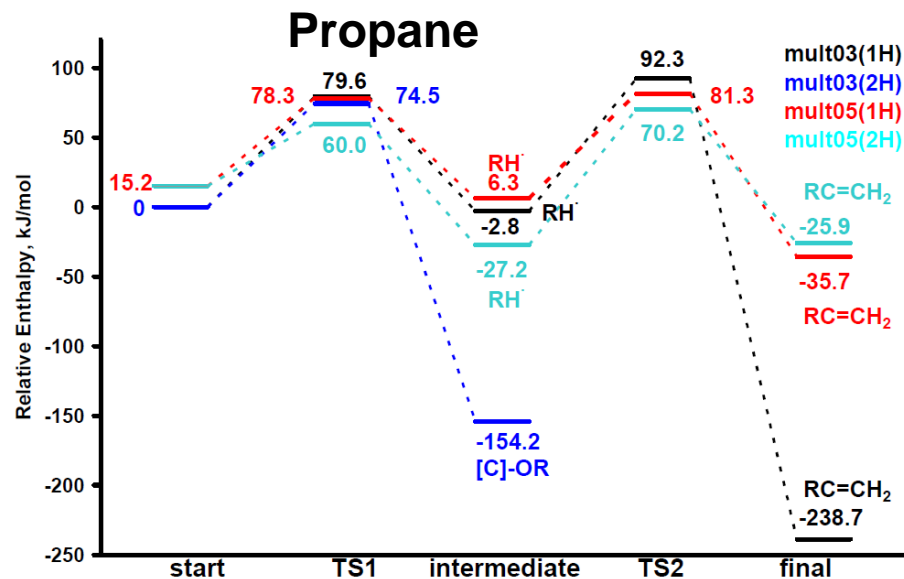


Temkin

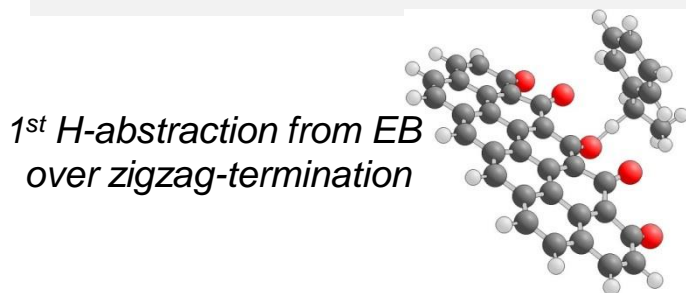


	<i>K</i> (Langmuir adsorption constant)	<i>p</i>[*] (Temkin factor, combining surface and molecular properties)
oCNT	2250 bar ⁻¹ (45kJ/mol)	0.0065 bar
B₂O₃-oCNT	370 bar ⁻¹ (40kJ/mol)	0.048 bar

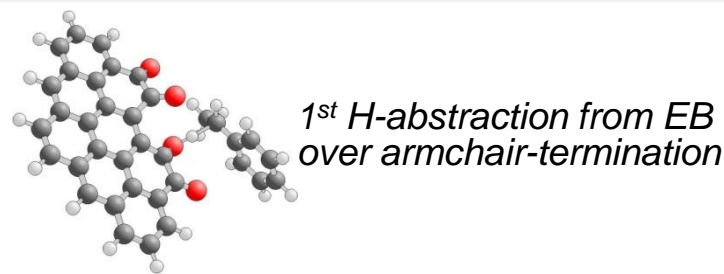
Energy Diagram for ODH of propane and EB (1st H-abstraction) over zigzag-termination of the carbon cluster



- the barrier for activation of propane is higher than for EB
- the zigzag-termination is much more active than the armchair geometry



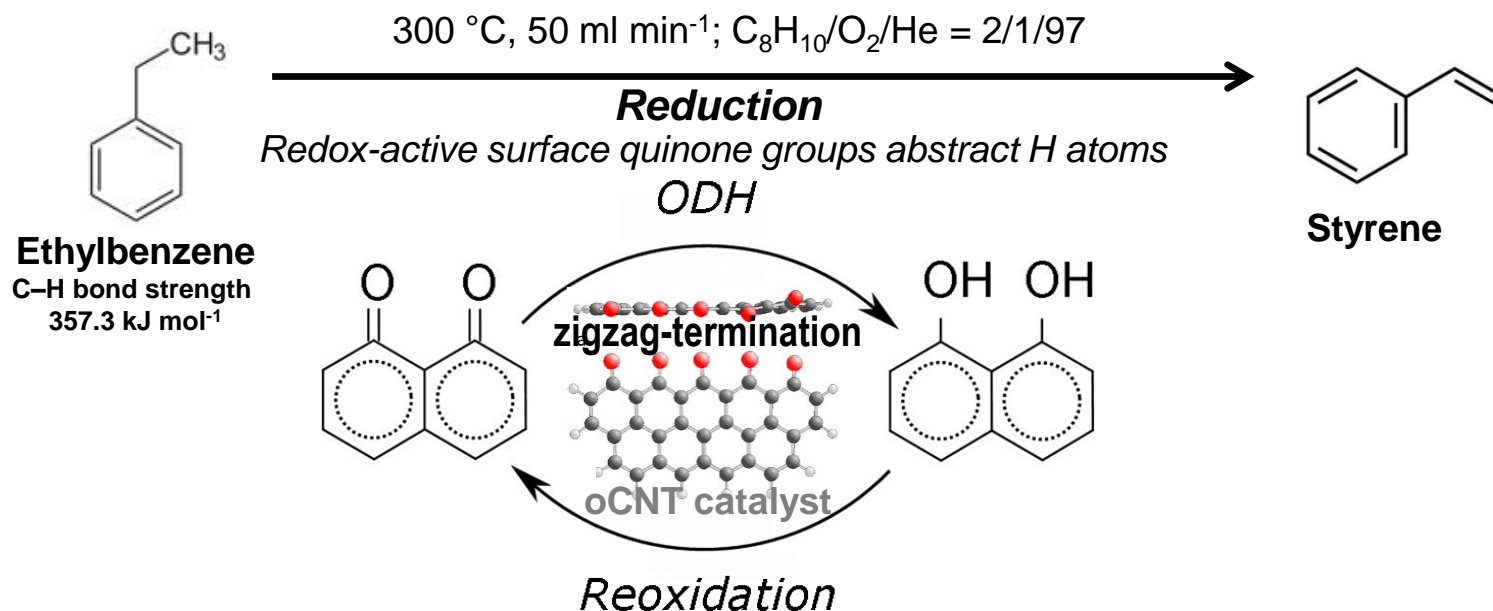
Quinones
Hydrogen
Carbon



[1] O. V. Khavryuchenko, B. Frank, A. Trunschke, K. Hermann, R. Schlögl, J. Phys. Chem. C 117 (12) (2013) 225

- Classification and quantification of the of the carbon surface under reaction conditions.
- EB: lower activation barriers and stronger irreversible adsorption well correlate with the lower stability of the benzylic C-H bond over the aliphatic C-H bond in propane

two-site redox kinetics:

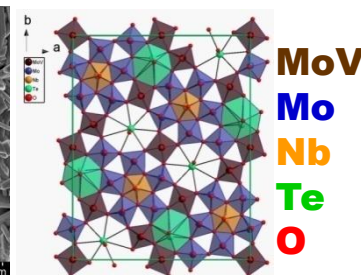
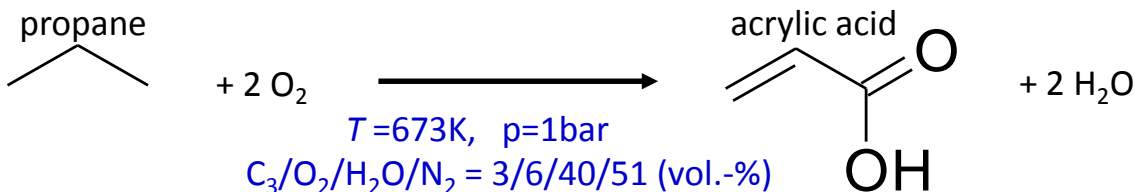


- The redox cycle of surface C=O and C-OH groups is the key process, which includes only a small fraction of surface O species (2.4 m² g⁻¹, 8 μmol/g, 3-5% _{Calo/XPS}) and favorably occurs at the zigzag-termination of sp² carbon planes.



Study of catalytic relevant sites
via calorimetry close to the reaction conditions:

**Selective oxidation of propane to acrylic acid
over MoVTeNb oxide catalyst**



Intention: study of the post-reaction state of the surface “used catalyst” in comparison with the prepared state of the surface “fresh catalyst” in order to describe a **structure-selectivity relationship**

Adsorption

★ propane as probe molecule

Microcalorimetry :

★ $T_{\text{adsorption}} = 313\text{K} < 673\text{K} = T_{\text{reaction}}$

★ selected catalysts: different selective catalysts

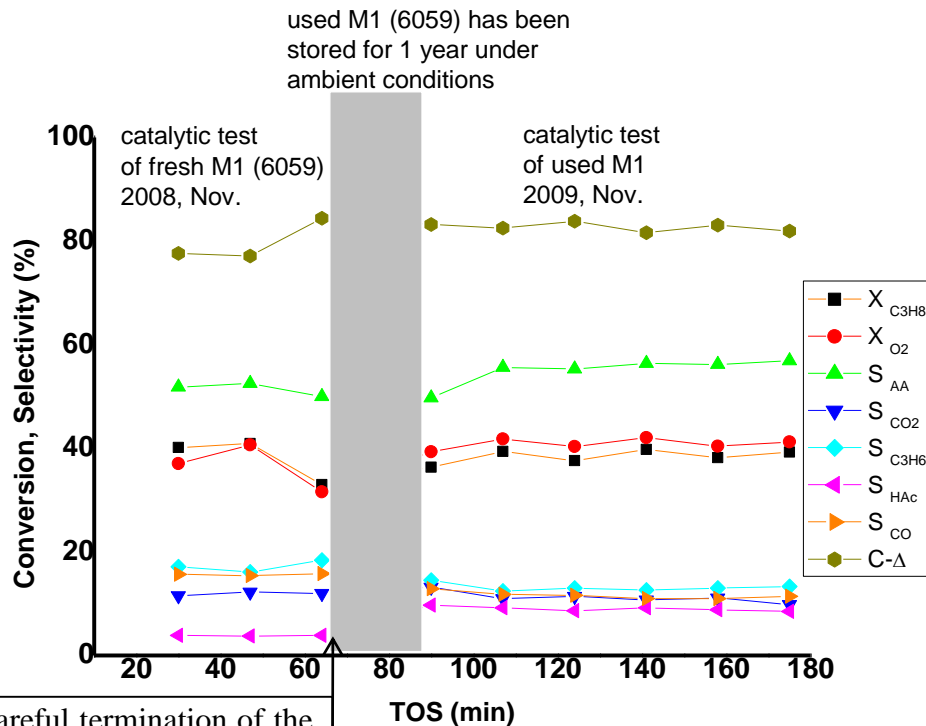
pure-phase MoVTeNb	S_{aa} = 53%
modified MoVTeNb by an oxidizing agent	S_{aa} = 37%
MoV oxide	S_{aa} = 1.8 %

[1] Botella, P., et al., *The preparation, characterization, and catalytic behavior of MoVTeNbO catalysts prepared by hydrothermal synthesis. Journal of Catalysis*, 2002. 209(2): p. 445-455.

[2] Ueda, W., et al., *Structural organization of catalytic functions in Mo-based oxides for propane selective oxidation. Catalysis Today*, 2004. 96(4): p. 235-240.

CATALYTIC TEST (fresh/used catalyst)

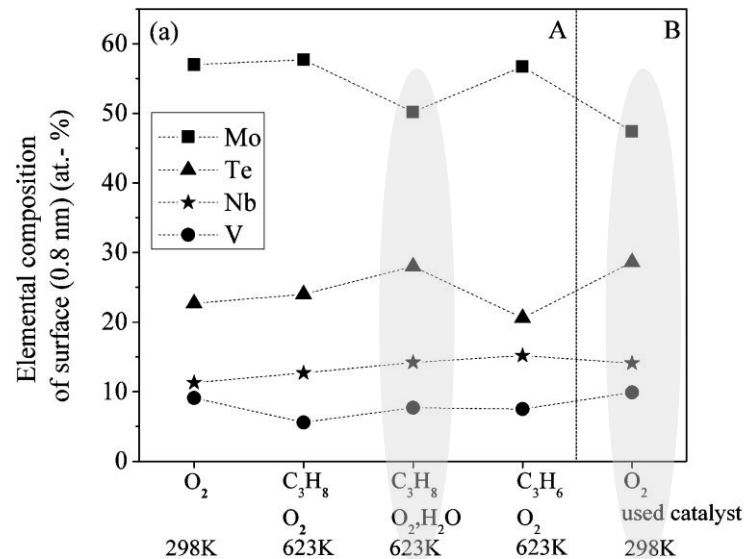
propane oxidation data obtained from fresh and used MoVTenb catalyst



Careful termination of the reaction under steam and N_2 with a cooling rate of 5 K/min.

SURFACE STUDY (fresh/used catalyst)

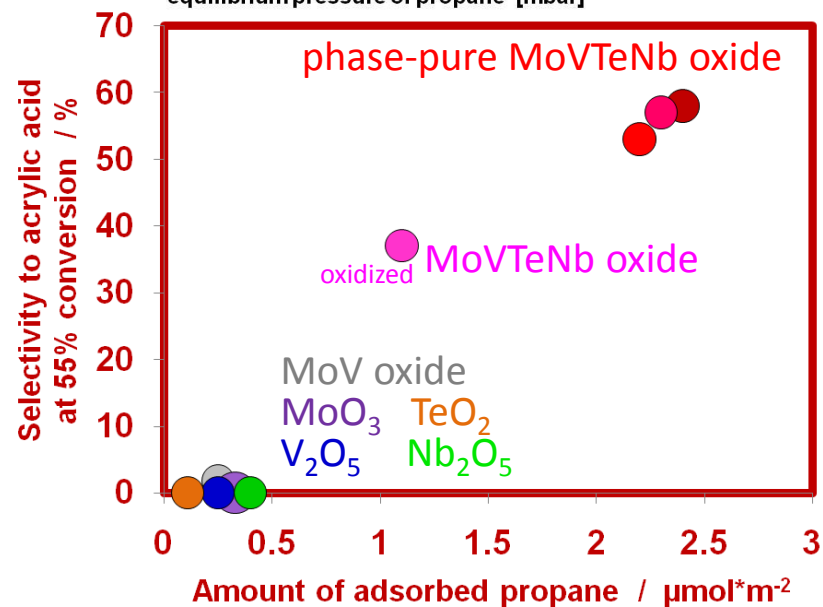
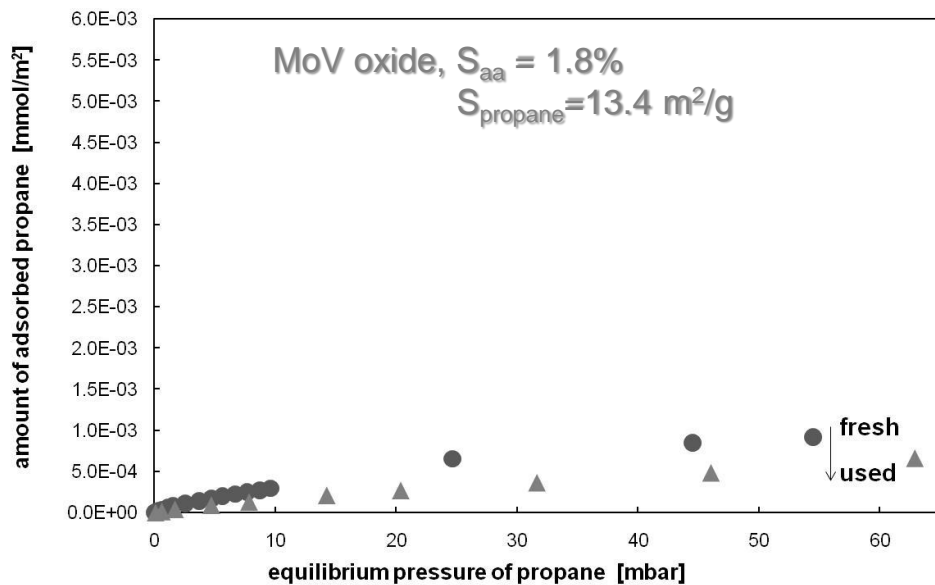
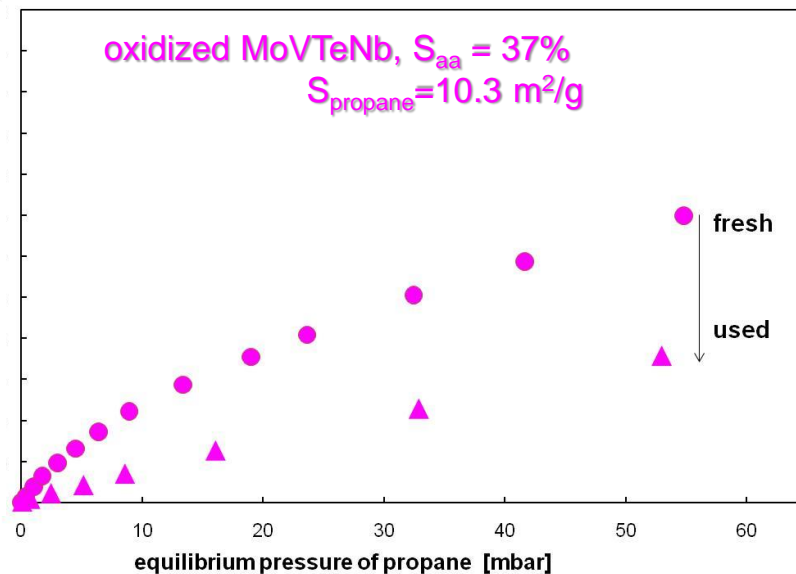
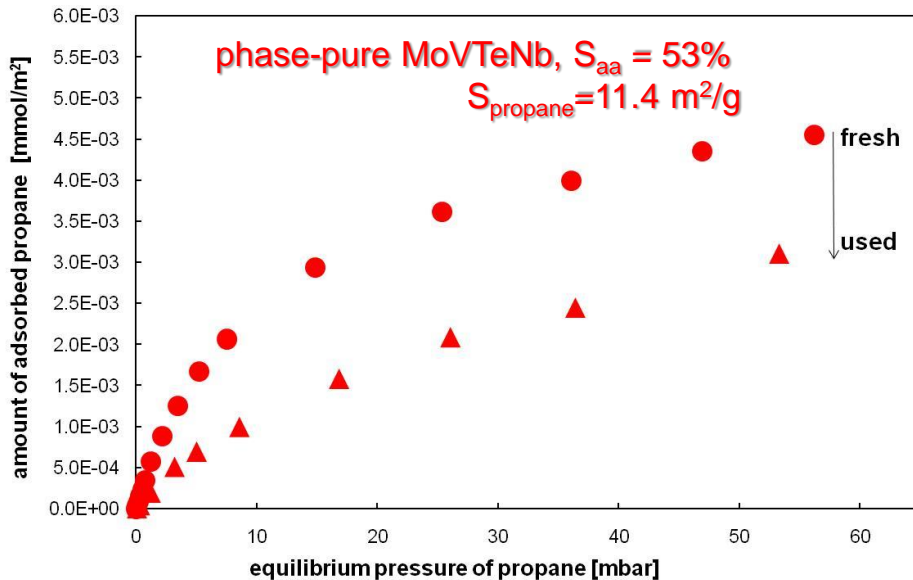
in situ XPS: surface element composition during and after PO over MoVTenb catalyst

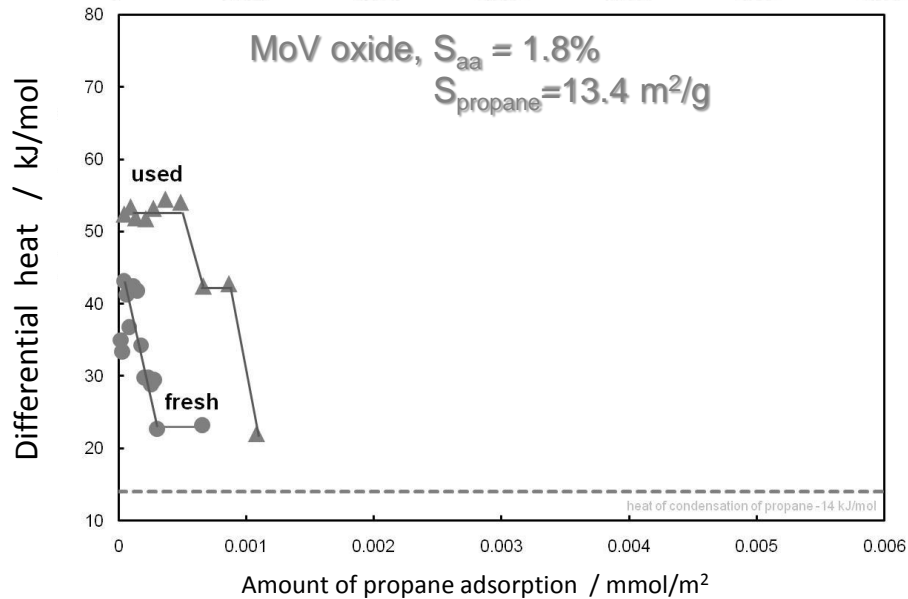
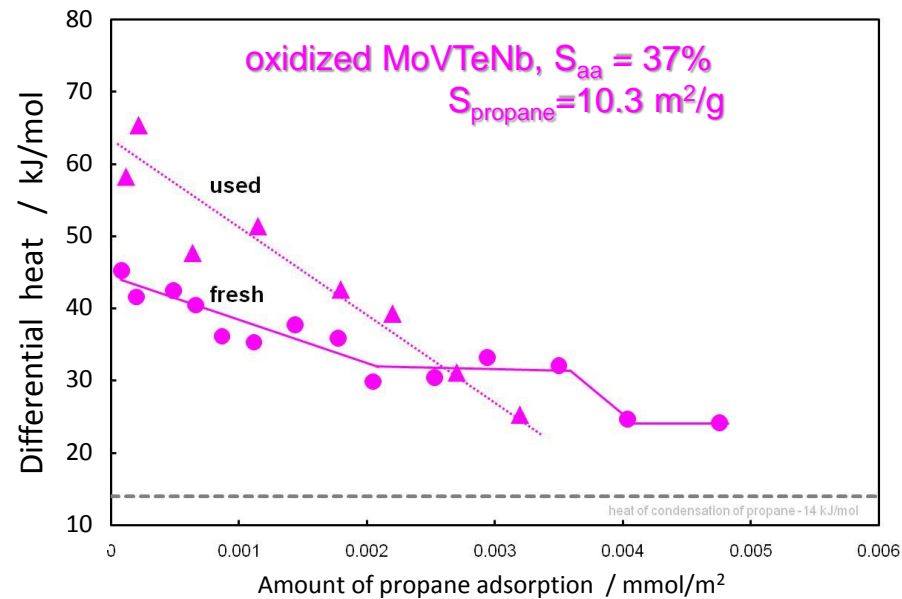
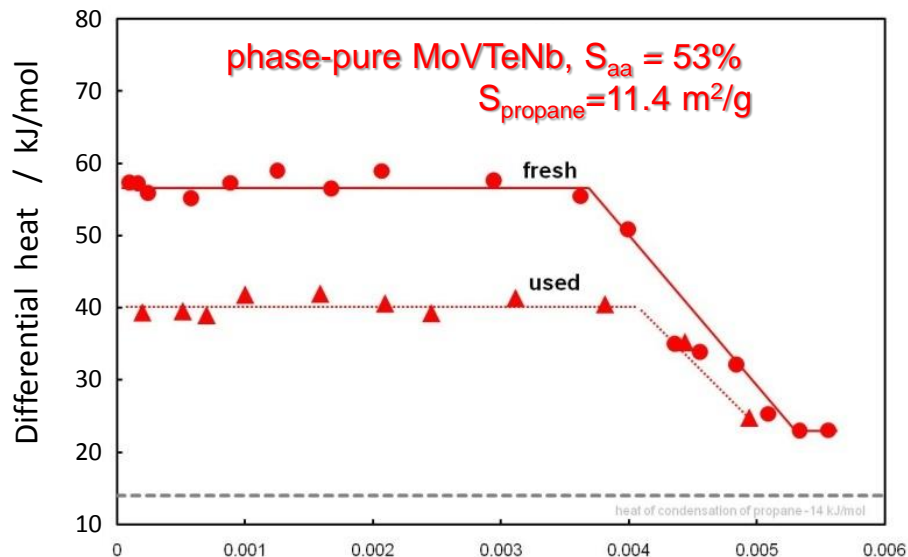


Surface composition of the used M1 is similar to the composition measured in the *in situ* experiment in the presence of steam.

[A. Celaya Sanfiz et al., *J. Phys. Chem. C*, 2010, 114, pp 1912]

***ex situ* surface analysis of the used catalyst can be done**





- ★ Strength of interaction of propane with the surface changes during reaction.
- ★ S_{aa} is correlated with energetically homogenous distributed propane adsorption sites
- ★ S_{aa} is associated with reduced interaction of propane and active surface sites
- ★ *CO & CO₂ ads. exp. : weak acid/basic sites*

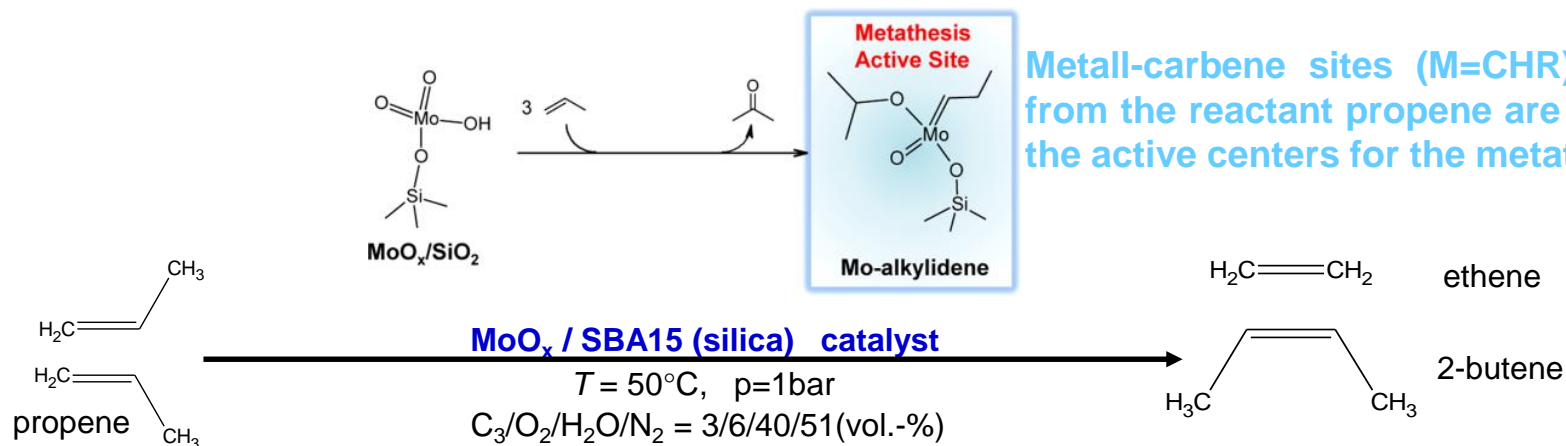
- ★ the prepared state of the surface is different from the post-reaction state of the surface
→ **dynamic surface during reaction**
- ★ remarkable selective ($S_{aa} = 53\%$) MoVTaNb oxide surface is characterized by
high density of energetically uniform propane adsorption sites
with weak acid-base character
- ★ The weaker interaction of propane with the post-reaction state of the surface is
apparently favorable for the catalytic performance;
perhaps because of facile product desorption.



Study of catalytic relevant sites
via calorimetry under reaction conditions:

**Active Site Quantification
on Propylene Metathesis over MoO_x/SBA-15**

Active Site Quantification on Propylene Metathesis over MoO_x/SBA-15



Intention: Studying of the catalytically active surface sites - quantification

Adsorption

★ propylene as probe molecule

Microcalorimetry :

★ $T_{\text{adsorption}} = 50^\circ\text{C} = T_{\text{reaction}}$

★ selected catalysts: different activity

13 % MoO_x/SBA15

Metathesis rate = **3.0** $\mu\text{mol}/\text{m}^2\cdot\text{h}$

10 % MoO_x/SBA15

Metathesis rate = **13.0** $\mu\text{mol}/\text{m}^2\cdot\text{h}$

5 % MoO_x/SBA15

Metathesis rate = **1.5** $\mu\text{mol}/\text{m}^2\cdot\text{h}$

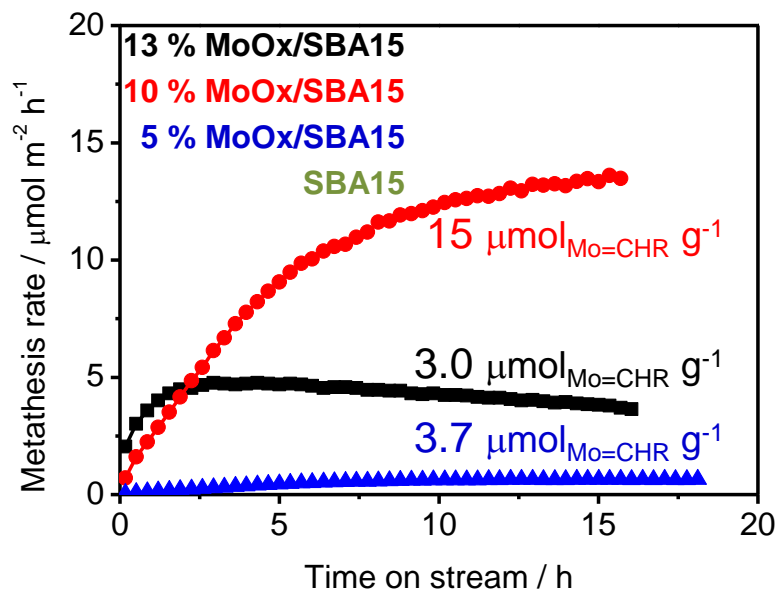
SBA15

Metathesis rate = **0.0** $\mu\text{mol}/\text{m}^2\cdot\text{h}$

Microcalorimetry

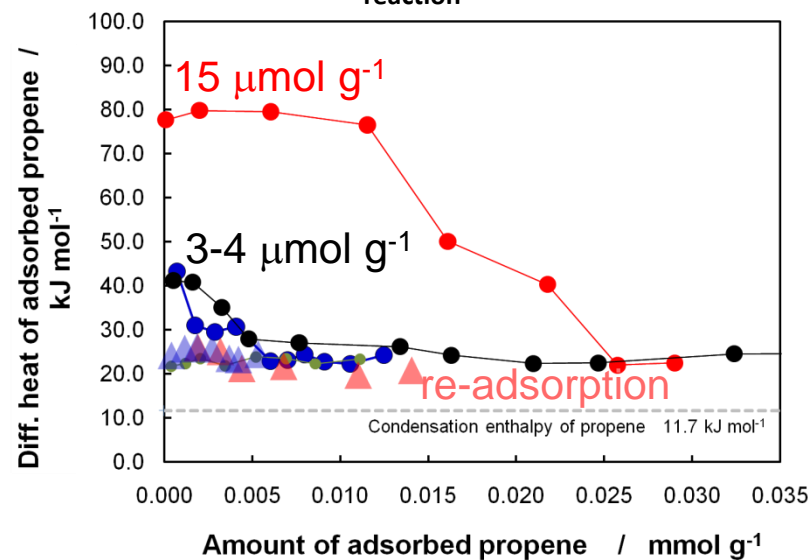
Propene Metathesis Activity

T = 50 °C



Differential heat of propene adsorbed on MoOx/SBA15

T_{reaction} = 50 °C

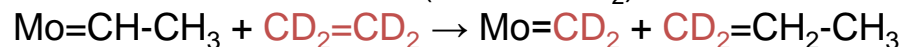


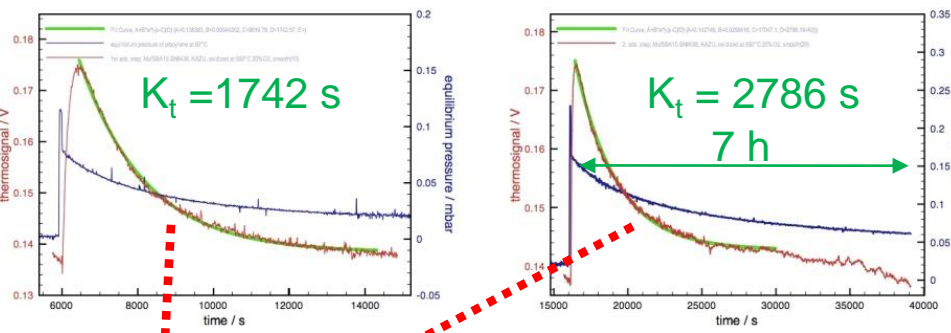
➤ Activity strongly depends on the Mo loading

➤ Correlation between amount & strength of C_3H_6 adsorption sites and catalytic activity.

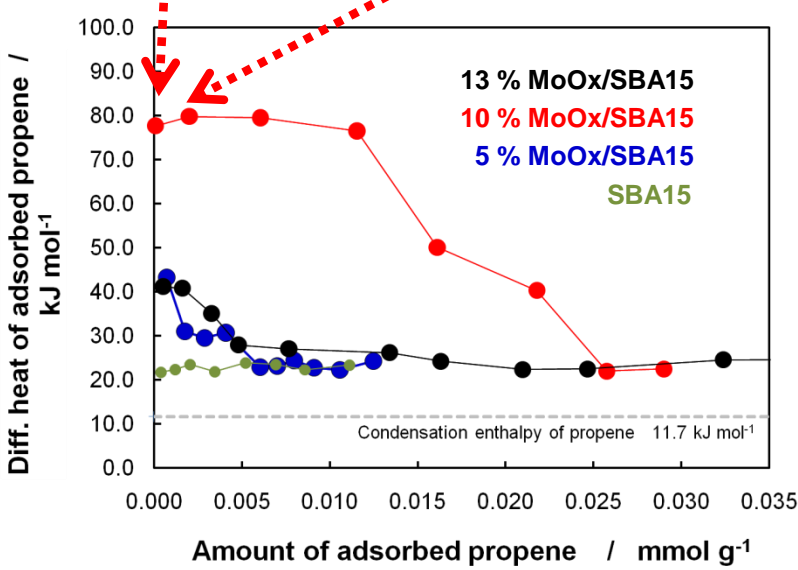
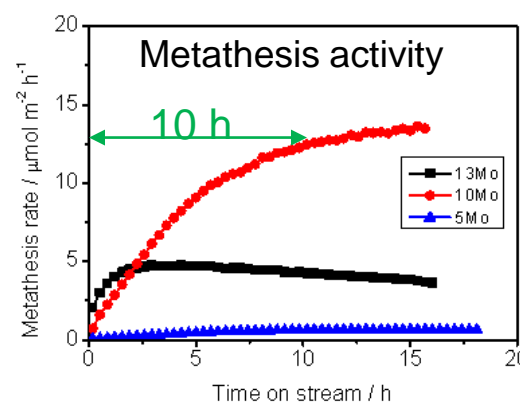
Post-reaction carbene titration

Active site counting was performed after metathesis using post-reaction ethene- d_4 ($\text{CD}_2=\text{CD}_2$) metathesis to titrate the formed metal-carbene ($\text{Mo}=\text{CH}-\text{CH}_2$) sites.

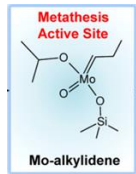
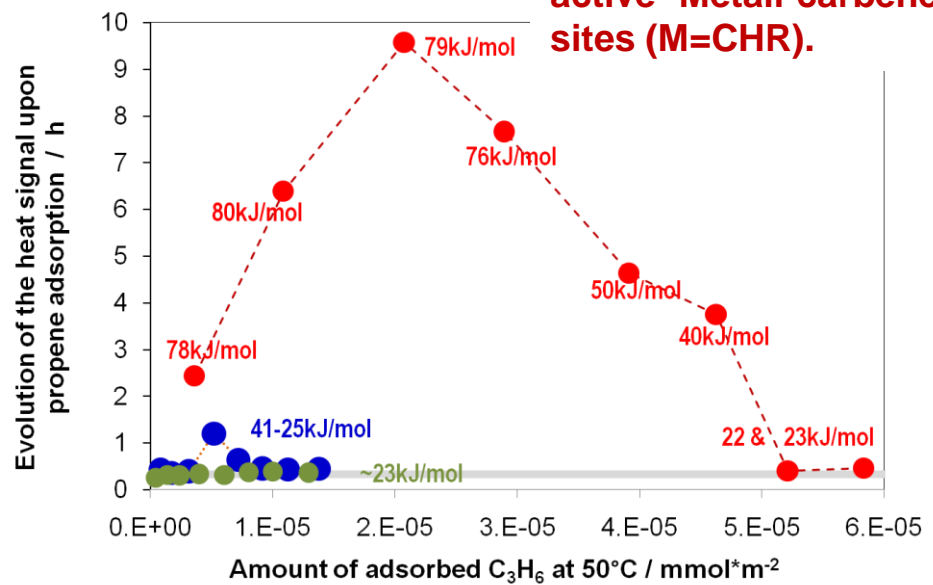




A long decay time and fine structure in the exothermic signal indicate reactive adsorption.



Generation of the active Metall-carbene sites ($\text{M}=\text{CHR}$).

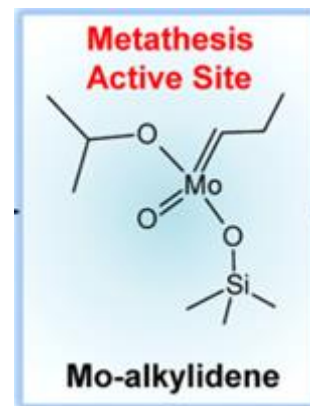


Active Site Quantification on Propylene Metathesis over MoO_x/SBA-15

- The active catalyst is characterized by:
- higher amount of ads. sites for propylene
 - strong and irreversible adsorption of propylene on MoO_x sites
 - energetically homogenously distributed active sites

- Catalytic activity is directly correlated with the strength of the propylene interaction with the active surface site.

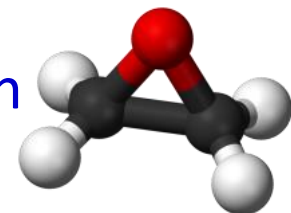
- ca. 1% of Mo atoms formed active sites





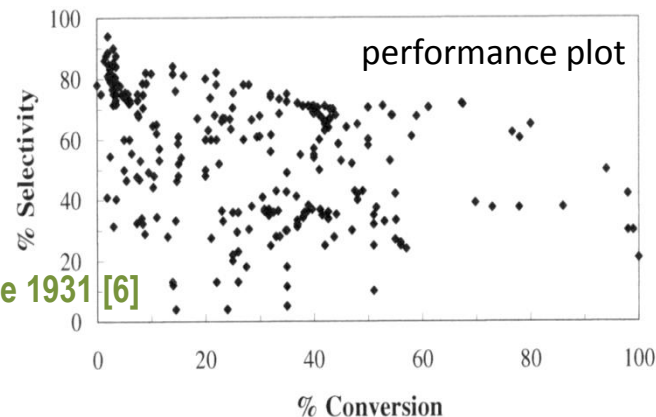
Study of catalytic relevant sites via calorimetry under reaction conditions:

Silver as a catalyst for the ethylene epoxidation
- Ag-O system in catalysis -



- **Ag** is used as a catalyst in two important large scale processes in the chemical industry, the **ethylene epoxidation** and **methanol oxidation**.

The **economic relevance** of these processes motivated the extensive investigation of the Ag-O system in past years. The mechanisms behind the **remarkable selectivity** are still unclear.



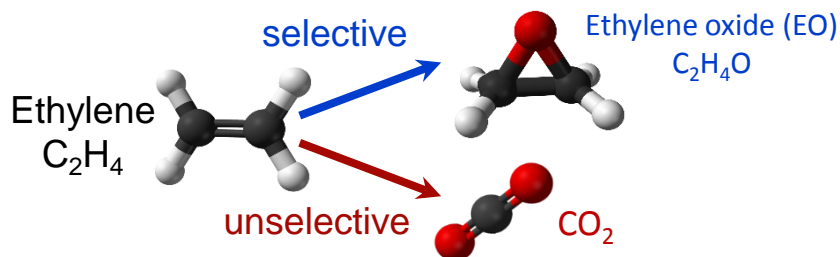
- The current understanding of oxidation reactions on Ag catalysts rely on the knowledge about the **oxygen species formed on silver** [1].
- Final goal is to safely **translate the electronic signatures** obtained by X-ray spectroscopies **into structural information**, which can be used to construct reaction mechanisms [4,5].

- [1] C. Hess, R. Schlögl, A. T. Bell, A. Trunschke, A. Knop-Gericke, Nanostructured Catalysts: Selective Oxidations, Royal Society Of Chemistry, 2011.
- [2] T. C. R. Rocha, A. Knop-Gericke, R. Schlögl, The Journal of Physical Chemistry C 2012, 116, 11408–11409.
- [3] R. Reichelt, S. Gunther, J. Winterlin, Journal of Physical Chemistry C 2011, 115, 17417–17428.
- [4] T. C. R. Rocha, A. Oestereich, D. V Demidov, M. Hävecker, S. Zafeiratos, G. Weinberg, V. I. Bukhtiyarov, A. Knop-Gericke, R. Schlögl, Phys. Chem. Chem. Phys. 2012, 14, 4554–64.
- [5] V. I. Bukhtiyarov, M. Hävecker, V. V. Kaichev, A. Knop-Gericke, R. W. Mayer, R. Schlögl, Phys. Rev. B 2003, 67, 235422.
- [6] B. K. Hodnet, Heterogeneous Catalytic Oxidation, John Wiley & Sons, New York, 2000.

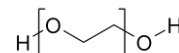
The Ag-O system in catalysis

epoxidation of ethylene over silver catalyst

$T = 180 - 230 \text{ }^\circ\text{C}$



versatile
intermediate

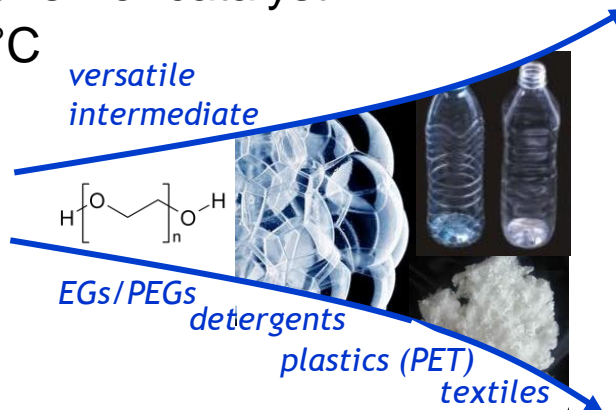


EGs/PEGs

detergents

plastics (PET)

textiles



Intention: to construct reaction mechanisms. The energetic data provided by calorimetry is essential to any reaction mechanism. It will provide additional information to interpret the spectroscopic measurements and it will also be used as **reality check for the predictions of the computational calculations.**

quasi in situ

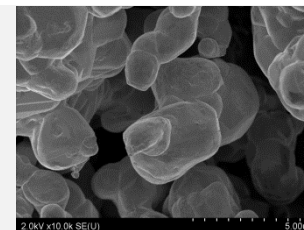
★ Oxygen

Adsorption:

★ $T_{\text{reaction}} = 230 \text{ }^\circ\text{C}$

Microcalorimetry

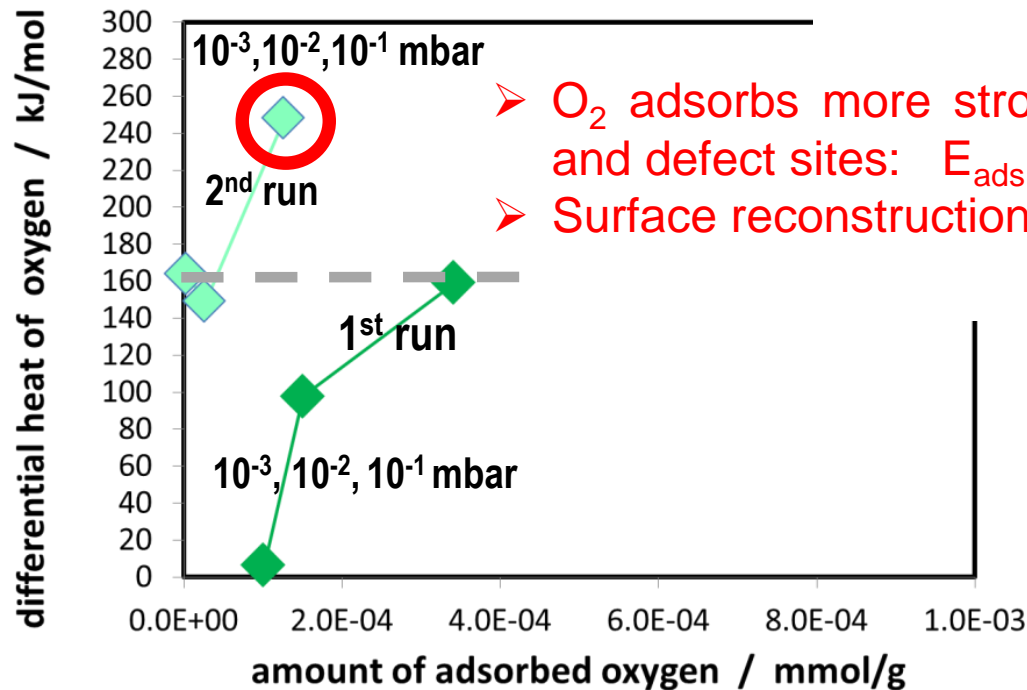
★ selected catalyst: Ag powder <45micron



Initial State

Cleaning of the silver surface observed by calorimetry

Differential heat of O₂ ads. at 150°C



DFT

- O₂ adsorbs more strongly on Ag modified by O_{sub} and defect sites: E_{ads.} = 180 – 240 kJ/mol
- Surface reconstructions: E_{ads.} = 120 – 160 kJ/mol

$q_{\text{diff}} \uparrow$ is due to the exothermic reaction of oxygen atoms with the carbon contaminants (CH_x/CO₃).

References:

- 200 to 400 kJ/mol: combustion of impurities [4]
- 50 to 420 kJ/mol : combustion of contaminants [5]
- 171 kJ/mol at 170° C: combustion of impurities [6]

Note: mild pre-treatment (150° C, 0.1 mbar, 2h) is enough to clean the samples also observed by NAP-XPS

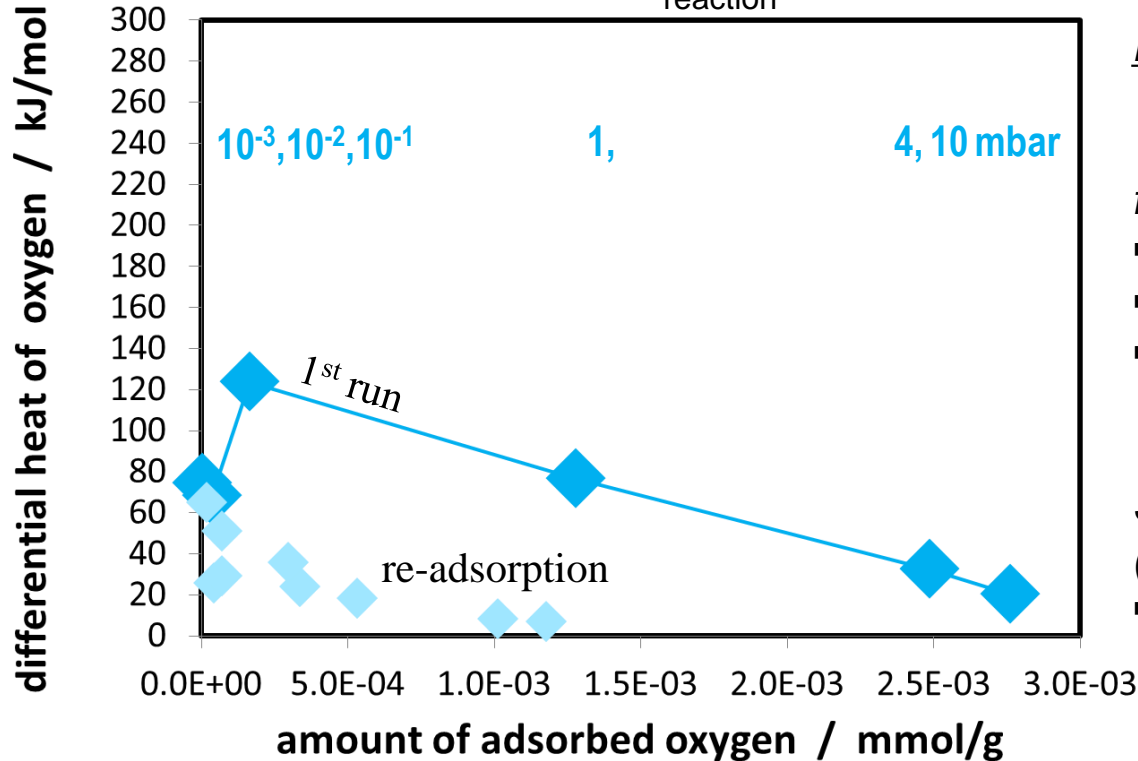
[4] Auroux, A. & Gravelle, P.C., 1981. Comparative study of the bond energy of oxygen at the surface of supported silver catalysts and of the activity of these catalysts for ethylene epoxidation. *Thermochemica Acta*, 47, pp.333–341.

[5] Anderson, K.L., Plischke, J.K. & Vannice, M., 1991. Heats of Adsorption of Oxygen, Ethylene, and Butadiene on Al₂O₃-Supported Silver. *J. of Catalysis*, 160, pp.148–160.

[6] Anderson, K.L., Plischke, J.K. & Vannice, M., 1991. Heats of Adsorption of Oxygen, Ethylene, and Butadiene on Al₂O₃-Supported Silver. *Journal of Catalysis*, 160, pp.148–160.]

Steady State

Differential heat of O₂ ads. on the clean Ag surface
at 230°C = T_{reaction}



References:

[12]

H is the standard enthalpy of formation for model adsorbates at 298.15 K

- O_{ads.} : H = -63.0 kJ/mol
- O_{2 ads.} : H = -44.5 kJ/mol
- O_{ads.} / O_{surface} : H = -103.0 kJ/mol

[13]

Standard enthalpies of formation at 298 K (ΔH_f°) of O adatoms on Pt(111):

- 109 – 99 kJ/mol

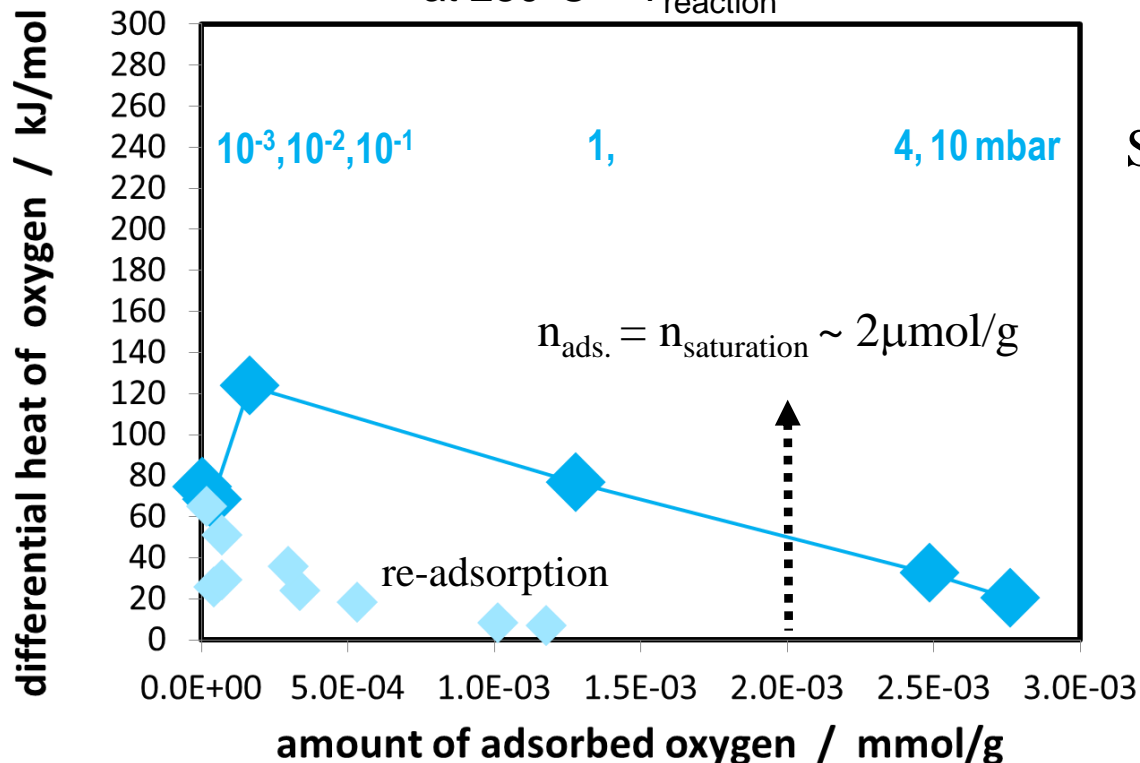
Note: The enthalpy is insignificantly affected by the temperature (DFT)

[12] C. Stegelmann, N.C. Schiødt, C.T. Campbell, and P. Stoltze, J. Of Catal. 221 (2004) 630-649.

[13] Eric M. Karp, Charles T. Campbell, Felix Studt, Frank Abild-Pedersen and Jens K. Nørskov; SLAC-PUB-15339.

Steady State

Differential heat of O₂ ads. on the clean Ag surface
at 230°C = T_{reaction}



Specific surface area of Ag for O₂
at T_{reaction} = 230°C

$$S_{\text{Ag}} = \frac{n_{\text{ads.}} \cdot \text{Avogadro constant}}{\text{Surface sites density } \Gamma_{\text{fcc lattice, Ag}}}$$

$$\frac{2 \cdot 10^{-6} \text{ mol} \cdot 6.022 \cdot 10^{23} \text{ particles} \cdot \text{cm}^2}{\text{g} \cdot 1.4 \cdot 10^{15} \text{ atoms} \cdot \text{mol}}$$

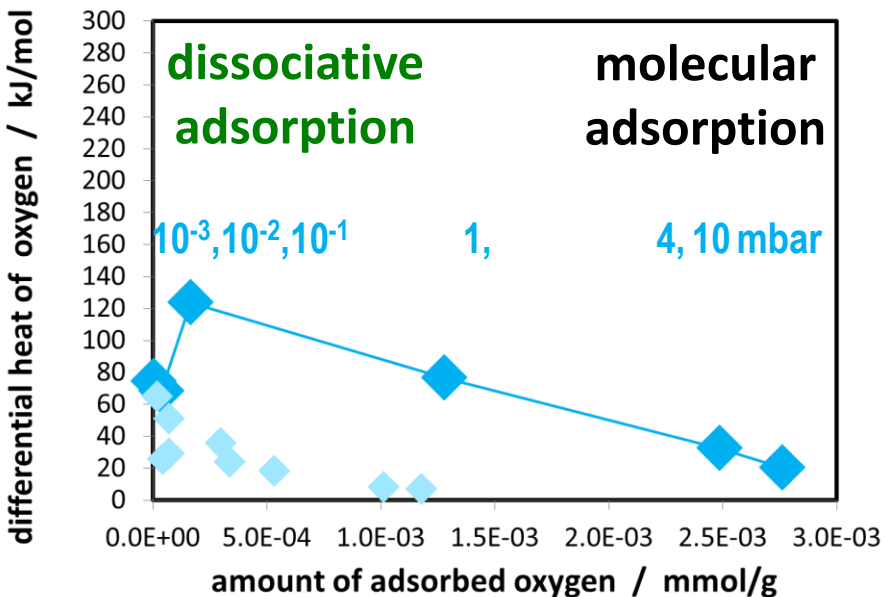
$$S_{\text{Ag-O}} = 0.86 \text{ m}^2/\text{g}$$

$$\text{BET}_{\text{N}_2, 77\text{K}} = 0.72 \text{ m}^2/\text{g}$$

$$\Delta S = 0.14 \text{ m}^2/\text{g}$$

The **excess** can be due to dissolving of oxygen into the Ag subsurface.

Experiment

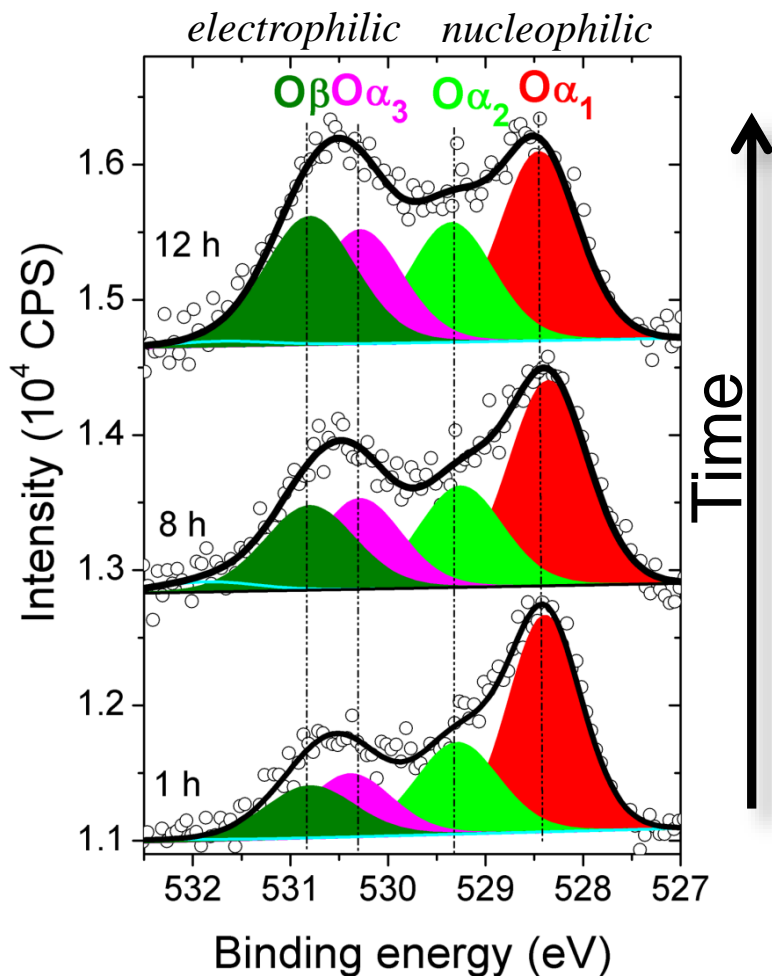


Theory

DFT calculations

system	E _{ads} per 1/2 O ₂ [kJ/mol]	E _{ads} per O ₂ [kJ/mol]
reconstructions O _{ads} stronger on Ag(110)	60-80	120-160
unreconstructed O _{ads} on hollow sites of Ag(111)	40-60	80-120
on subsurface O	110-120	220-240
surface defects	90-120	180-240
subsurface	<10	10
grain boundaries	10-20	20-40
O ₂ clean surface	5-10	10-20
O ₂ on sub O	10-20	20-40
O ₂ on defects	20-30	40-60

O1s XPS spectra for Ag powders measured in situ under 0.5 mbar O₂ at 180 °C



The **distribution of O species** on the Ag surface dynamically **changes with time** as the catalyst surface equilibrates with the gas phase at mbar pressure and temperatures typical of alkene (180-230 °C).
→ Dynamics at 180 °C

T ° C	p_{O_2} mbar	$n_{ads.}$ $\mu\text{mol}_{O_2}/g_{Ag}$	q_{diff} kJ/mol	Ag-O dynamics	DFT
$T_{cleaning}$ 150	$< 10^{-1}$	0.5	$>120 - 260$	<ul style="list-style-type: none"> ➤ dissociative adsorption ➤ cleaning the surface from CH_x/CO_3 ➤ initial formation of the surface reconstructions 	
$T_{reaction}$ 230	$10^{-1} - 1$	1.5	$>50 - 120$	<ul style="list-style-type: none"> ➤ extensive structural changes * ➤ oxygen begins to dissolve to subsurface ** ➤ oxide-like structures = $60 - 80 \text{ kJ/mol}^{[8]}$ ➤ chemisorbed oxygen modified by a subsurface oxygen *** 	
$T_{reaction}$ 230	$>1 - 10$	1	< 50	<ul style="list-style-type: none"> ➤ molecular oxygen adsorbed on surface vacancies **** ➤ formation of electrophilic oxygen ***** ➤ O_2 on subsurface oxygen 	

* Ag atoms moving from defects and edges to form the reconstructions. Island formation at low coverages.

** Formation of oxide like reconstruction and/or surface oxide layer.

*** Depends on time/temperature because its formation is limited by oxygen diffusion to subsurface.

**** Proposed by theory and calorimetry. In this case the time/temperature dependence is related to the defect formation.

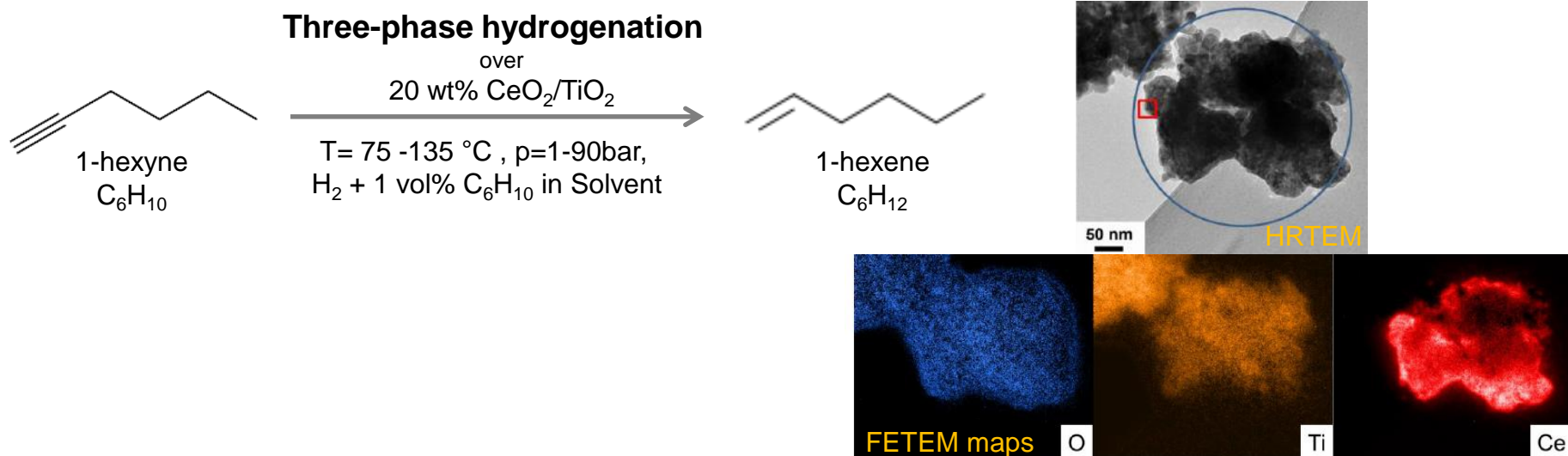
***** The active site for epoxidation! Two interpretations are believed: O_2 stabilized on defects on O covered surface (DFT) or surface oxygen modified by sub-surface species (XPS)



Study of catalytic relevant sites via calorimetry under reaction conditions:

1-hexyne adsorption at $T_{\text{react.}}$ on supported ceria ,
being unexpectedly active in the hydrogenation of 1-hexyne

1-hexyne adsorption at $T_{\text{react.}} = 80^\circ\text{C}$ on supported ceria



Intention: Does calorimetry offers the possibility to distinguish between catalysts of similar characteristic properties ($\text{IR}, \text{XRD}, \text{TEM}, \text{XPS}, \text{BET}$), but different catalytic activity?

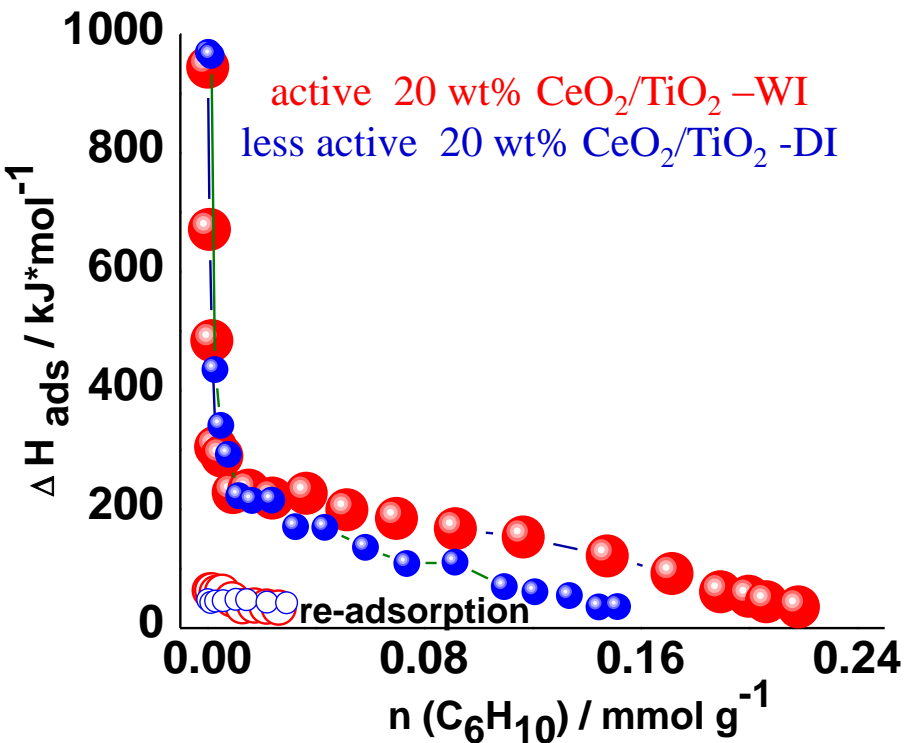
Adsorption
Microcalorimetry :

- ★ 1-hexyne as probe molecule
- ★ $T_{\text{adsorption}} = 80^\circ\text{C}$ ← as the Arrhenius plot of 1-hexyne hydrogenation is smooth in the whole 75 - 135 °C range
- ★ selected catalysts: different active catalysts

20 wt% $\text{CeO}_2/\text{TiO}_2$ -WI	very active	(wet impregnation; # 17380)
20 wt% $\text{CeO}_2/\text{TiO}_2$ -DI	less active	(dry impregnation; # 17378)

1-hexyne adsorption at $T_{\text{react.}} = 80^\circ\text{C}$ on supported ceria

Differential heats



$\Delta H_{\text{ads.}, \text{initial stage}} : < \mathbf{200 - 900 \text{ kJ/mol}}$ $10 \mu\text{mol/g}$

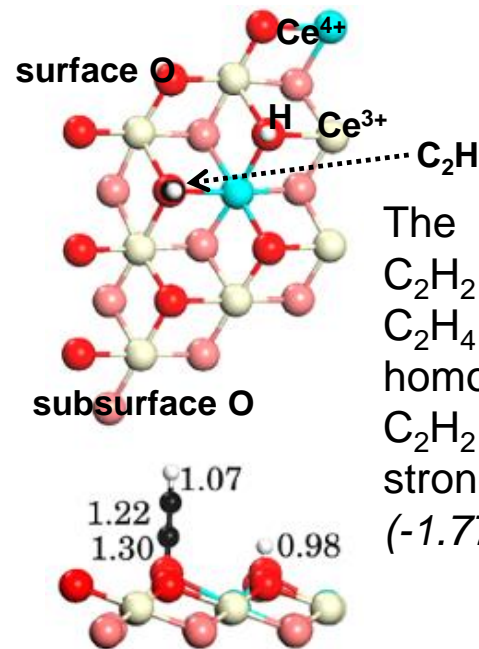
→ very strong irreversible ads.
→ multiple dehydrogenation steps ^[1]

formation of stable surface intermediates ^[2]

$\Delta H_{\text{ads.}, \text{plateau}} \sim \mathbf{200 \text{ kJ/mol}}$ $60 \mu\text{mol/g}$

→ dissociative homolytic adsorption of C_6H_{10}
→ single dehydrogenation step ^[1]

DFT calculations ^[1]



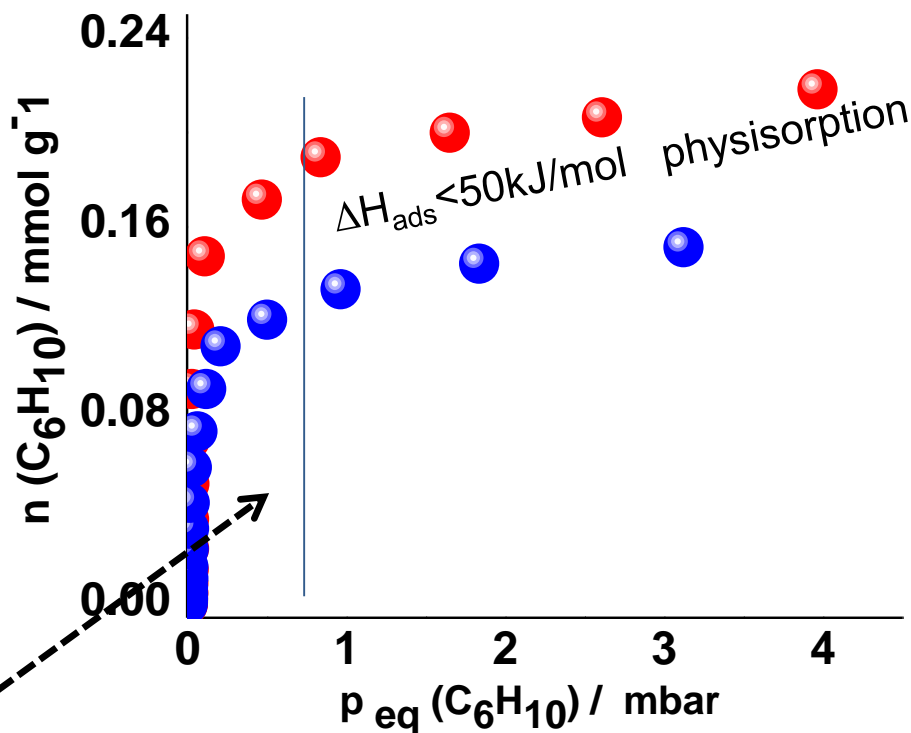
The initial step of the C_2H_2 hydrogenation to C_2H_4 is the dissociative homolytic adsorption of C_2H_2 . This process is strongly exothermic. (-1.77eV)

[1] J. Carrasco, G. Vilé, D. Fernández-Torre, R. Pérez, J. Pérez-Ramírez, M. V. Ganduglia-Pirovano, *J. Phys. Chem. C* 2014, 118, 5352.

[2] Claire L. Pettiette-Hall, Donald P. Land, Robert T. McIver, Jr.,* and John C. Hemminger, *J. Am. Chem. Soc.* 1991, 113, 2755-2756.

1-hexyne adsorption at $T_{\text{react.}} = 80^\circ\text{C}$ on supported ceria

Adsorption Isotherm



$\Delta H_{\text{ads}} > 50 \text{ kJ/mol}$ - chemisorption

very active 20 wt% $\text{CeO}_2/\text{TiO}_2$ -WI \rightarrow 190 $\mu\text{mol/g}$ reacted 1-hexyne molecules

less active 20 wt% $\text{CeO}_2/\text{TiO}_2$ -DI \rightarrow 130 $\mu\text{mol/g}$ reacted 1-hexyne molecules

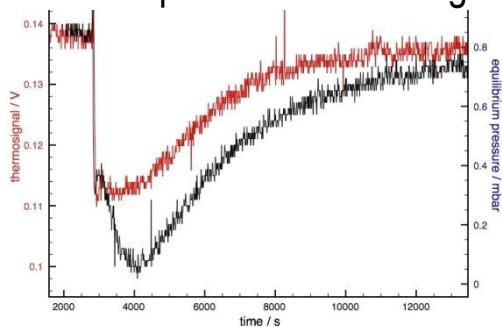
1-hexyne adsorption at $T_{\text{react.}} = 80^\circ\text{C}$ on supported ceria

Corresponding integral heats

The temporal evolution of the thermo signal during 1-hexyne ads.

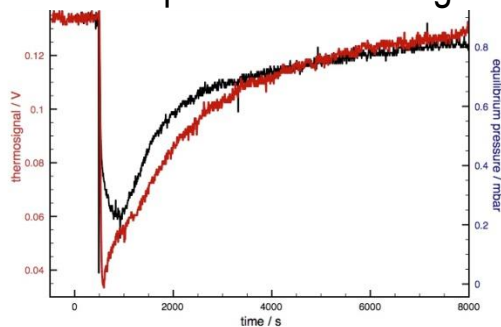
1st ads. step = 0.0023 mmol/g

1st ads. step = 0.00039 mmol/g



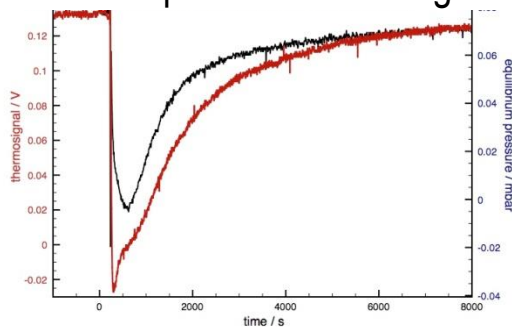
4th ads. step = 0.0031 mmol/g

3rd ads. step = 0.0029 mmol/g



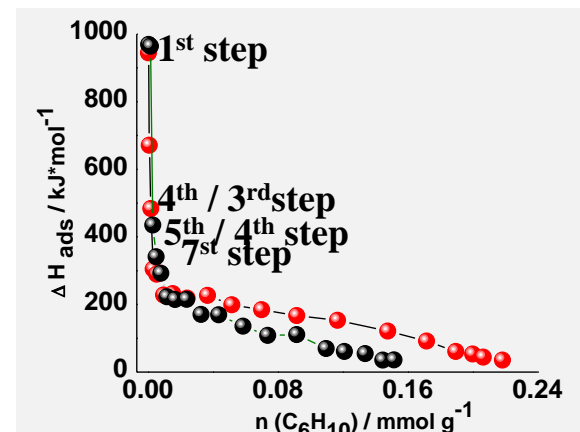
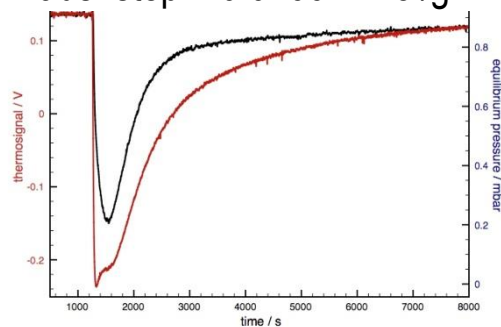
5th ads. step = 0.0053 mmol/g

4th ads. step = 0.0050 mmol/g



7th ads. step = 0.0153 mmol/g

7th ads. step = 0.0166 mmol/g



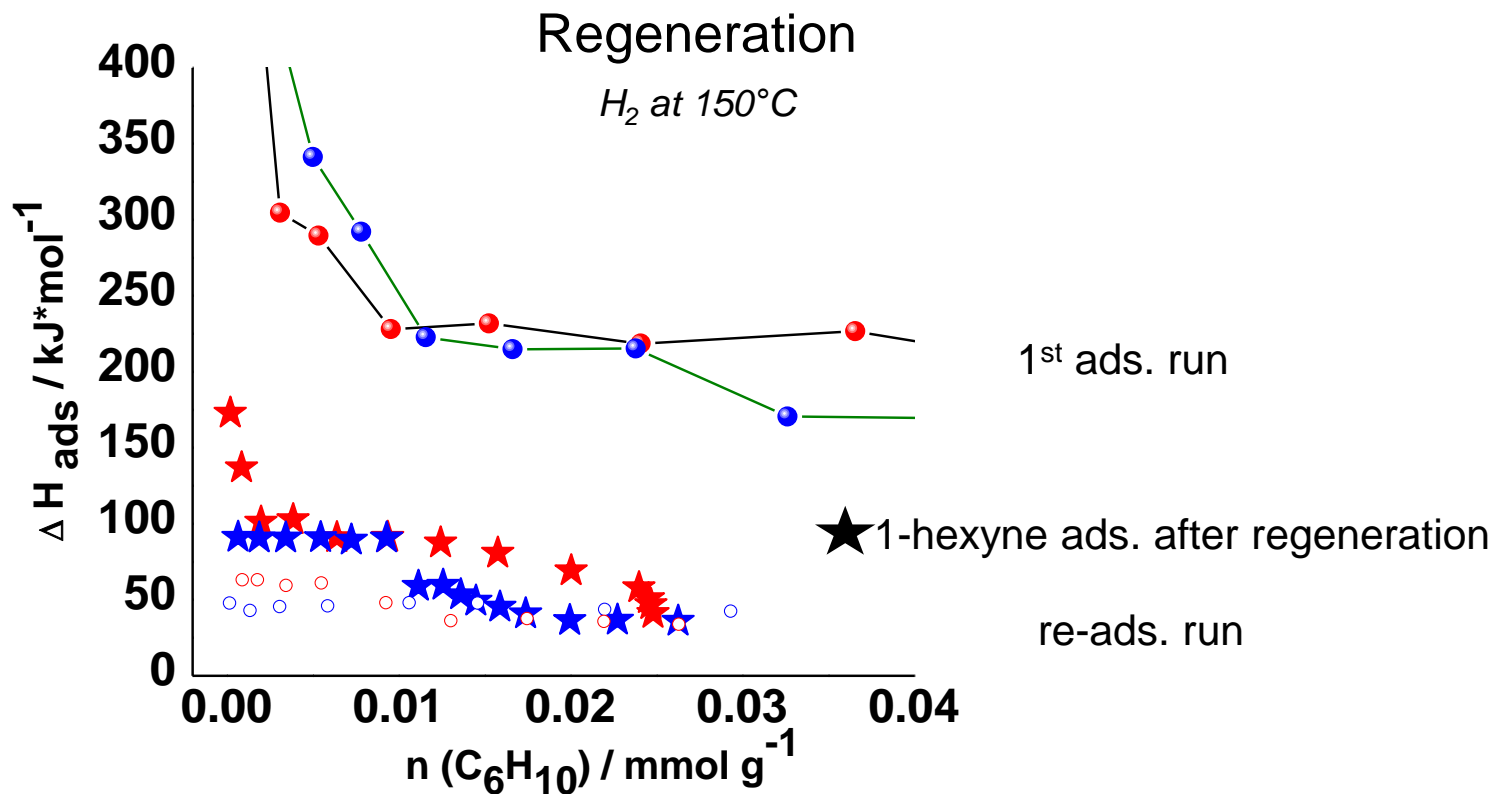
The adsorption signature is composed of two main contributions:

- physisorption / *fast-signal*
- reaction / *delayed signal*

The most active sample has such sites that will hold 1-hexyne very weakly until the molecule chemisorbs stronger. **dynamic**

In the less active sample the physisorbed molecule undergoes much faster side reactions or strong chemisorption.

1-hexyne adsorption at $T_{\text{react.}} = 80^\circ\text{C}$ on supported ceria



The regeneration of the catalyst surface using H_2 (at 150°C) has been somewhat more successful for the more active catalyst.

Summary

Yes, calorimetry is a useful tool to distinguish between catalysts of similar characteristic properties.

Key-note:

under reaction conditions a significant portion of the surface sites is covered by dehydrogenated species and is not available for hydrogenation. Nevertheless, the remaining small number of surface sites is active and selective in alkyne hydrogenation.

The ads. of 1-hexyne at T_{react} is composed of 2 main processes:

- 1) unspecific adsorption (physisorption $<50\text{kJ/mol}$)
- 2) time-consuming secondary process is due to single or multiple dehydrogenation steps and potentially oligomerization. ^[10] ($>50 - 900\text{ kJ/mol}$)

The most active catalyst is characterize by:

- higher amount of adsorption places for 1-hexyne $190\ \mu\text{mol/g}$
- slightly easier regeneration of the surface after 1-hexyne contact at T_{react} .
- pronounced trapped and phys. state of the adsorbates to find the most suitable place for reaction \rightarrow dynamic surface is apparently favorable for the catalytic performance



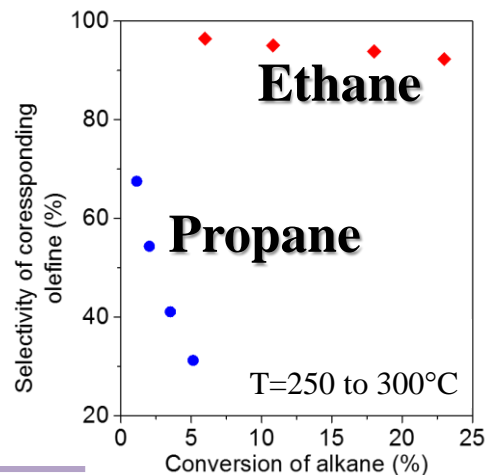
Reactants induced responses of catalyst surface:

Propane and ethane ads./des. cycles (40°C) on MoV oxide model catalyst for oxidative dehydrogenation of alkanes.

MoV oxide¹ has been studied as a **model system** for a better understanding of the **complex V-containing bulk MoVTaNb** oxide catalyst



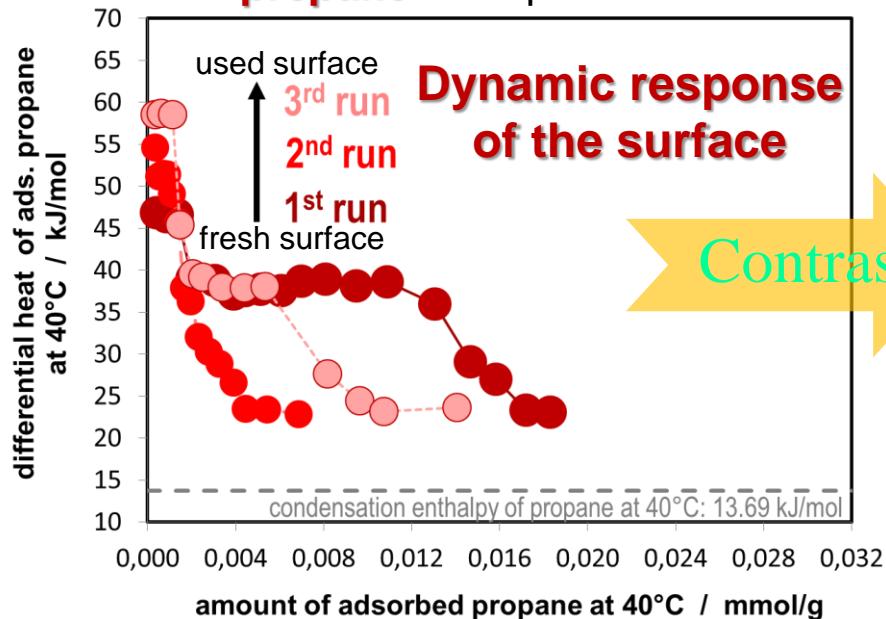
→ different dynamic behavior of the MoV oxide surface under reaction conditions due to the different chemical potential of the feeds while the chemical potential of the solid remains the same



Microcalorimetry

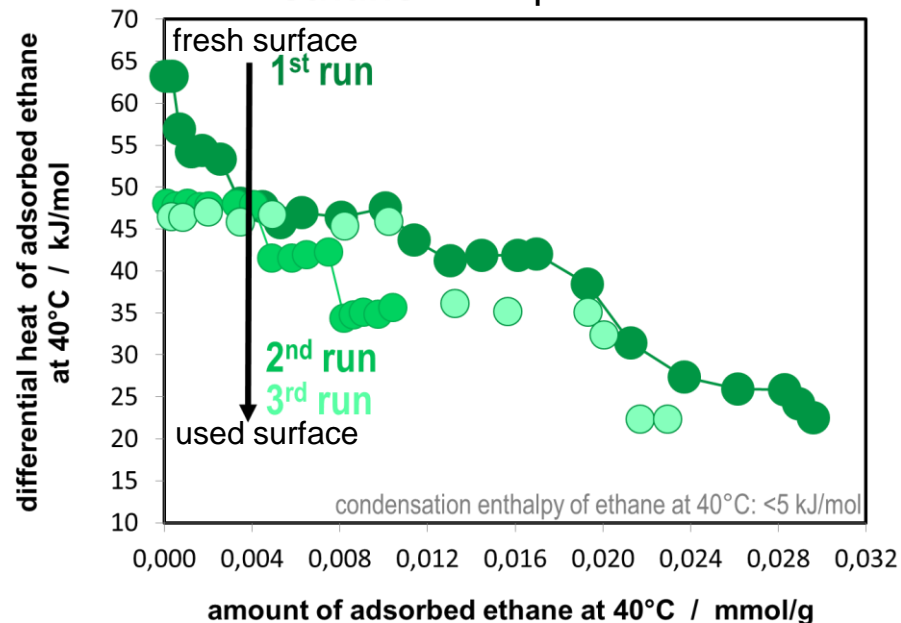
- specific ads. phenomena of PROPANE and ETHANE at 40°C
- reactants induced response of the MoV oxide surface via ads./des. cycles.

Differential heat of propane adsorption at 40°C



➤ $S_{\text{specific for propane}} \sim 3.6 \text{ m}^2/\text{g}$
 $BET = 25.52 \text{ m}^2/\text{g}$

Differential heat of ethane adsorption at 40°C



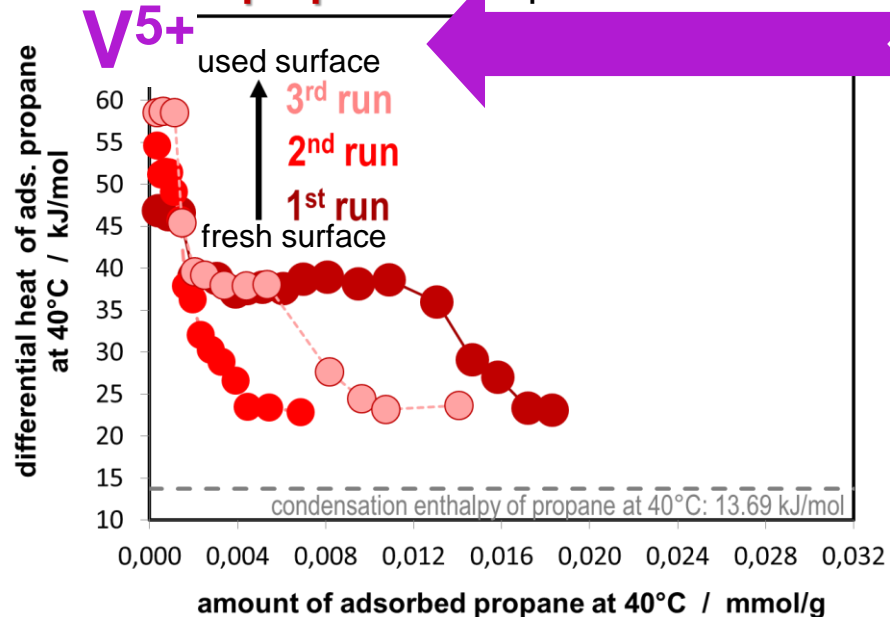
➤ $S_{\text{specific for ethane}} \sim 2.9 \text{ m}^2/\text{g}$
 $BET = 25.52 \text{ m}^2/\text{g}$

$$S_{\text{MoV oxide}} = n_{\text{ads.}} \cdot \text{Avogadro const.} \cdot S_{1:1} \cdot \text{cross-section area}$$

assumed

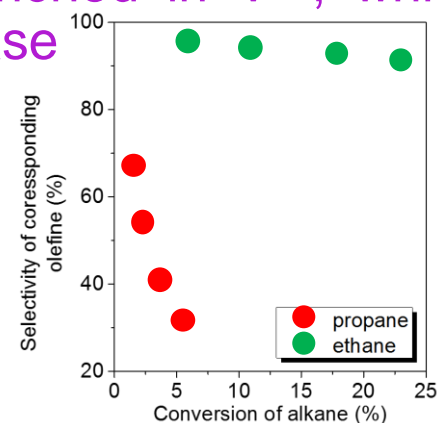
39\AA^2 for propane
 22\AA^2 for ethane

Differential heat of
propane adsorption at 40°C



In-situ photoelectron spectroscopy

with TOS (presents of H₂O) the surface is progressively enriched in V⁵⁺, which leads to a decrease in selectivity ¹



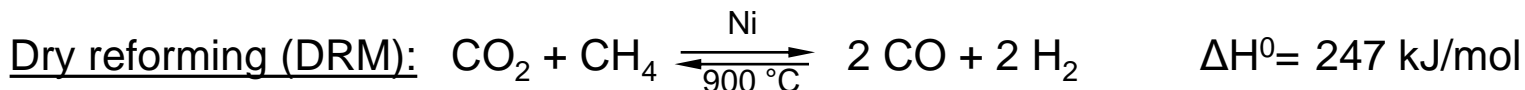
- ✓ segregation of V⁵⁺ occurs already at r.t.
- ✓ alkanes are already activated at r.t.
- ✓ dynamic nature of the surface
- ✓ very strong interaction of propane with used surface explains the decrease in selectivity caused by V-segregation



Reactants induced dynamic responses of catalyst surface:

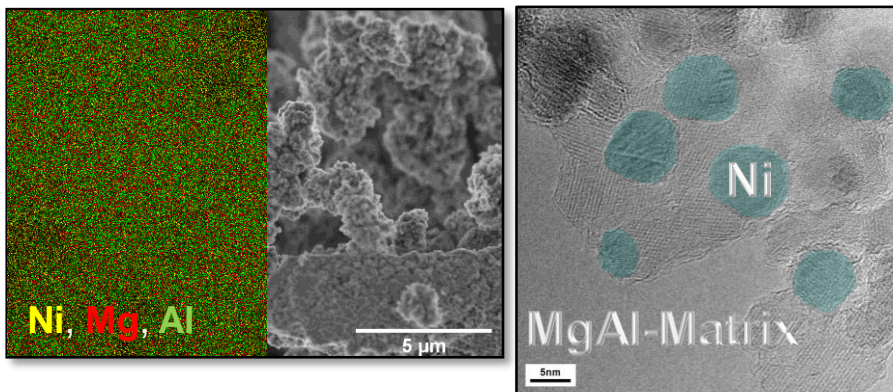
CO chemisorption cycles (30°C) on Ni/MgAl oxide catalyst
for dry reforming of methane (DRM)

Task: study the influence of structural and compositional properties of nickel catalysts on the catalytic performance during DRM



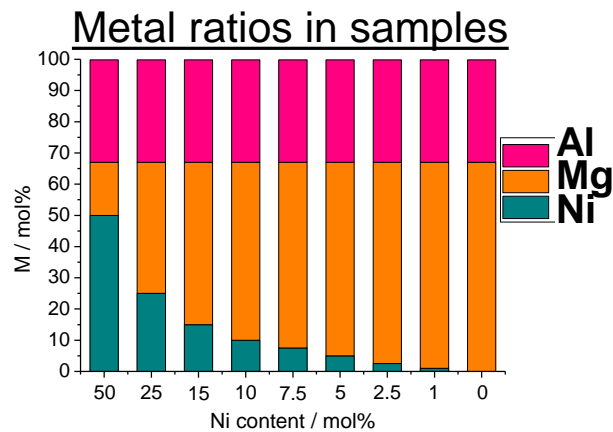
Catalyst preparation pathway:

- synthesized by constant pH co-precipitation with Ni contents between 0 and 55 wt.-%.
- decomposition to mixed oxides by calcination at 600°C

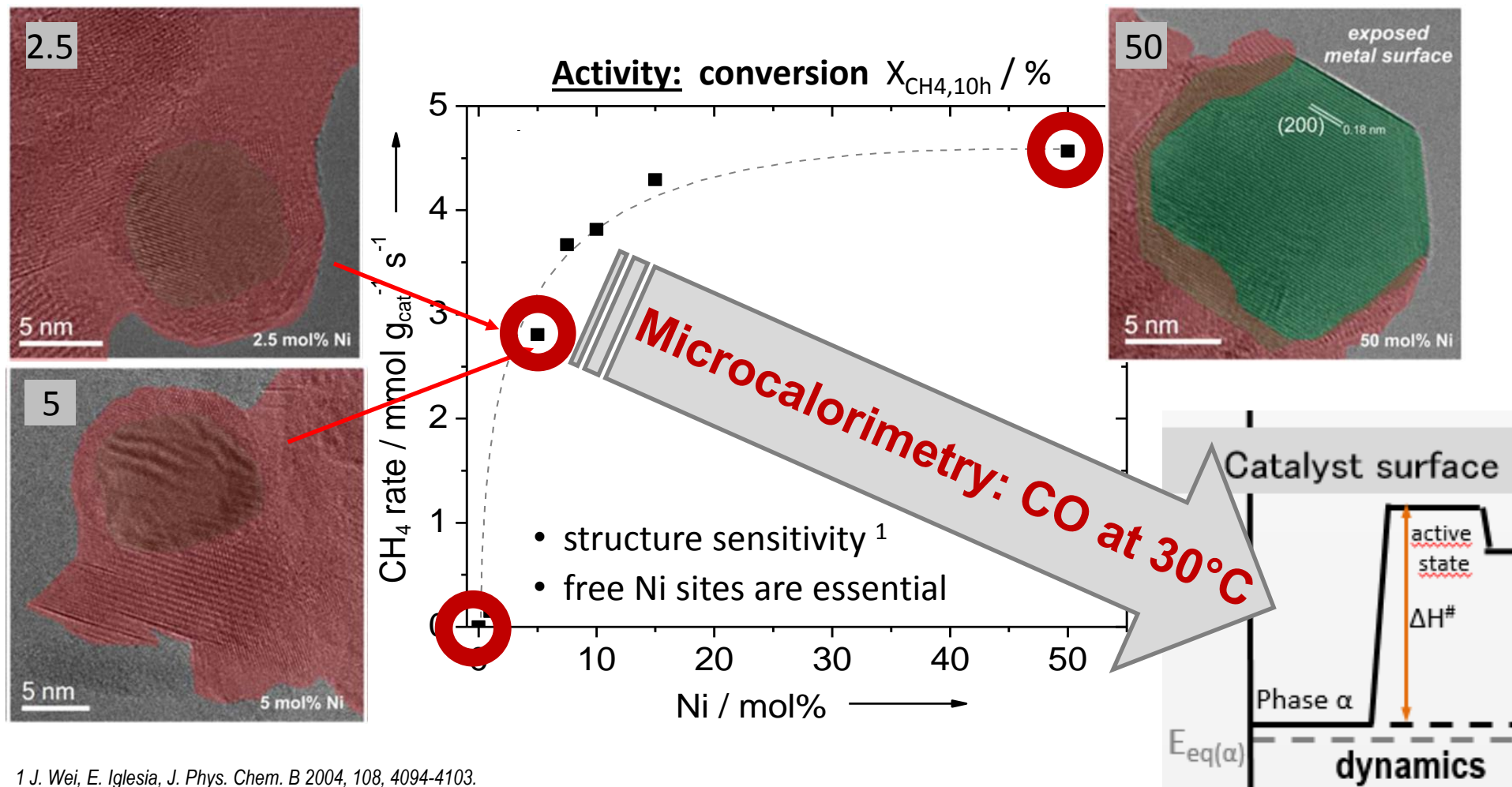


Obtained Ni/MgAl oxide catalyst

- reduction at 1000°C
- $d_{\text{P, Ni}} = 7 - 9 \text{ nm}$ in all samples
- $d_{\text{P, Ni}} = 7 - \mathbf{20} \text{ nm}$ only in the 50wt% sample



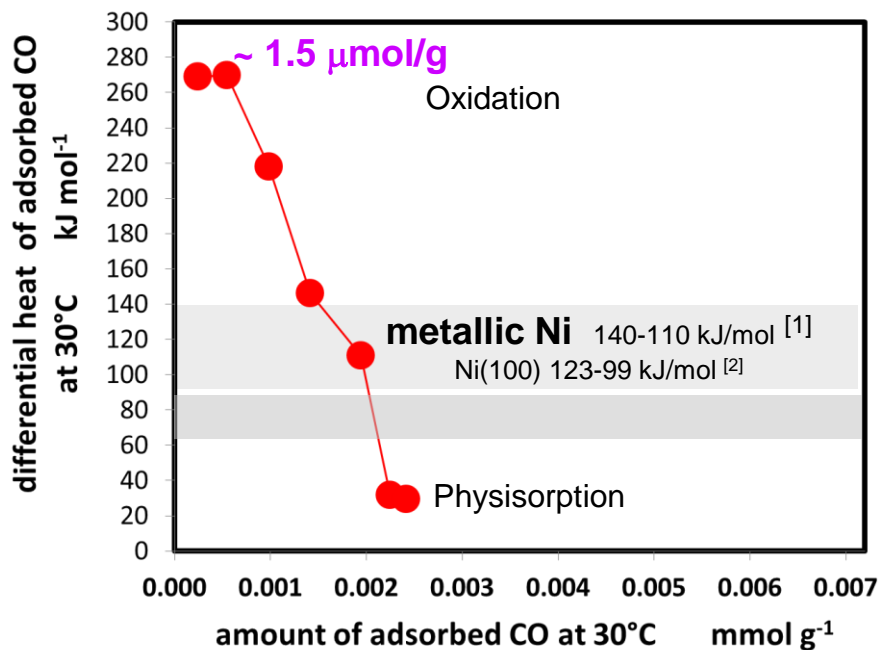
- HR-TEM images of 2.5, 5 and 50 mol% Ni/MgAl oxide
- EDX, NEXAFS & FTIR/CO/77K: overgrowth might be interpreted as a NiAl_2O_4 spinel



¹ J. Wei, E. Iglesia, *J. Phys. Chem. B* 2004, 108, 4094-4103.

50mol% Ni/MgAl oxide

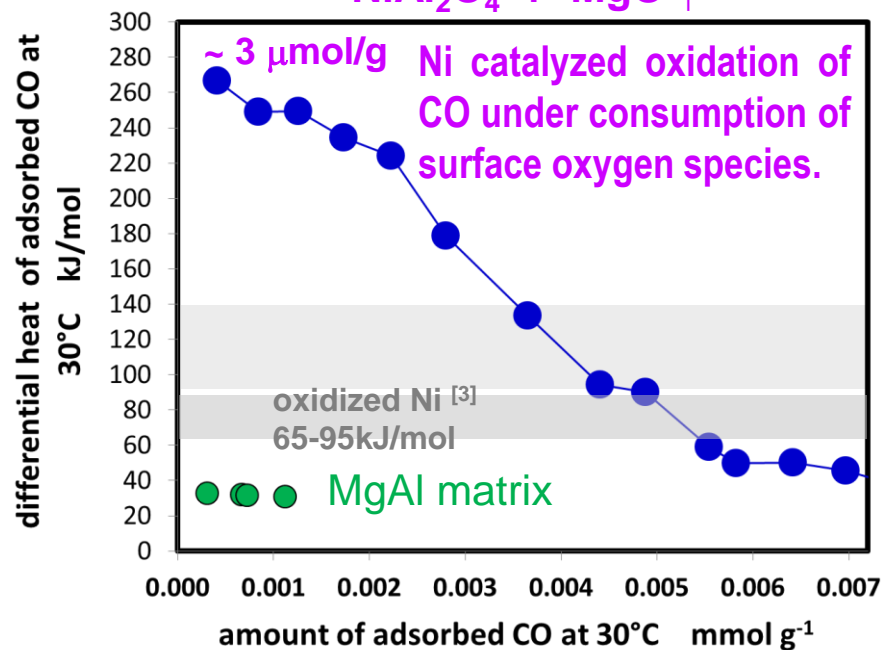
$X_{\text{CH}_4, 10\text{h}} = 73\%$



5 mol% Ni/MgAl oxide

$X_{\text{CH}_4, 10\text{h}} = 50\%$

$\text{NiAl}_2\text{O}_4 + \text{MgO} \uparrow$



➤ The differential heat profiles are dominated by the presence of nickel

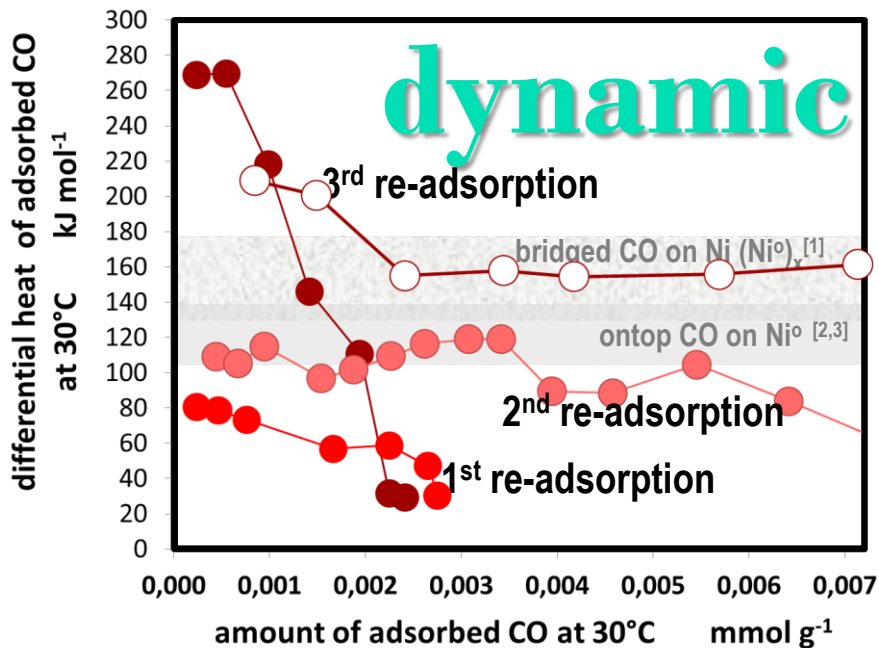
[1] A. Tanksale, J.N. Beltramini, J.A. Dumesic, G.Q. Lu, *Journal of Catalysis* 258 (2008) 366–377.

[2] J. T. Stuckless, N. Al-Sarraf, C. Wartnaby, D. A. King, *J. Chem. Phys.* **1993**, 99, 2202-2212.

[3] M. Cerro-Alarcó, B. Bachiller-Baeza, A. Guerrero-Ruiz, I. Rodríguez-Ramos, *J. Mol. Catal. Chem.* 2006, 258, 221-230.

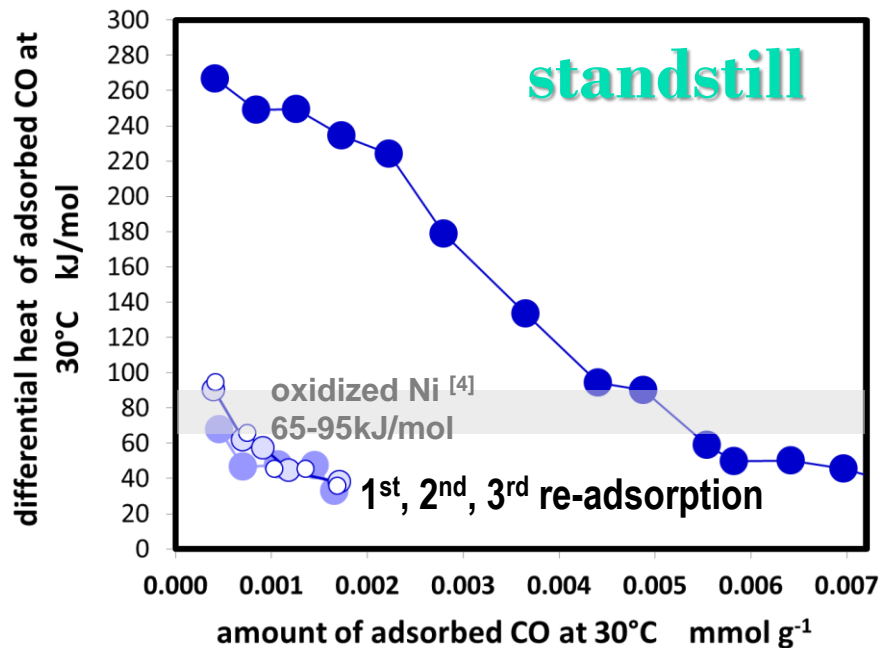
50mol% Ni/MgAl oxide

$X_{\text{CH}_4, 10\text{h}} = 73\%$



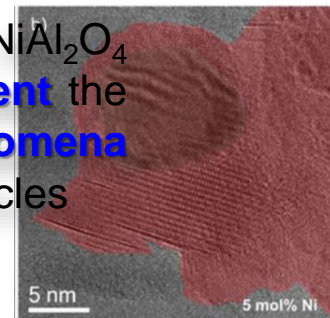
5 mol% Ni/MgAl oxide

$X_{\text{CH}_4, 10\text{h}} = 50\%$



Catalytically relevant Ni⁰ is back again !

➤ **Overgrowth** NiAl₂O₄ seems to **prevent** the **dynamic phenomena** on Ni nanoparticles



[1] R. S. Bordoli, J. C. Vickerman, J. Wolstenholme, *Surf. Sci.* **1979**, 85, 244-262.

[2] A. Tanksale, J.N. Beltramini, J.A. Dumesic, G.Q. Lu, *J. of Catalysis* **258** (2008) 366–377.

[3] J. T. Stuckless, N. Al-Sarraf, C. Wartnaby, D. A. King, *J. Chem. Phys.* **1993**, 99, 2202-2212

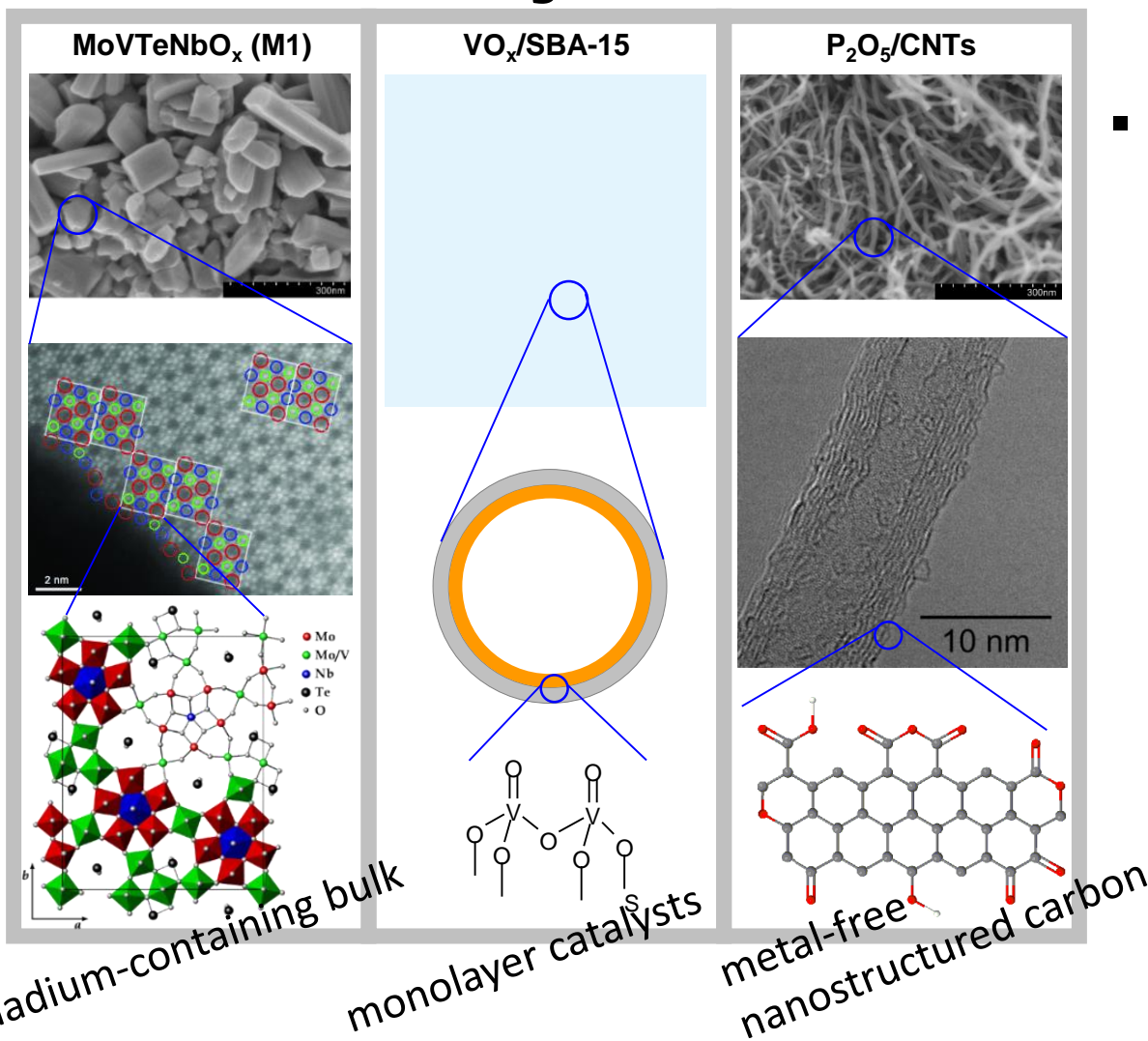
[4] M. Cerro-Alarcó, B. Bachiller-Baeza, A. Guerrero-Ruiz, I. Rodríguez-Ramos, *J. Mol. Catal. Chem.* **2006**, 258, 221-230.



Estimation of the enthalpy of formation of the transition state (activation barrier):

ethane & ethylene and propane & propylene ads. on the Vanadium oxide-based and Metal-free catalysts for ODH

Catalysts



- Identification of differences and similarities in the reaction network.

structurally similar functional groups:

V-OH / C-OH

V=O / C=O

V-O-V / C-O-C

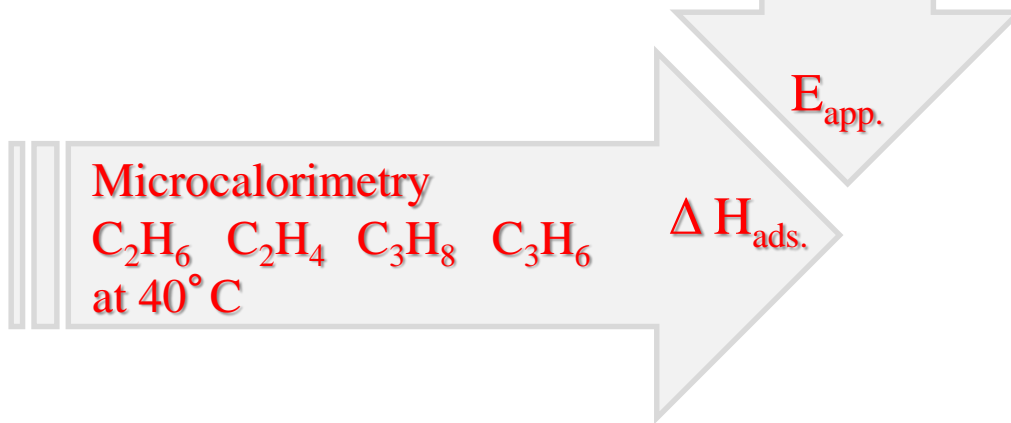
[1] P. Kube, B. Frank, S. Wrabetz, J. Kröhnert, M. Hävecker, J. Valasco-Vélez, J. Noack, R. Schlögl, A. Trunschke, *ChemCatChem* 9 (2017) 1-14.

Catalytic Performance

- Bulk MoVTenb oxide, 6V/SBA-15 and P/oCNT have been compared in the **ODH of C₂H₆ and C₃H₈ under identical conditions.**¹

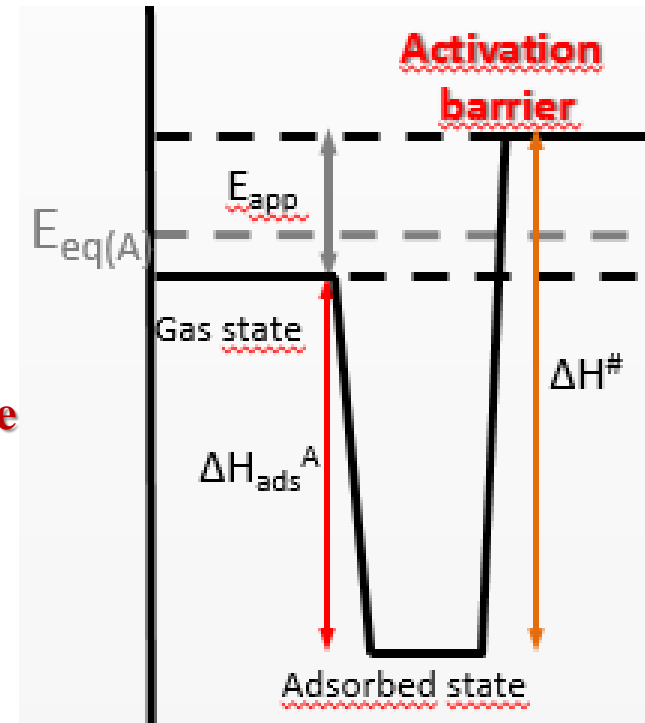
Similarities and Differences in the reaction network

Strong temperature dependence → **different transition states**



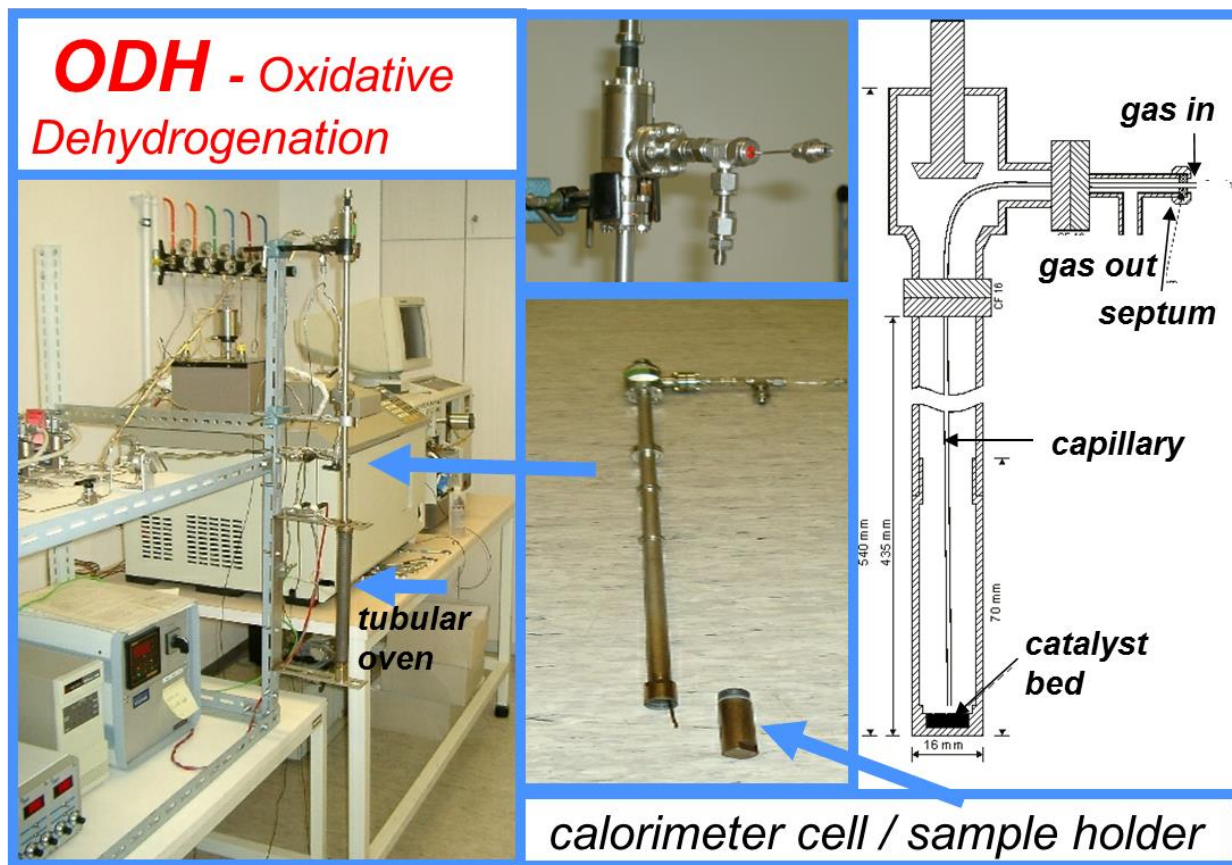
enthalpy of formation of the transition state

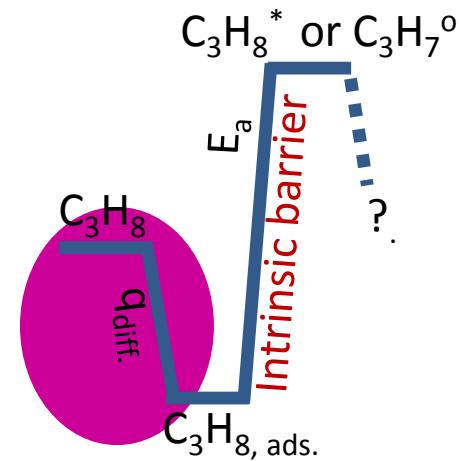
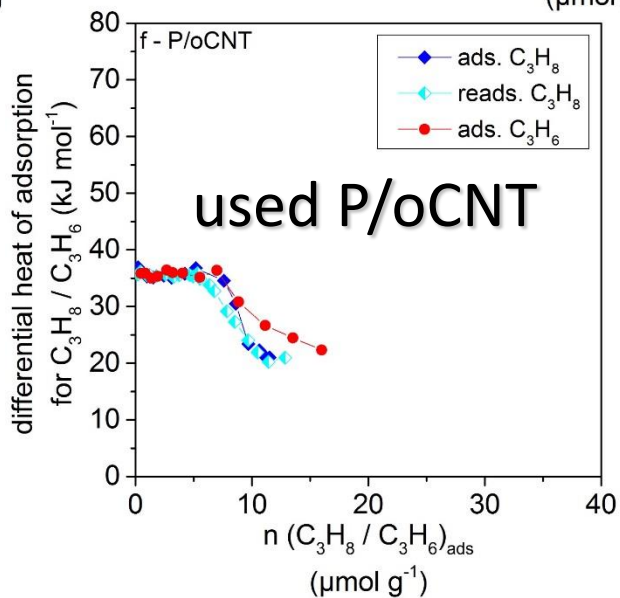
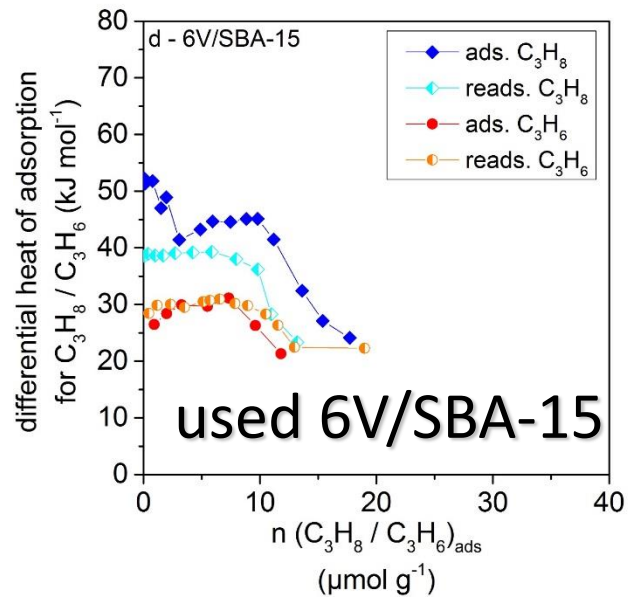
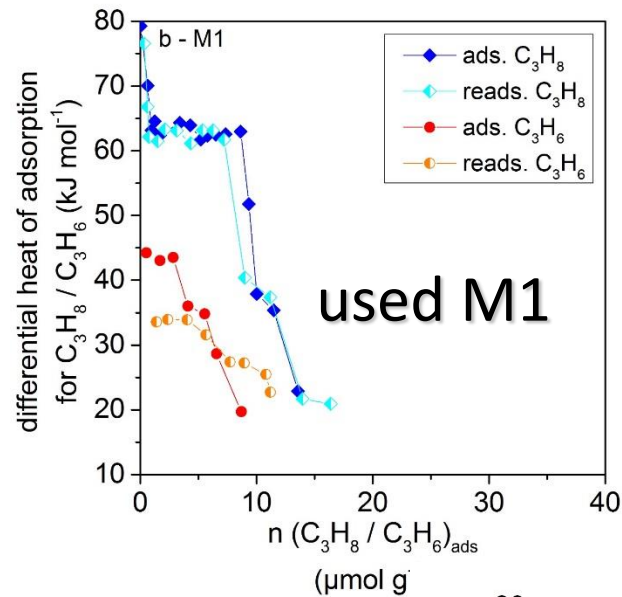
Note: $\Delta H_{ads.} \neq T_{ads.}$ ²; ads. in quasi-equilibrium³; intermediates occur in pseudo-steady-state

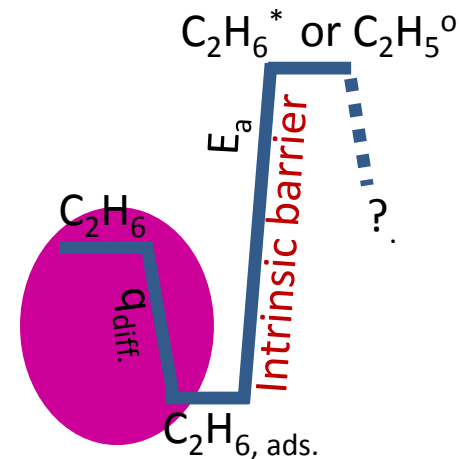
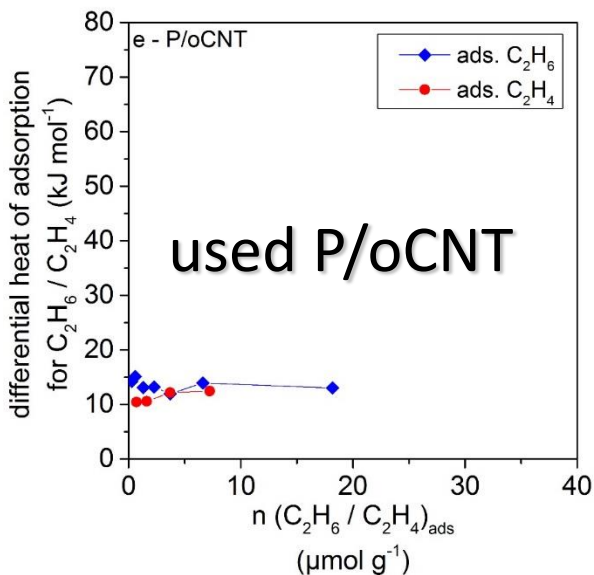
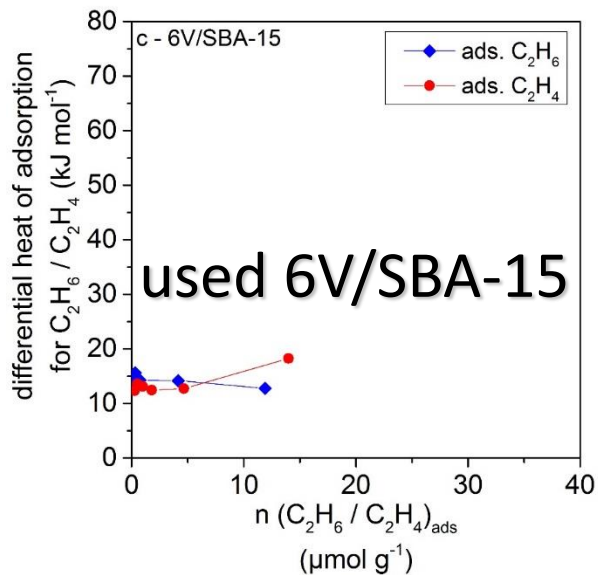
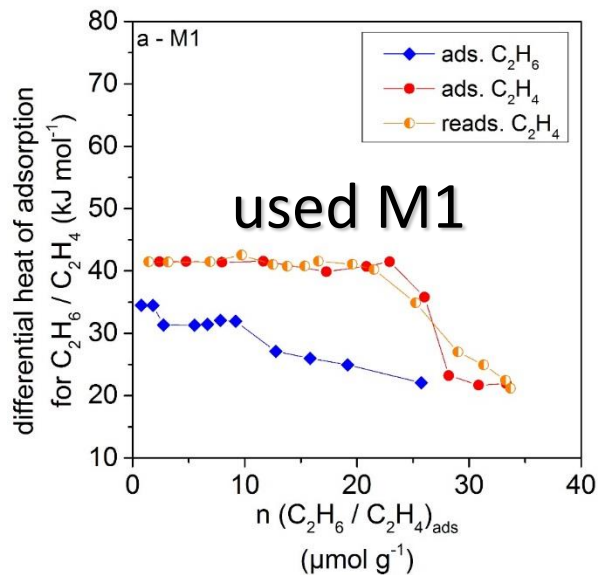


1 P. Kube, B. Frank, S. Wrabetz, J. Kröhnert, M. Hävecker, J. Valasco-Vélez, J. Noack, R. Schlögl, A. Trunschke, *ChemCatChem* 9 (2017) 1-14.
 2 a) D. C. Tranca, N. Hansen, J. A. Swisher, B. Smit, F. J. Keil, *J. Phys. Chem. C* 2012, 116, 23408–23417; b) E. J. Maginn, A. T. Bell, D. N. Theodorou, *J. Phys. Chem.* 1995, 99, 2057–2079.
 3 K. Chen, A. T. Bell, E. Iglesia, *J. Phys. Chem. B* 2000, 104, 1292–1299

- Feed of 10% hydrocarbon (C_3H_8 or C_2H_6) and 5% oxygen in helium with a total flow rate of 20 mLmin^{-1} .
- $T_{\text{reaction}} = 400^\circ\text{C}$ for 6V/SBA-15, 360°C for P/oCNT and 350°C for M1
- The reaction was performed at a **steady state for 20 h**, subsequently, the cell was **cooled down to RT in pure helium**.







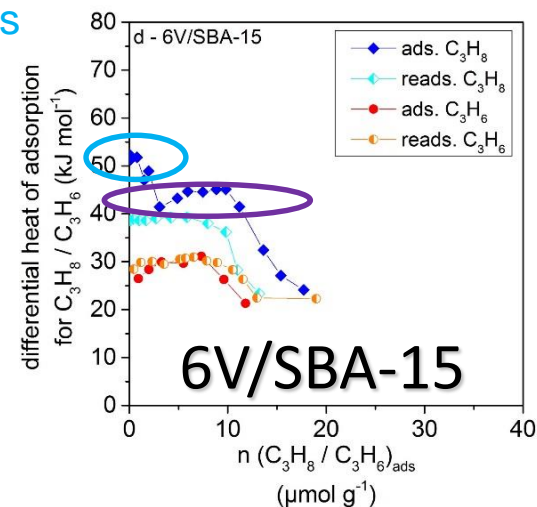
	M1	6V/SBA-15	P/oCNT
S_{BET} m ² g ⁻¹	10.6	355	229
$V_{\text{surf.}}$; $O_{\text{surf.}}$	30	1113	1063
Γ_{V} atoms nm ⁻²	1.7	1.9	2.8
$\Gamma_{\text{C}_3\text{H}_8}$ molecules nm ⁻²	0.44 (63 kJ/mol)	0.0014 (52 kJ/mol) 0.0114 (44 kJ/mol)	0.013 (36 kJ/mol)
$V_{\text{surf.}}/C_3H_6$ ads.	~4	~150	
$r_{\text{C}_3\text{H}_8, \text{consumption}, 0}$ mmol g ⁻¹ h ⁻¹	5.3 ±0.2	0.45 ±0.006	0.21 ±0.004
$r_{\text{C}_2\text{H}_6, \text{consumption}, 0}$ mmol g ⁻¹ h ⁻¹	5.4 ±0.2	0.055 ±0.001	0.03 ±0.001
$q_{\text{diff}}(C_3H_8)$	79 / 63 rev. ads.	52 / 44 rev. ads.	36 rev. ads.
$q_{\text{diff}}(C_3H_6)$	44 irrev. ads.	30 rev. ads.	36 rev. ads.
$q_{\text{diff}}(C_2H_6)$	34 rev. ads.	14 *	14 *
$q_{\text{diff}}(C_2H_4)$	41 rev. ads.	14 *	14 *
E_a , propane	80 ±3	110 ±2	103 ±7
E_a , ethane	90 ±2	121 ±2	110 ±7
intrinsic barrier for propane activation	143 (63 kJ/mol)	162 154	139
intrinsic barrier for ethane activation	124		

q_{diff} - Differential heat of adsorption of hydrocarbons (kJ mol⁻¹)
 $V_{\text{surf.}}$, $O_{\text{surf.}}$: Surface concentration of V (M1 and 6V/SBA-15) and O (P/oCNT) atoms (μmol g⁻¹)
 $\Gamma_{\text{C}_3\text{H}_8}$ - Density of adsorbed propane (molecules nm⁻²)
 Γ_{V} - Surface density of V or O (atoms nm⁻²)
 E_a : propane/ethane consumption, 0 (kJ/mol); initial rate
 * Differential heat near the condensation enthalpy of reaction molecules at 40°C
 intrinsic barrier = $E_a + q_{\text{diff}}$ (kJ mol⁻¹)

6V/SBA-15:

- $\Gamma_{\text{C}_3\text{H}_8} = 0.0014$ molecules nm⁻²
 - intrinsic barrier for C₃H₈ activation = 162 kJ/mol
 - DFT calculations by Rozanska² = 160 kJ/mol due to monomeric species
- ~0.1% of all V atoms.

~ 1%



- intrinsic barrier for C₃H₈ activation = 154 kJ/mol
 - DFT calculations by Rozanska² = 148 kJ/mol due to silica-supported vanadium oxide dimers
- ~ 0.6% of all V atoms

- Hävecker, M.; Wrabetz, S.; Kröhnert, J.; Csepei, L.-I.; Naumann d'Alnoncourt, R.; Kolen'ko, Y. V.; Girgsdies, F.; Schlögl, R.; Trunschke, A. *Journal of Catalysis* 2012, 285, 48.
- X. Rozanska, R. Fortrie, J. Sauer, *J. Am. Chem. Soc.* 2014, 136, 7751–776.
- P. Concepcijn, P. Botella, J. M. L. Nieto, *Appl. Catal. A* 2004, 278, 45–56; f) R. Coast, M. Pikus, P. N. Henriksen, G. A. Nitowski, *J. Phys. Chem.* 1996, 100, 15011–15014.

Conclusion

- Microcalorimetry and DFT : - quantification of propane adsorption sites in vanadium oxide monolayer catalysts
 - resolves different degrees of V_xO_y oligomerization

V_xO_y	<u>Microcalorimetry</u> Intrinsic barrier for C_3H_8 activation <i>kJ/mol</i>	<u>Density functional theorie DFT</u> ¹ Energy barriers <i>kJ/mol</i>	<u>Microcalorimetry</u> % of the total amount of $V_{surf.}$
Monomer (a)	162	160	0.1
Dimer (b)	154	148	0.6
trimer		143	
tetramer	143	139	

~ 1%

ODH of propane over M1 phase: tetramers of vanadium oxide species have been postulated to be the required ensemble size ²

- Structure - Activity Relationship
Higher activity correlates with:
 - **higher density of C_3H_8 adsorption sites**
 - **lower intrinsic barrier for C_3H_6 formation**

[1] X. Rozanska, R. Fortrie, J. Sauer, J. Am. Chem. Soc. 2014, 136, 7751–776.

[2] R. Schlögl, Top. Catal. 2011, 54, 627–638.

- Microcalorimetry and DFT : - quantification of propane adsorption sites in vanadium oxide monolayer catalysts
- resolves different degrees of V_xO_y oligomerization

V_xO_y	<u>Microcalorimetry</u> Intrinsic barrier for C_3H_8 activation <i>kJ/mol</i>	<u>Density functional theory DFT</u> ¹ Energy barriers <i>kJ/mol</i>
Monomer (a)	162	160
Dimer (b)	154	148
trimer		143
tetramer	143	139

J | A | C | S
JOURNAL OF THE AMERICAN CHEMICAL SOCIETY

Article
pubs.acs.org/JACS

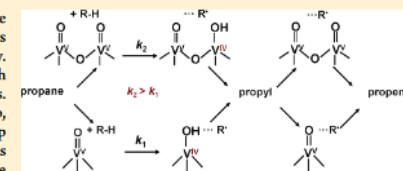
Size-Dependent Catalytic Activity of Supported Vanadium Oxide Species: Oxidative Dehydrogenation of Propane

Xavier Rozanska, Remy Fortrie, and Joachim Sauer*

Institut für Chemie, Humboldt Universität zu Berlin, Unter den Linden 6, D-10099 Berlin, Germany

Supporting Information

ABSTRACT: Possible reaction pathways for the oxidative dehydrogenation of propane by vanadium oxide catalysts supported on silica are examined by density functional theory. Monomeric and dimeric vanadium oxide species are both considered and modeled by vanadyl-substituted silsesquioxanes. The reaction proceeds in two subsequent steps. In a first step, hydrogen abstraction from propane by a vanadyl ($O=V$) group yields a propyl radical bound to a HOV^{IV} surface site. Propene is formed by a second hydrogen abstraction, either at the same vanadia site or at a different one. V^V/V^{IV} redox cycles are preferred over V^V/V^{III} cycles. Under the assumption of fast reoxidation, microkinetic simulations show that the first step is rate-determining and yields Arrhenius barriers that are lower for dimers (114 kJ/mol at 750 K) than for monomers (124 kJ/mol). The rate constants predicted for a mixture of monomers and dimers are 14% larger (750 K) than for monomers only, although the increase remains within experimental uncertainty limits. Direct calculations of energy barriers also yield lower values for dimeric species than for monomeric ones. Reactivity descriptors indicate that this trend will continue also for larger oligomers. The size distribution of oligomeric species is predicted to be rather statistical. This, together with the small increase in the rate constants, explains that turnover frequencies observed for submonolayer coverages of vanadia on silica do not vary with the loading within the experimental uncertainty limits.



1. INTRODUCTION

Supported transition metal oxides are an important class of solid catalysts that are industrially used in selective oxidation

but proving this appears difficult.^{10,11} For example, it has been shown that V–O–V bonds, which would be absent in monomeric species, cannot be identified in IR or Raman spectra because of overlap with bands of the supporting oxide.⁷ UV–vis absorption spectra are also not size-discriminating, although there is no doubt that the O 2p–V 3d charge transfer transitions will shift to lower energies with increasing particle size.^{8,12}

Here, we use density functional theory (DFT) to provide information that cannot be easily obtained from experiments. We construct models for monomeric, dimeric, and polymeric supported species, and we examine them in comparison to surfaces of the bulk crystal. We study the reaction mechanisms

Here, we use density functional theory (DFT) to provide information that cannot be easily obtained from experiments.

includes different types of active species, ranging from monomeric over oligomeric to polymeric transition metal oxide clusters anchored on the surface of the supporting oxide, to nanocrystallites of the active component with the structure

[1] X. Rozanska, R. Fortrie, J. Sauer, J. Am. Chem. Soc. 2014, 136, 7751–776.

[2] R. Schlögl, Top. Catal. 2011, 54, 627–638.



Limitations of method:

Propane ads. on vanadium-phosphorus-oxide / VPO
at $T_{\text{reaction}} = 100 - 400^{\circ}\text{C}$

Natural gas as raw material

Methane
Ethane
Propane
Butane

+ O₂ VPO

OCM
Oxidative Dehydrogenation
Selective Catalytic Oxidation

Olefines, Oxygenates

Ethane, Ethylene
Ethylene, Acetic acid
Propylene, Acrylic acid
Butylenes, Butadiene,
Maleic anhydride

Intention: Determination of kinetic data: N_o , K and ΔH_{ads} of alkanes on VPO at $T_{reaction}$

Adsorption

★ propane, ethane and n-butane as probe molecule

Microcalorimetry :

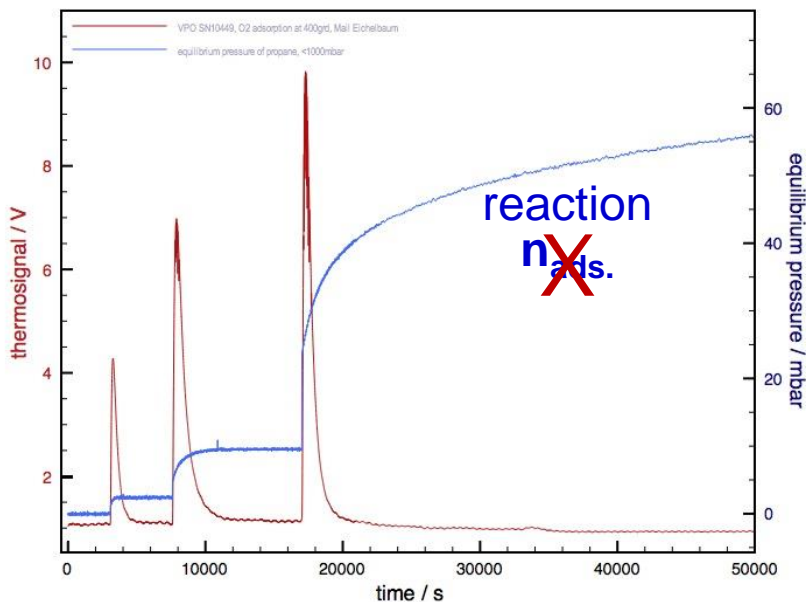
★ $T_{adsorption} = 400, 300, 200, 100$ and 40°C

★ selected catalyst: VPO #10449

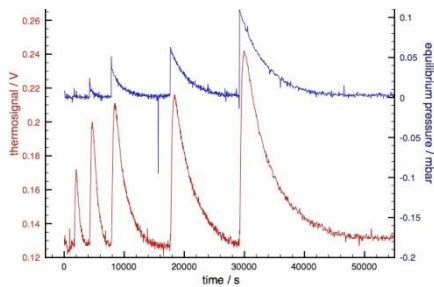
The temporal evolution of the thermo signal during propane ads. at 400°C

Catalyst was oxidized at 400°C for 2h

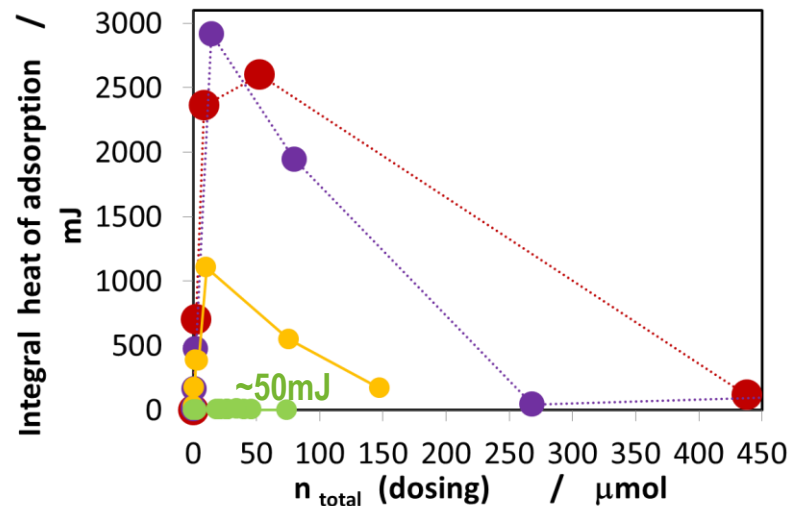
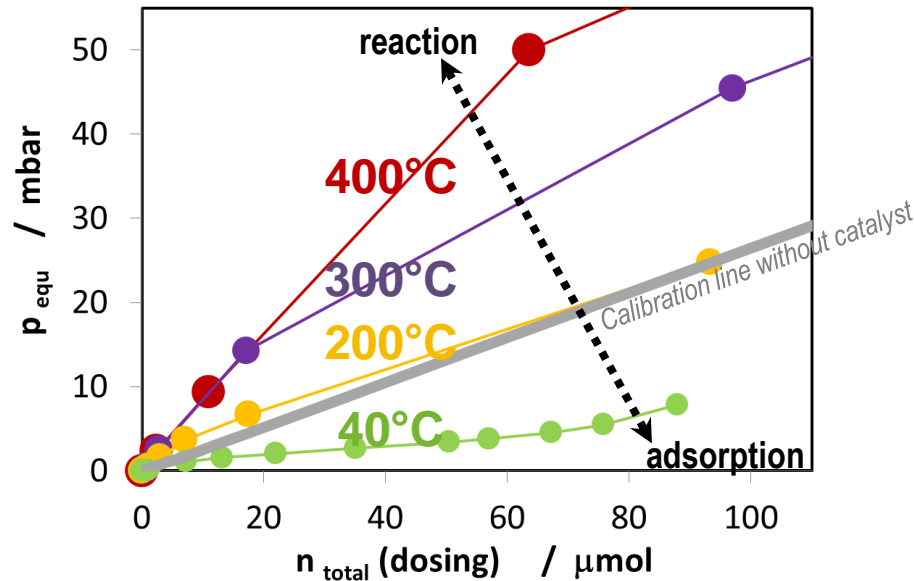
Integral heat / pressure



Classical pressure profile

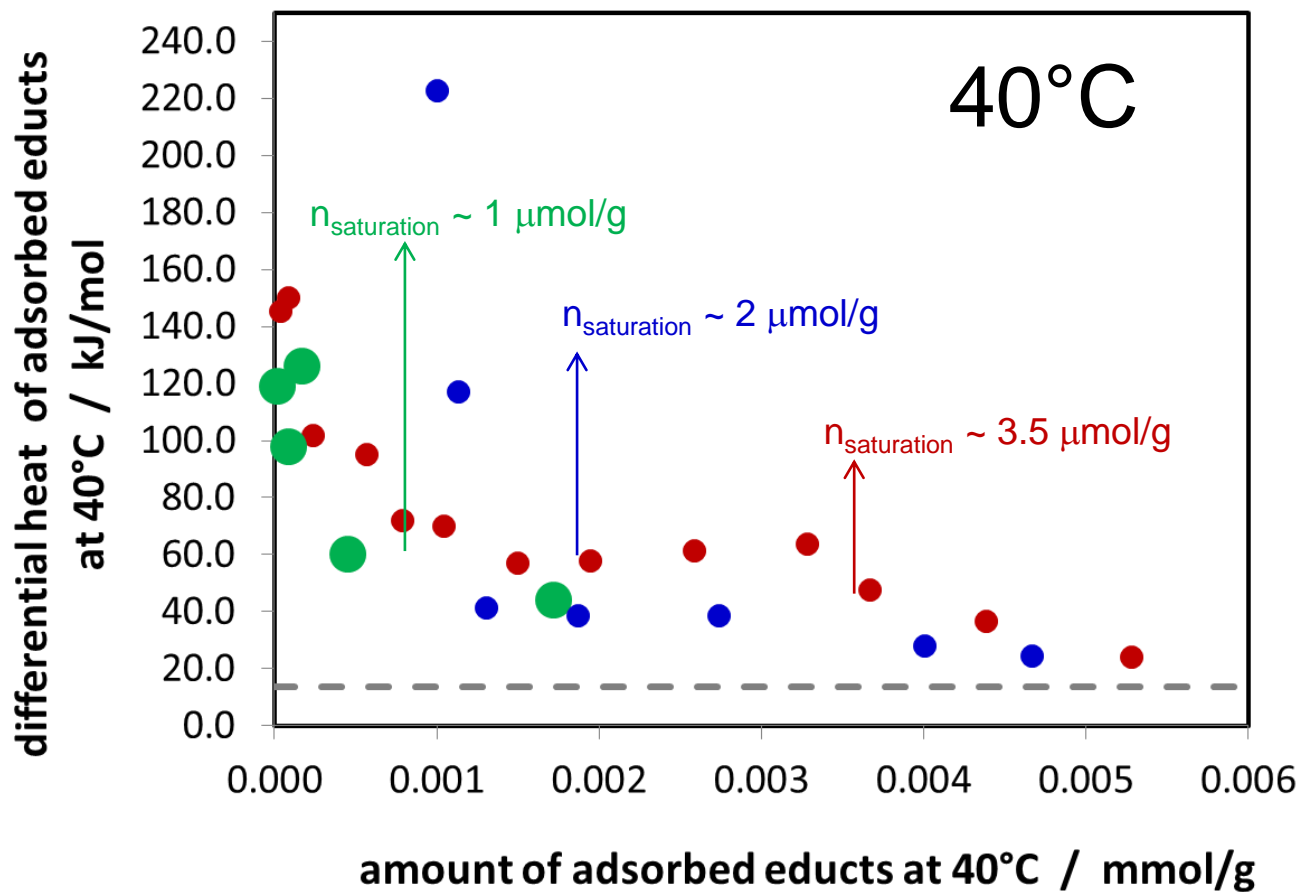


Calorimetric experiments at 400, 300, 200 and 40°C



Differential heat of propane / ethane / n-butane

Catalyst was oxidized at 400°C for 2h





Microcalorimetry alone or combined with to other techniques is a very powerful/sensitive tool to probe catalytically active surfaces quantitatively.



Quantitative data (*reversibility, heat of adsorption, number of adsorption sites, equilibrium constant*) provide a basis for theoretical modeling and can contribute to a better understanding of the complex microkinetics.



Microcalorimetry can applied under or close to reaction conditions !
→ investigation of the catalytic relevant surface sites

➤ **Calorimetry and Thermal Methods in Catalysis - Aline Auroux**
Springer –Verlag Berlin Heidelberg 2013



- ◆ A. Auroux “Thermal Methods: Calorimetry, Differential Thermal Analysis, and Thermogravimetry” in “Catalyst characterization: physical techniques for solid materials”, Eds. B. Imelik, J.C. Vedrine, Plenum Pr., New York 1994
- ◆ E. Calvet, H. Prat, H.A. Skinner “Recent progress in microcalorimetry”, Pergamon Pr., Oxford 1963
- ◆ B. E. Handy, S.B. Sharma, B.E. Spiewak and J.A. Dumesic, “A Tian-Calvet heat-flux microcalorimeter for measurement of differential heats of adsorption”, Meas. Sci. Technol. 4 (1993) 1350-1356.
- ◆ N. C. Cardona-Martinez and J.A. Dumesic, “Application of Adsorption Microcalorimetry to the Study of heterogeneous Catalysis”, Advances in Catalysis 38 150-243.
- ◆ Z. Knor, “Static Volumetric Methods for Determination of Adsorbed Amount of Gases on Clean Solid Surface”, Catalysis Reviews 1 (1) (1968) 257-313.
- ◆ S. Černý and V. Ponec, „Determination of Heat of Adsorption on Clean Solid Surfaces”, Catalysis Reviews 2 (1) (1969) 249-322.



Thank you for your attention



<http://www.fhi-berlin.mpg.de>

Dept. of Inorganic Chemistry, Director: Prof. R. Schlögl

